2-5-4 Mahab Area

(1) Lines location

During this field season, a total of 8 lines (from 000N to 1400N) were surveyed along N45°E direction with a line spacing of 200m. Each line had a length of 2.0 km with a total length of 14 km. Fig.II-2-23 shows the location of all the IP lines surveyed in Mahab.

(2) Results

The results of the TDIP survey in Mahab area are presented here in terms of pseudo-sections of apparent resistivity, chargeability and metal factor from Fig.II-2-24 to Fig.II-2-26, respectively. Contour maps of apparent resistivity, chargeability and metal factor for N=1 to 4 are indicated from Fig.II-2-27 to Fig.II-2-30, respectively.

The apparent resistivity map of Fig.II-2-27 shows a strong boundary running E-W that separates high resistivities in the south side from low resistivities in the north side. In the north side, from N=1 to 4, extremely low resistivities of few Ω-m are widely distributed. As seen in Fig. II-2-24, the boundary seems to dip at depth toward the south.

According to the Fig. II-2-29, the chargeability distribution shows almost the same distribution pattern as the apparent resistivity, i.e., the south part show high chargeabilities, while the north part low chargeabilities.

Due to the influence of the extremely low resistivity values, the metal factor distribution indicated in Fig. II-2-29 show high values widely distributed. However, the chargeability values are also low and therefore the existence of mineralization can not be suggested.

(3) 2D analysis

2D analysis was performed for all the lines. However in this report only the sections containing representative anomalies will be described (Fig.II-2-31).

By looking at the line 800N, it can be seen that its resistivity distribution is almost same as the apparent resistivity section indicated previously, i.e., presents high values in the south side and low in the north. In relation to the low resistivity zone in the north side, because the direction of resistivity changes, it can be expected sedimentary rocks from surface to intermediate depth. High resistivity zone in the south side agrees with the distribution of extrusive rocks.

Chargeability distribution presents almost same distribution pattern shown by the resistivity, namely, low chargeability in the north and high chargeability in the south. A fault can be expected around station No. 7, where is recognized the boundary between the low chargeability and high chargeability distributions.

The metal factor distribution presents high values everywhere from station No. 6 to the north. However, these high values are caused only by the extremely low resistivity because the chargeability distribution presents low values and therefore, this anomaly does not seem to be related to mineralization.

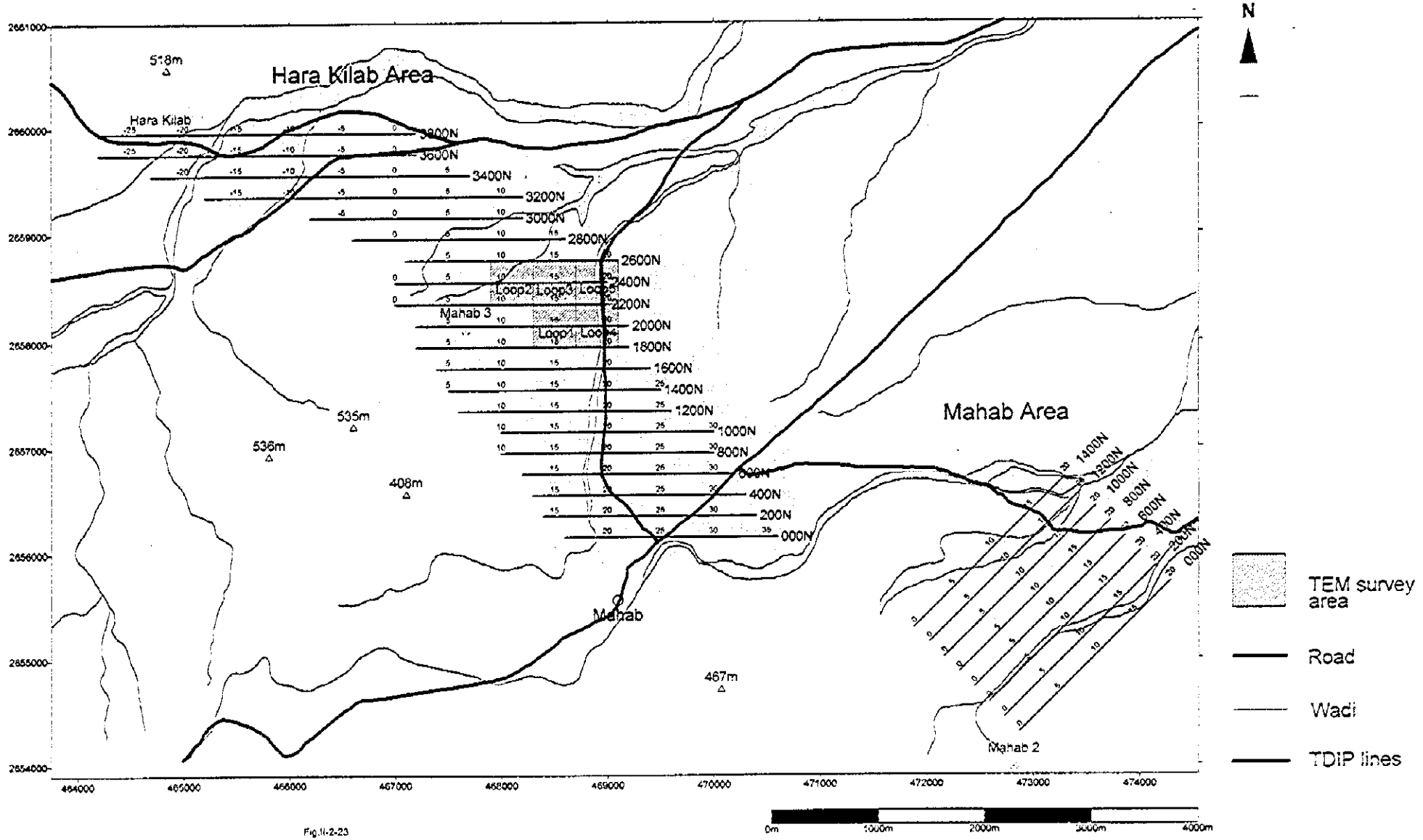

Fig. II -2-23 Geophysical survey location in Mahab and Hara Kilab area

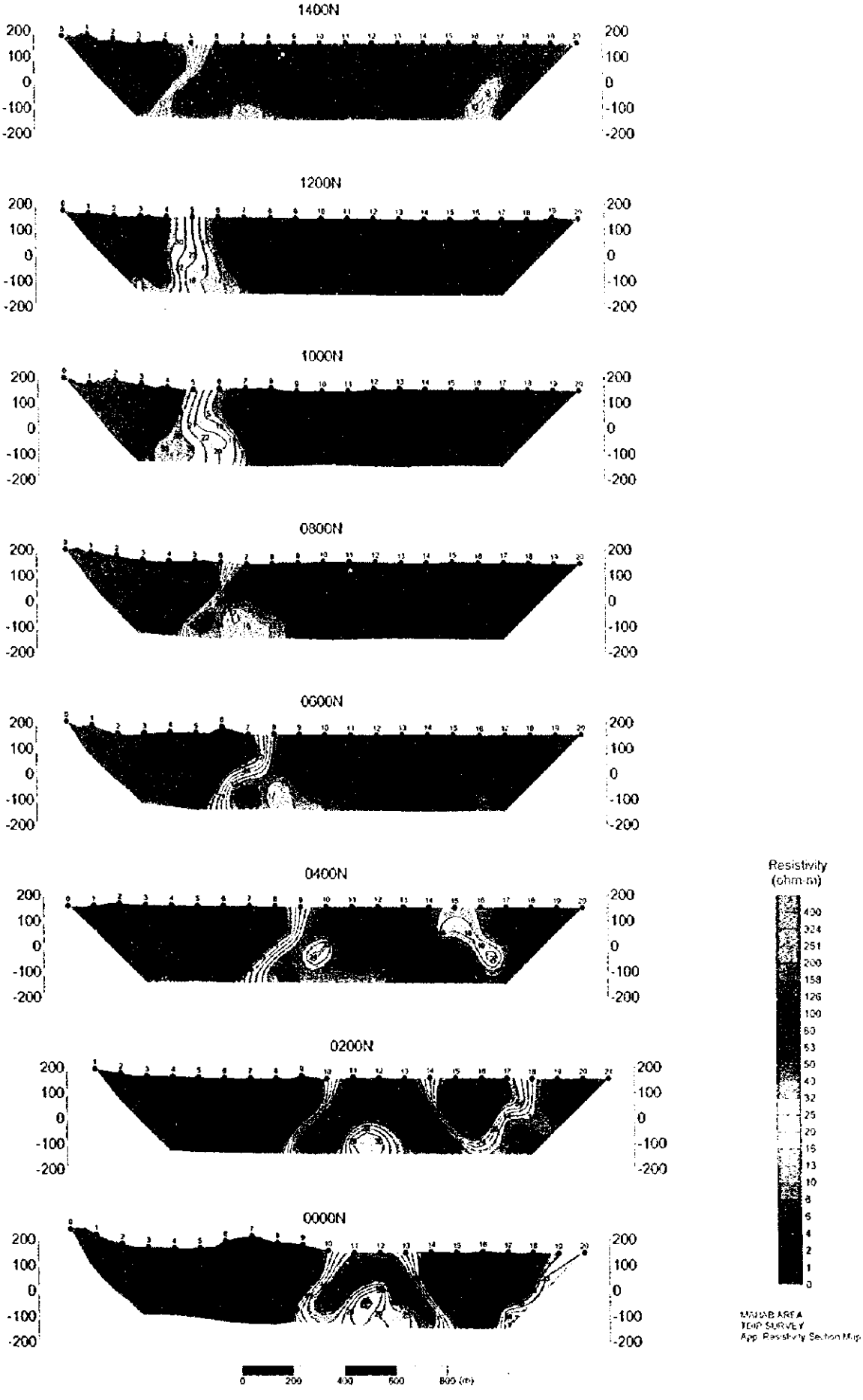

Fig. II-2-24 Apparent resistivity pseudo-sections in Mahab area

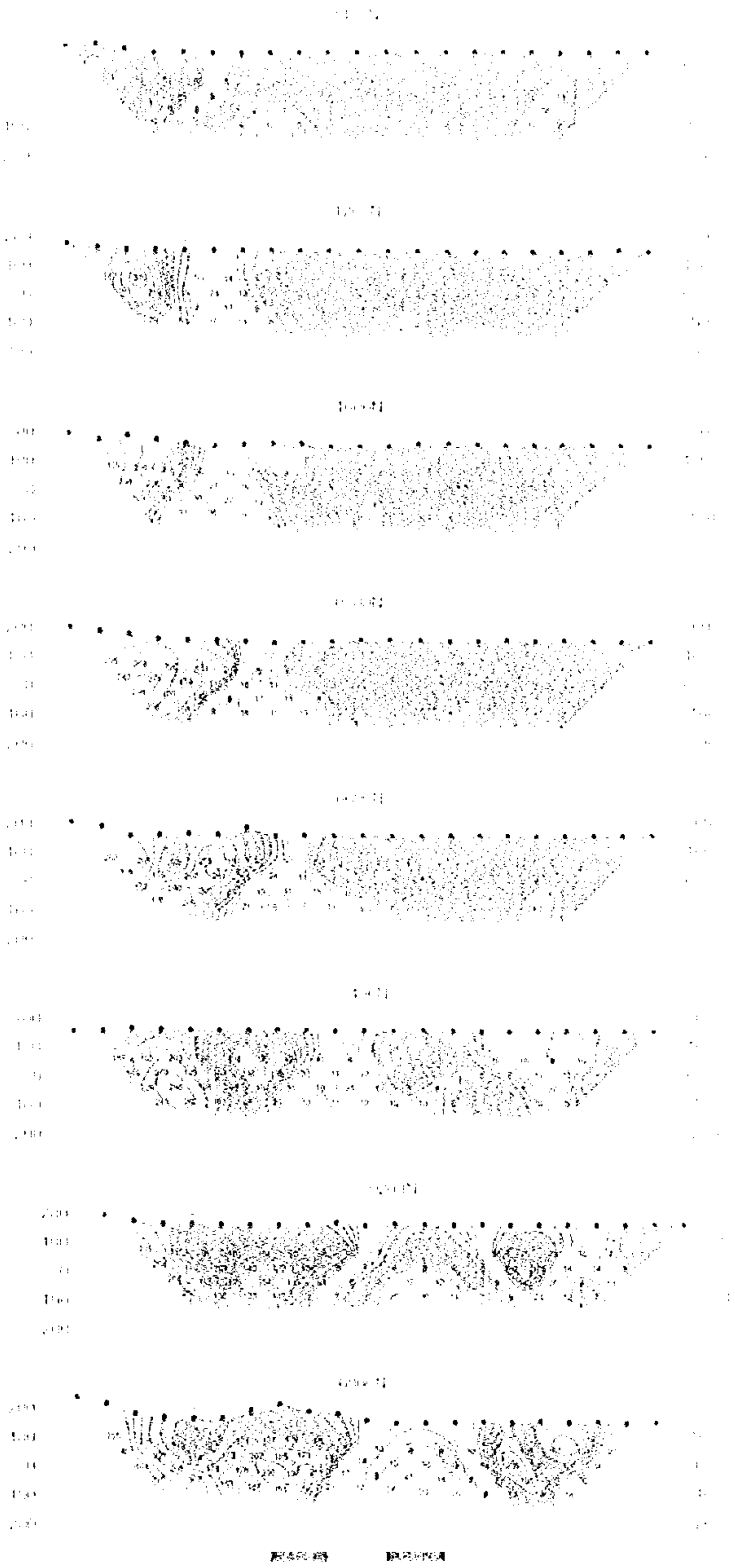

Fig. II.2.21 Apparent resistivity pseudo-sections in Malaba area

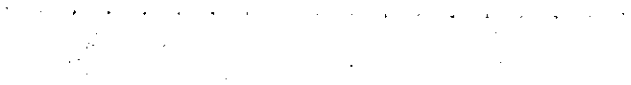

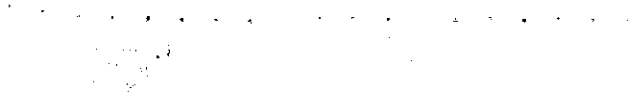

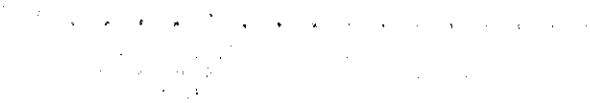

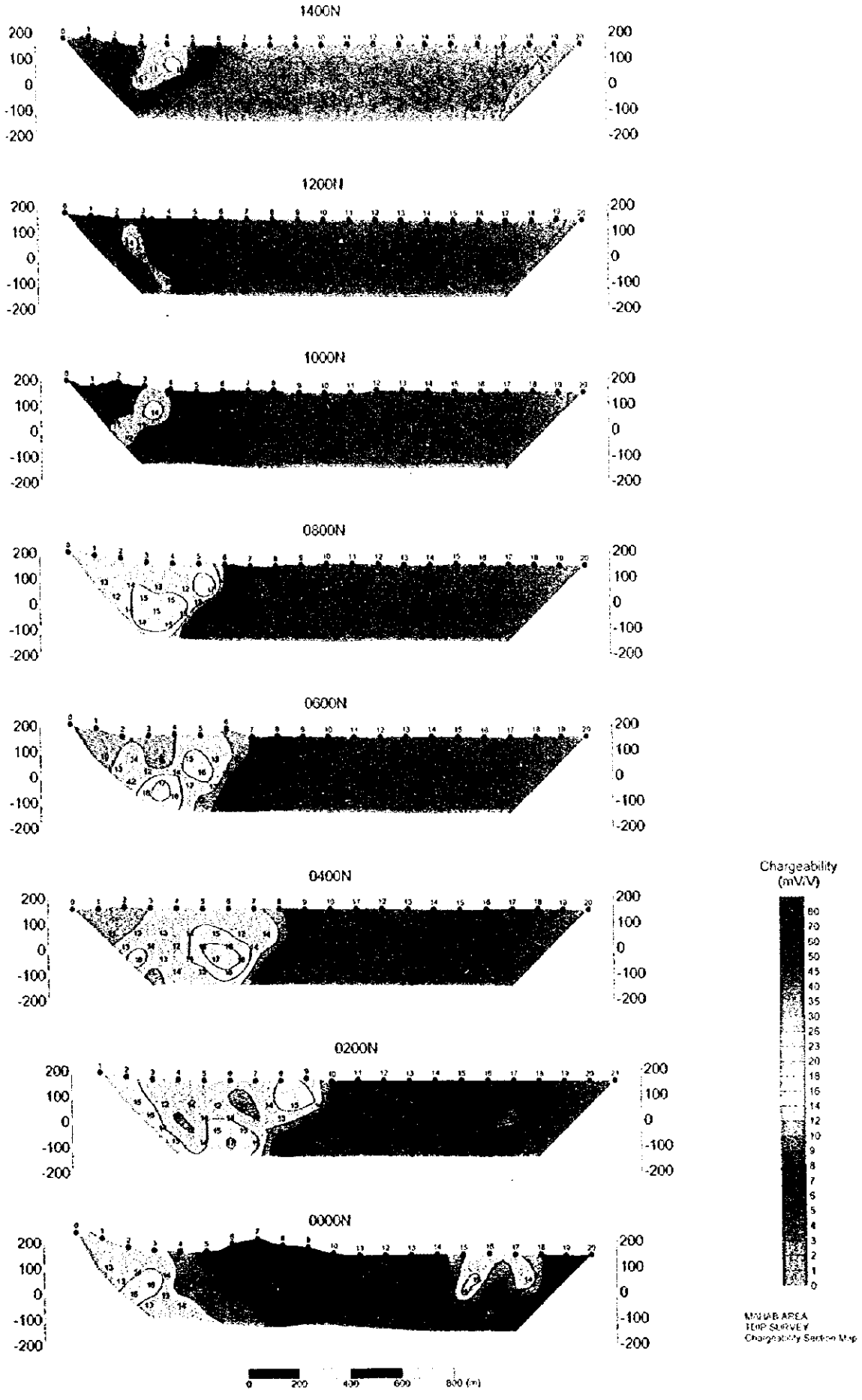

Fig. II -2-25 Chargeability pseudo-sections in Mahab area

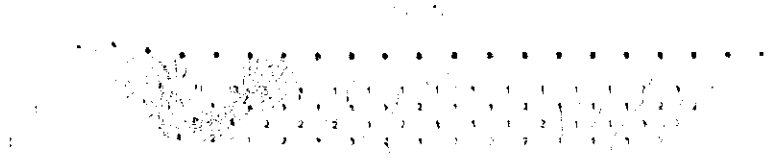

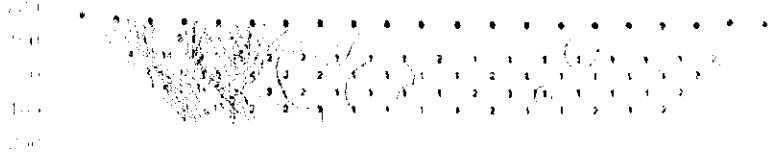

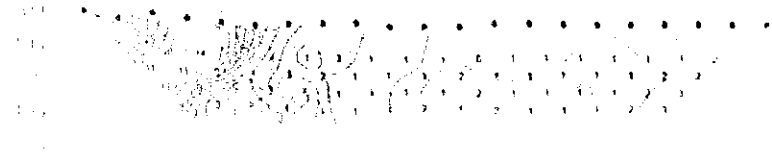

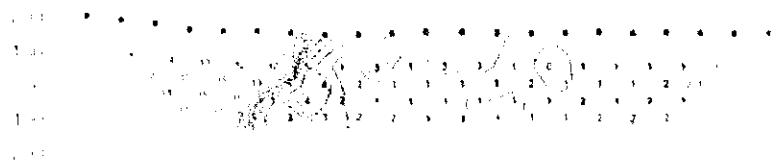

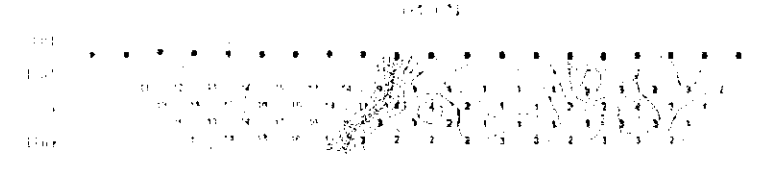

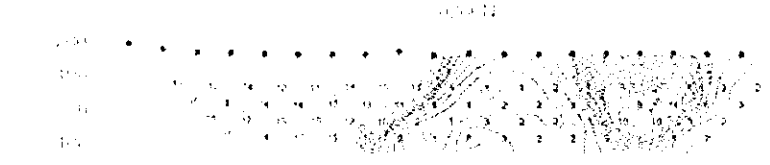

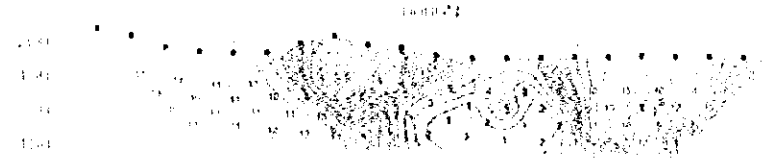

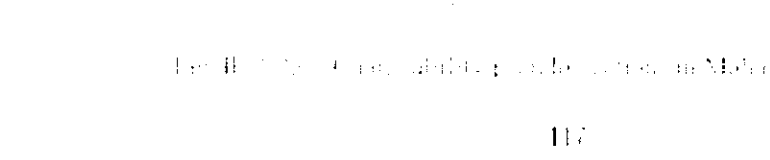

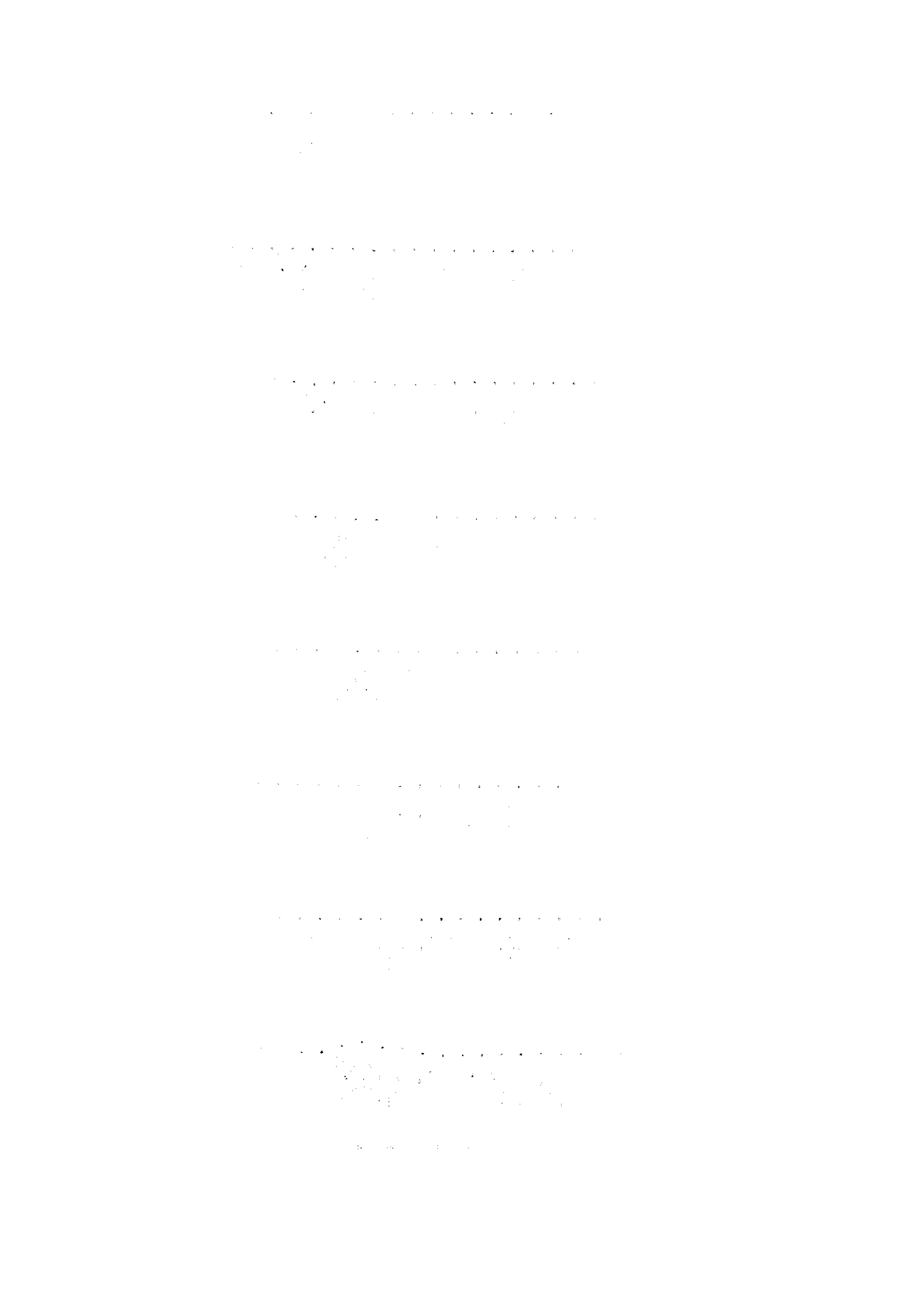

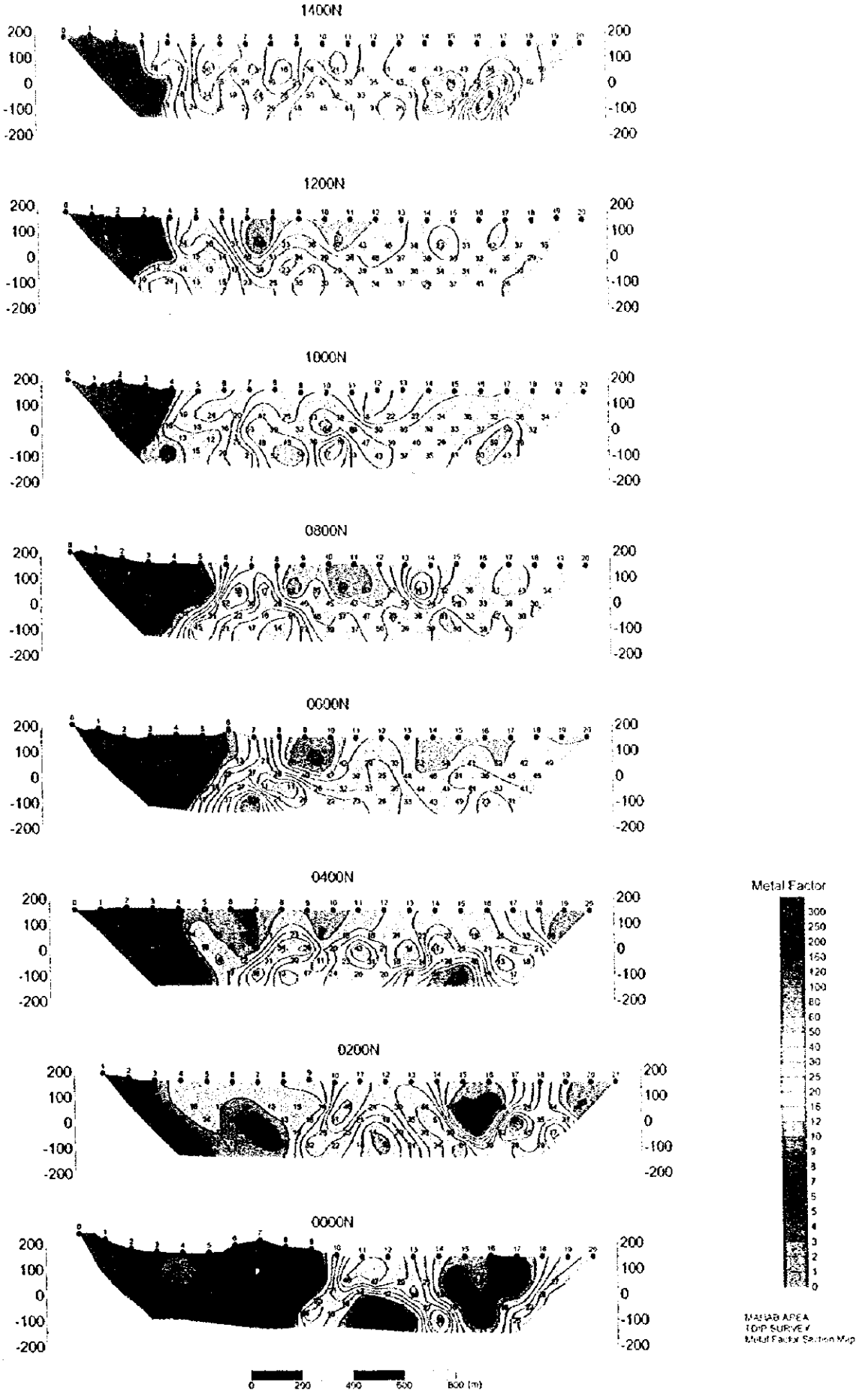

Fig. II -2-26 Metal factor pseudo-sections in Mahab area

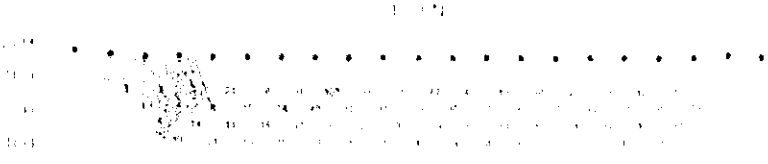

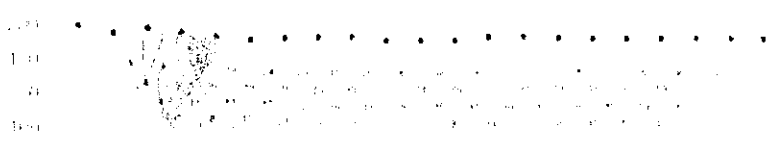

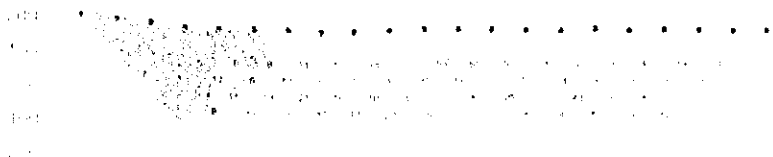

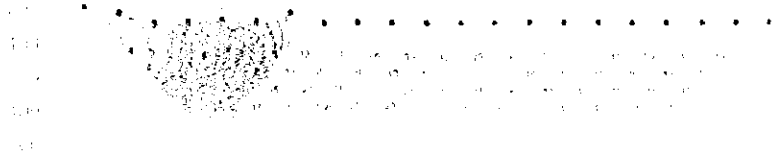

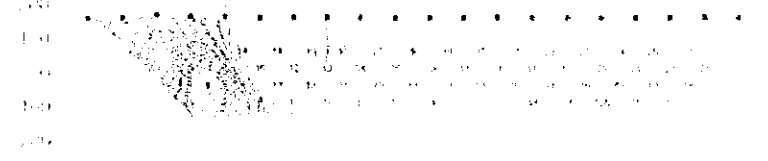

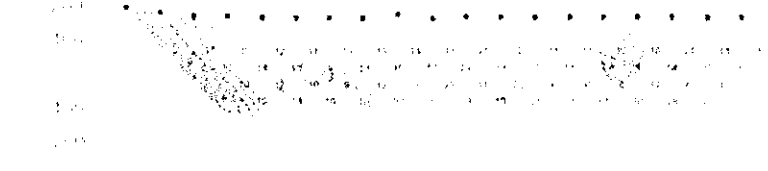

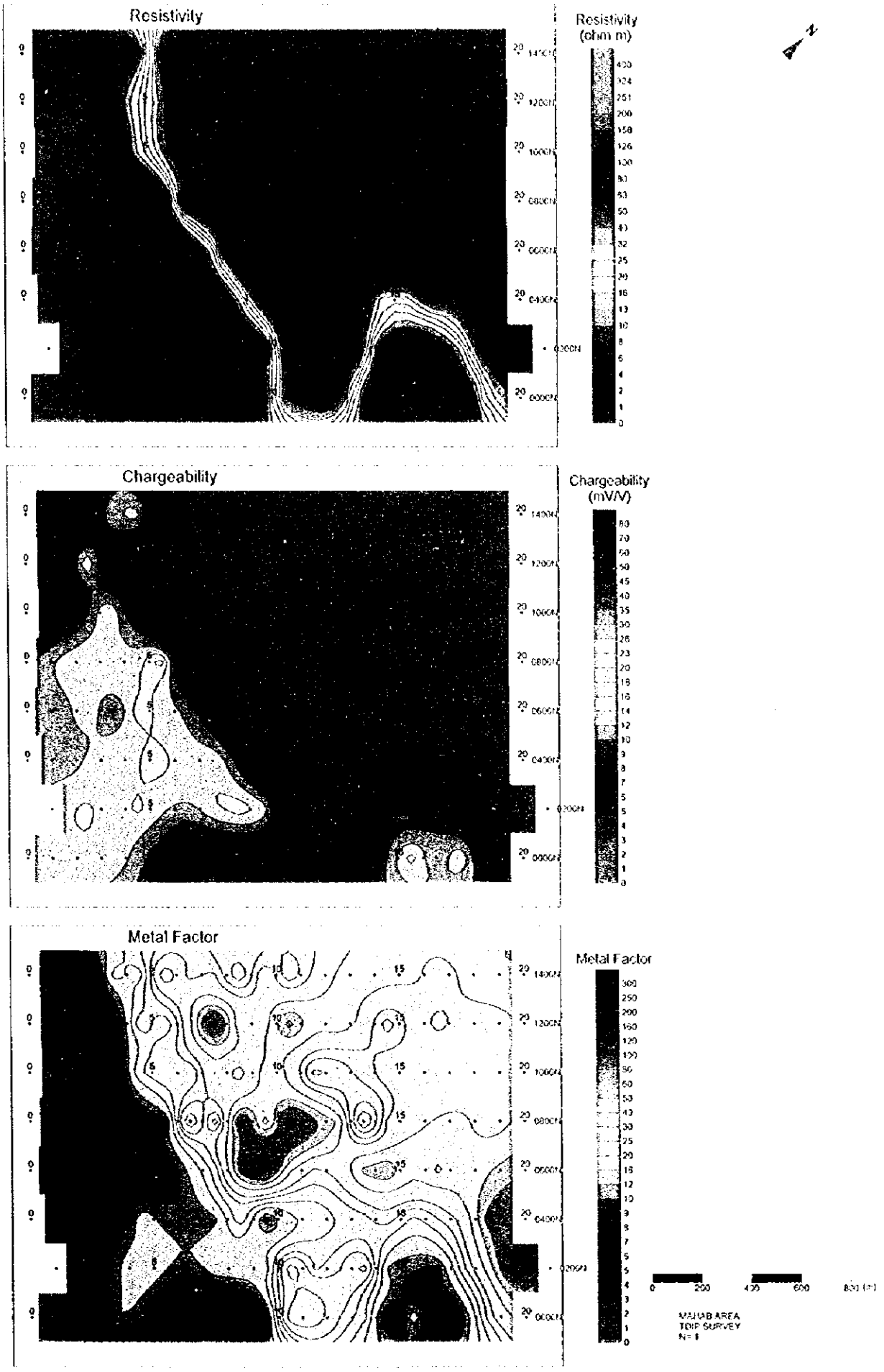

Fig. II -2-27 IP plane map of n=1 in Mahab area

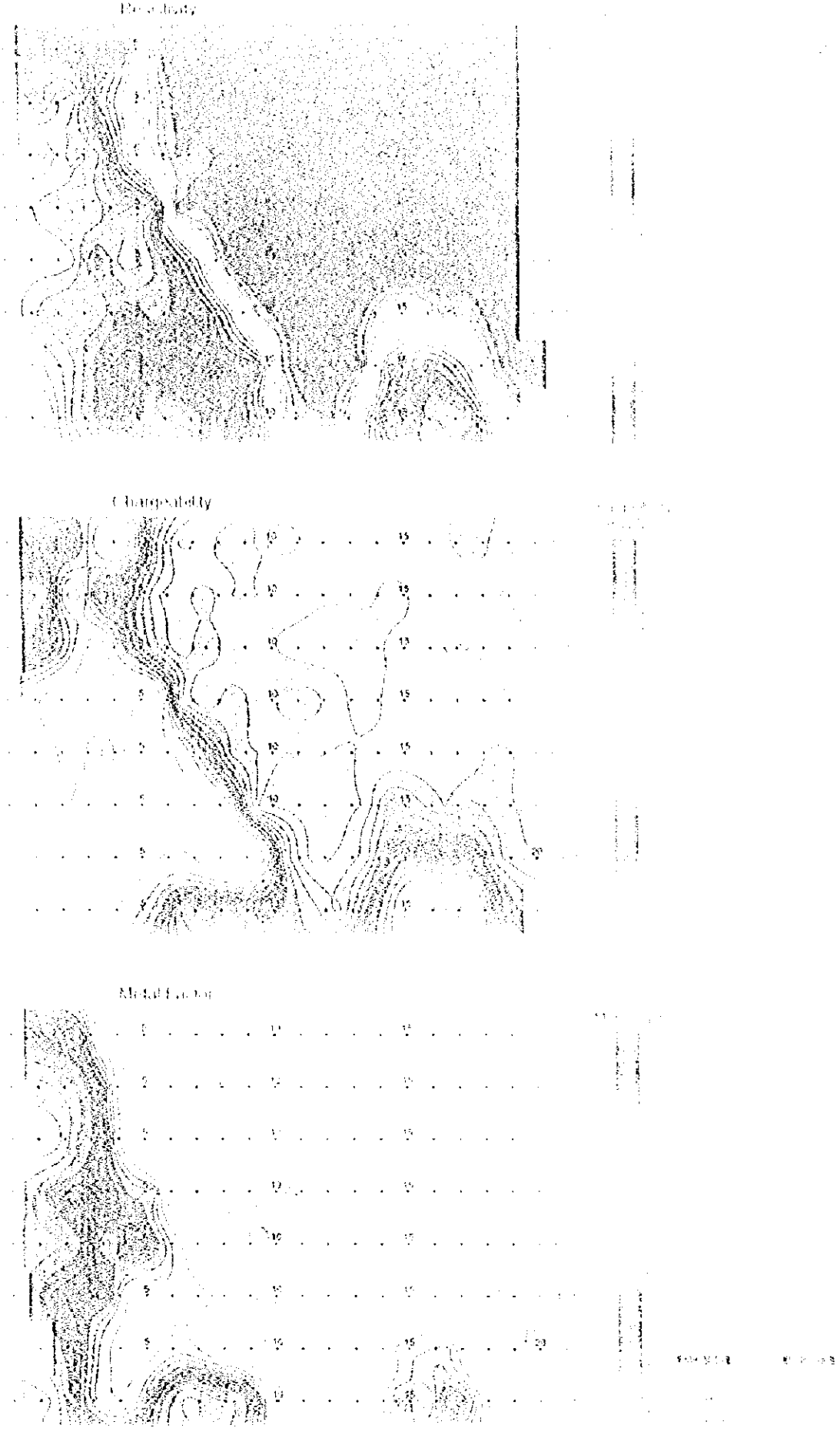

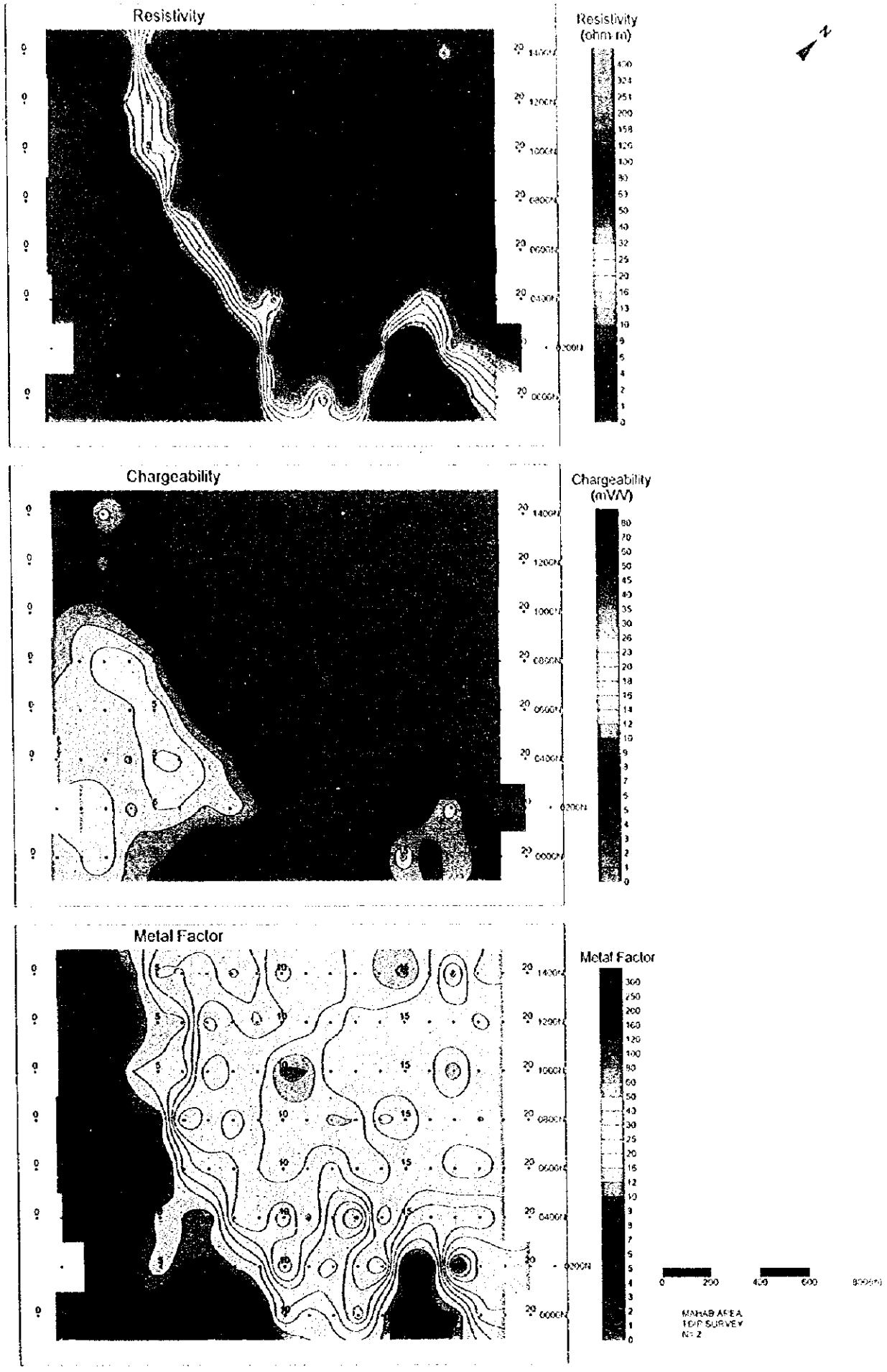

Fig. II -2-28 IP plane map of n=2 in Mahab area

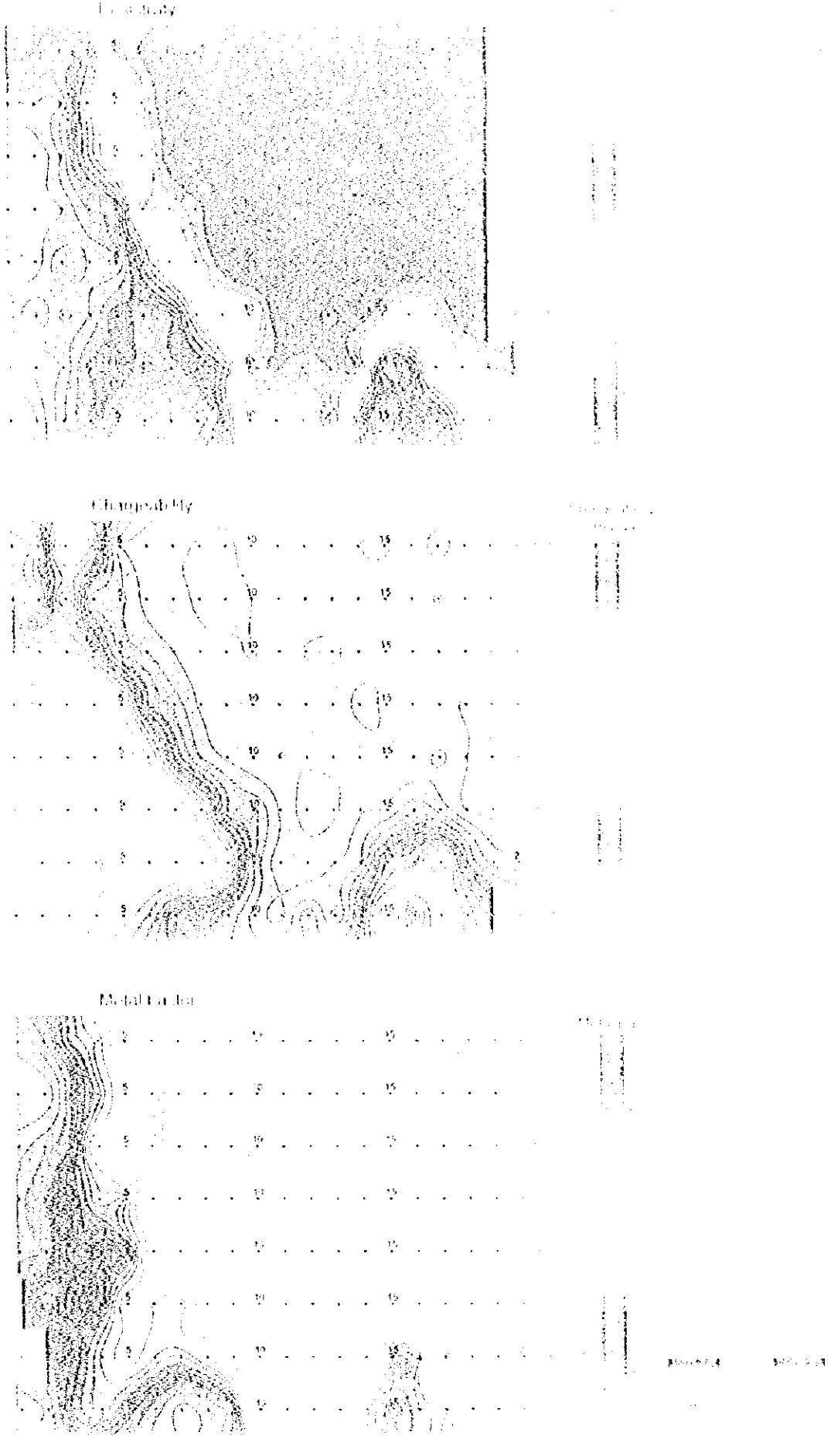

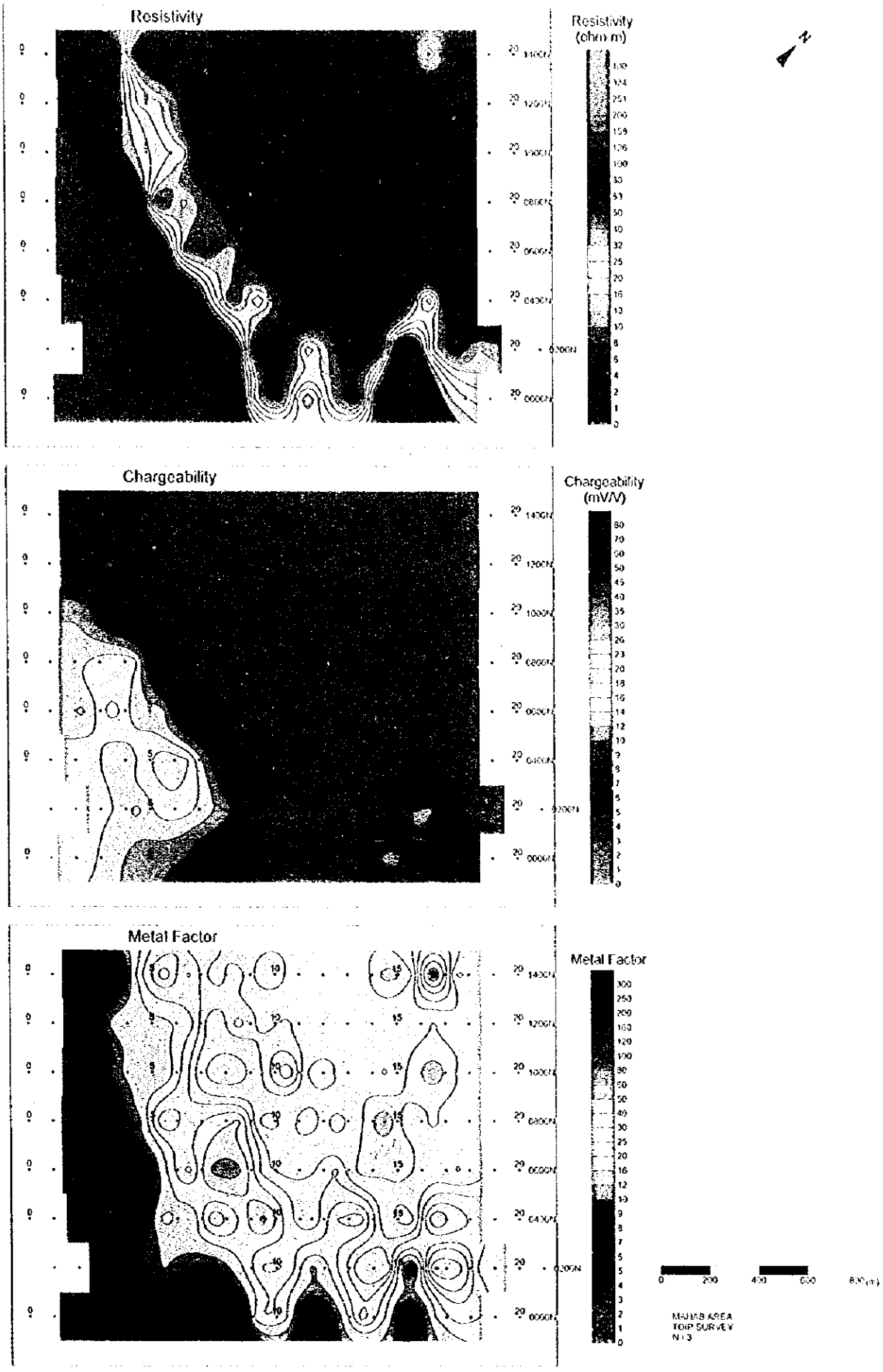

Fig. II-2-29 IP plane map of n=3 in Mahab area

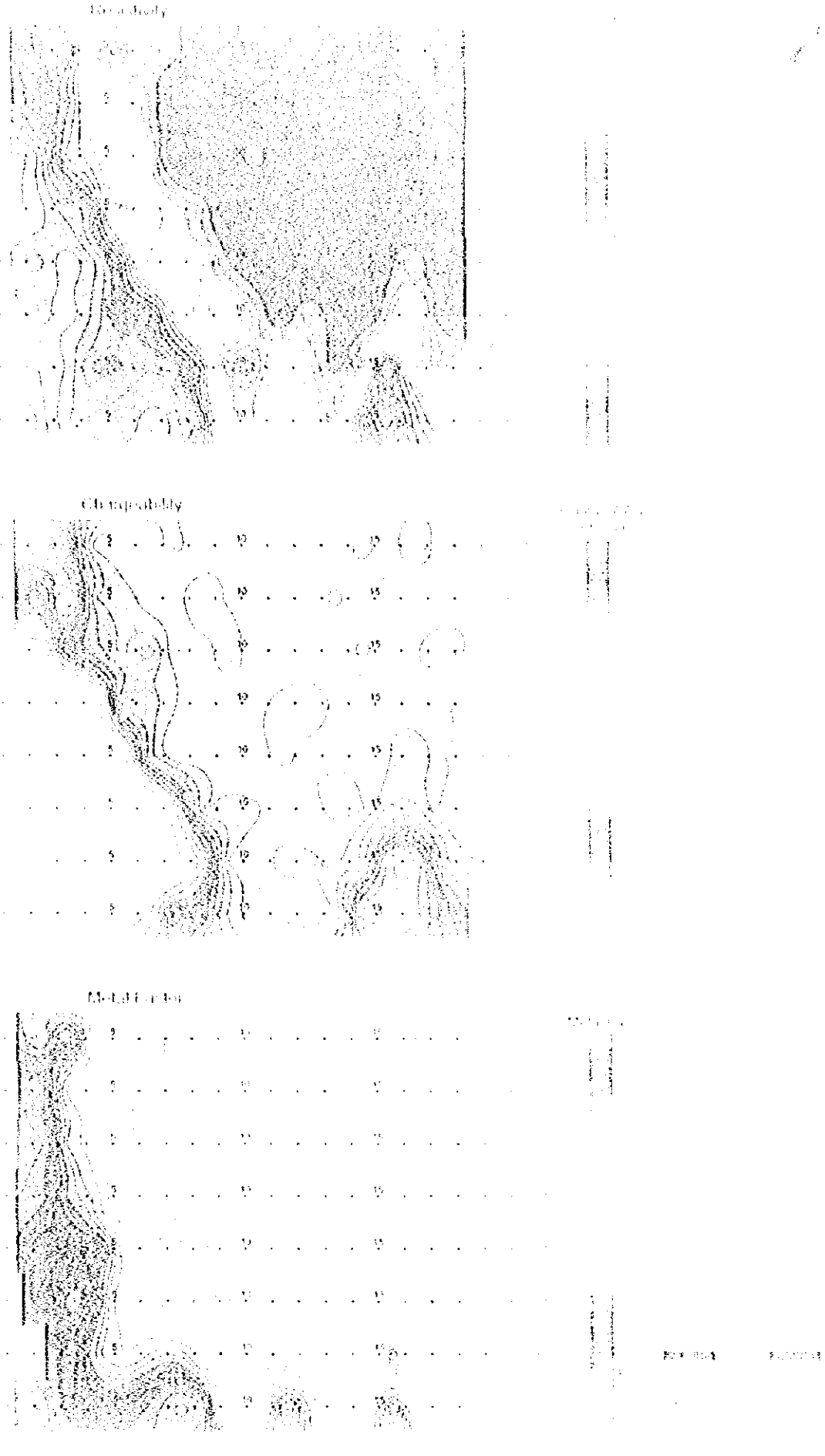

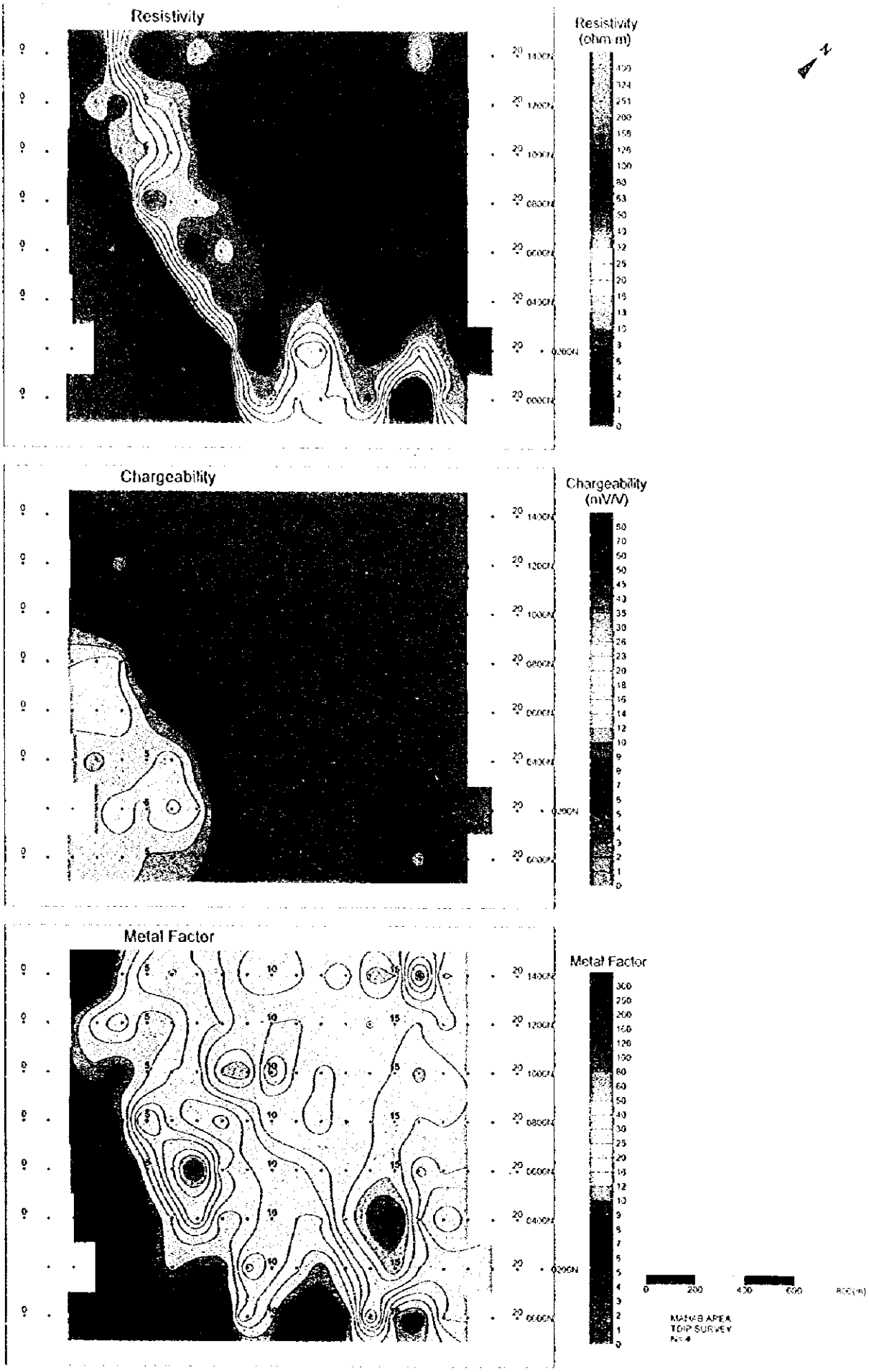

Fig. II-2-30 IP plane map of n=4 in Mahab area

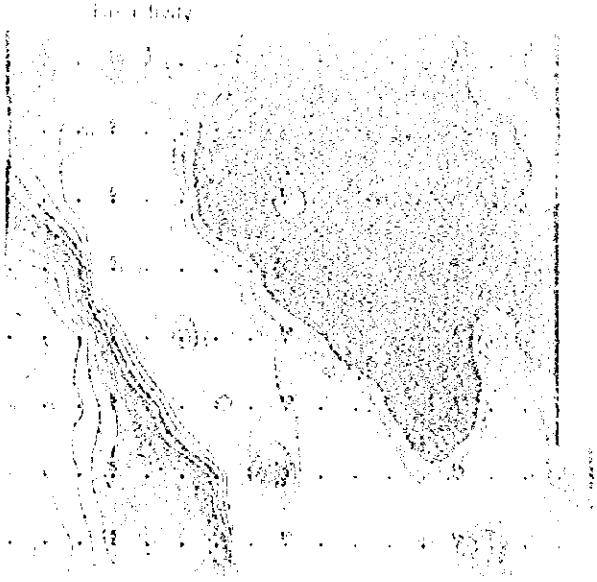

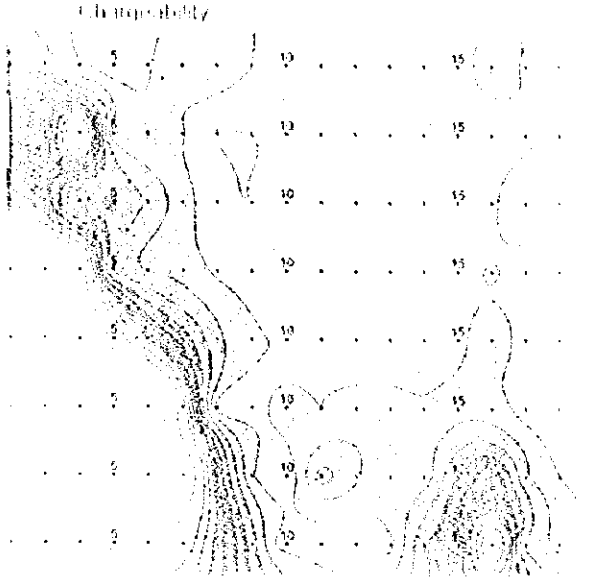

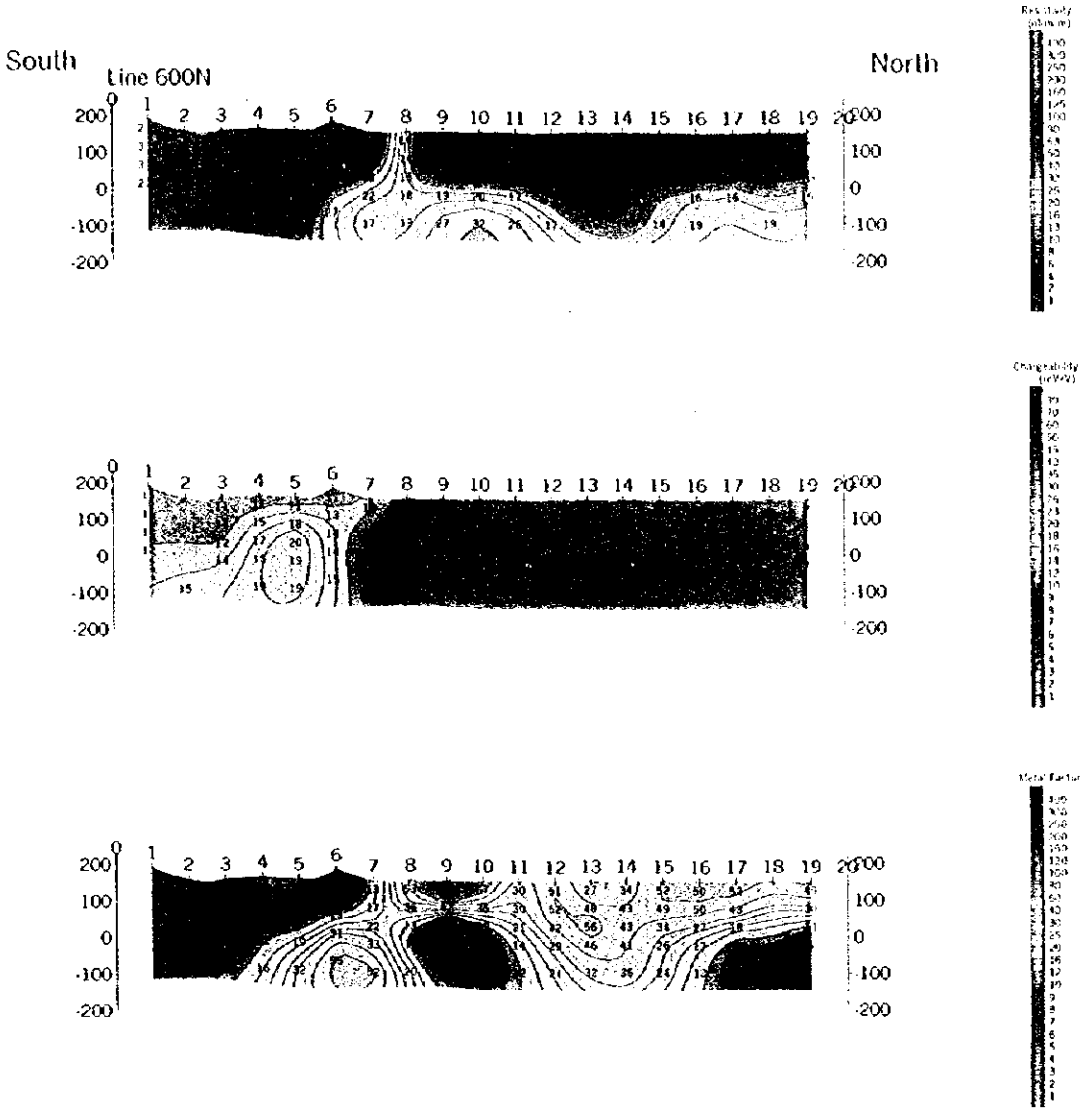

Fig. II -2-31 IP 2D model simulation on line 800N in Mahab area

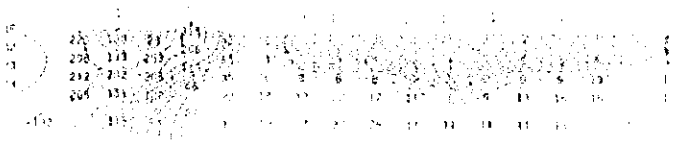

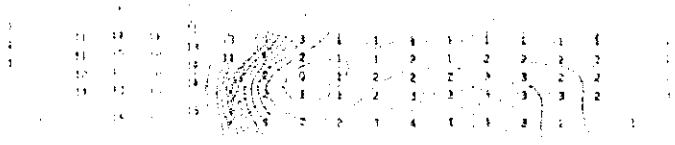

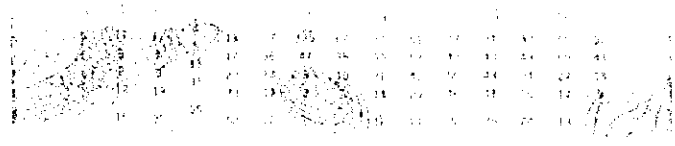

2-5-5 Hara Kilab area

(1) Lines location

During this field season, a total of 20 lines (from 000N to 3800N) were surveyed along E-W direction with a line spacing of 200m. Among these lines, 4 of them (3200N to 3800N) had a length of 3.0 km, while the remaining 16 (000N to 3000N) had a length of 2.0 km.

Fig.II-2-23 shows the location of all the IP lines surveyed in Hara Kilab.

(2) Results

The results of the TDIP survey in Hara Kilab area are presented here as pseudo sections of apparent resistivity (Fig.II-2-32(1) to Fig.II-2-32(3)), chargeability (Fig.II-2-33(1) to Fig.II-2-33(3)) and metal factor (Fig.II-2-34(1) to Fig.II-2-34(3)). Contour maps of apparent resistivity, chargeability and metal factor for N=1 to 4 are indicated respectively in Figs.II-2-35 to Fig.II-2-38.

In relation to the apparent resistivity distribution (Fig.II-2-37), a resistivity structure is seen in the north of the line 3000N along WNW-ESE direction and in the south of same line but along NNW-SSE direction. High resistivities are entirely seen to the west of the area, while low resistivities to the east. The high resistivities detected in the west part seem to be due to the effect of sheeted dikes, lower extrusives, intrusive trondhjemite, etc.

In the northeast part of the line 3200N, low resistivity values below 10 Ω-m are widely seen in a zone where Quaternary sediments are distributed. In the southeast part of the line 2800N and along NNW-SSE direction, medium to low resistivities values are distributed. Also within this part and in the vicinity of the stations Nos. 15 and 16 around the central part of the line 2200N, it is seen extended a low resistivity distribution from N=2 to 4 about 400m along N-S direction (Fig.II-2-37(2)).

In relation to the south part of the surveyed area, in the vicinities of station No.15 of line 800N, small scaled low resistivity distribution at N=3 to 4 are recognized trending NNW-SSE direction and continued up to the line 1200N (Fig.II-2-37 and Fig.II-2-32(1)). In this zone, the surroundings of the boundary between VI-1 and VI-2 are seen intruded by trondhjemite.

With reference to chargeability, it presents almost the same pattern as the apparent resistivity distribution, indicating high chargeability in the west part and low chargeability in the east part (Fig. II-2-37). In reference to the lines 2600N to 3000N, the west part presents a high chargeability distributed eastward in a concave pattern. In relation to the east part and within a zone of low chargeabilities, a high chargeability zone of trending N-S is recognized in the vicinity of the stations Nos.16 and 17 of the line 2000N. Since this zone coincides with a low resistivity distribution, there exists the possibility of the existence of intense mineralization. A high chargeability zone of above 10mV/V is recognized (Fig. II-2-33(1)) around the south of the stations Nos. 20 to 22 of the line 800N, however high resistivity values are seen distributed in the zone.

Concerning the metal factor, the east part of the lines 1600N to 2800N shows an extended zone of relatively high values. Within this zone, a N-S trending anomaly exists as a center in the vicinity of the

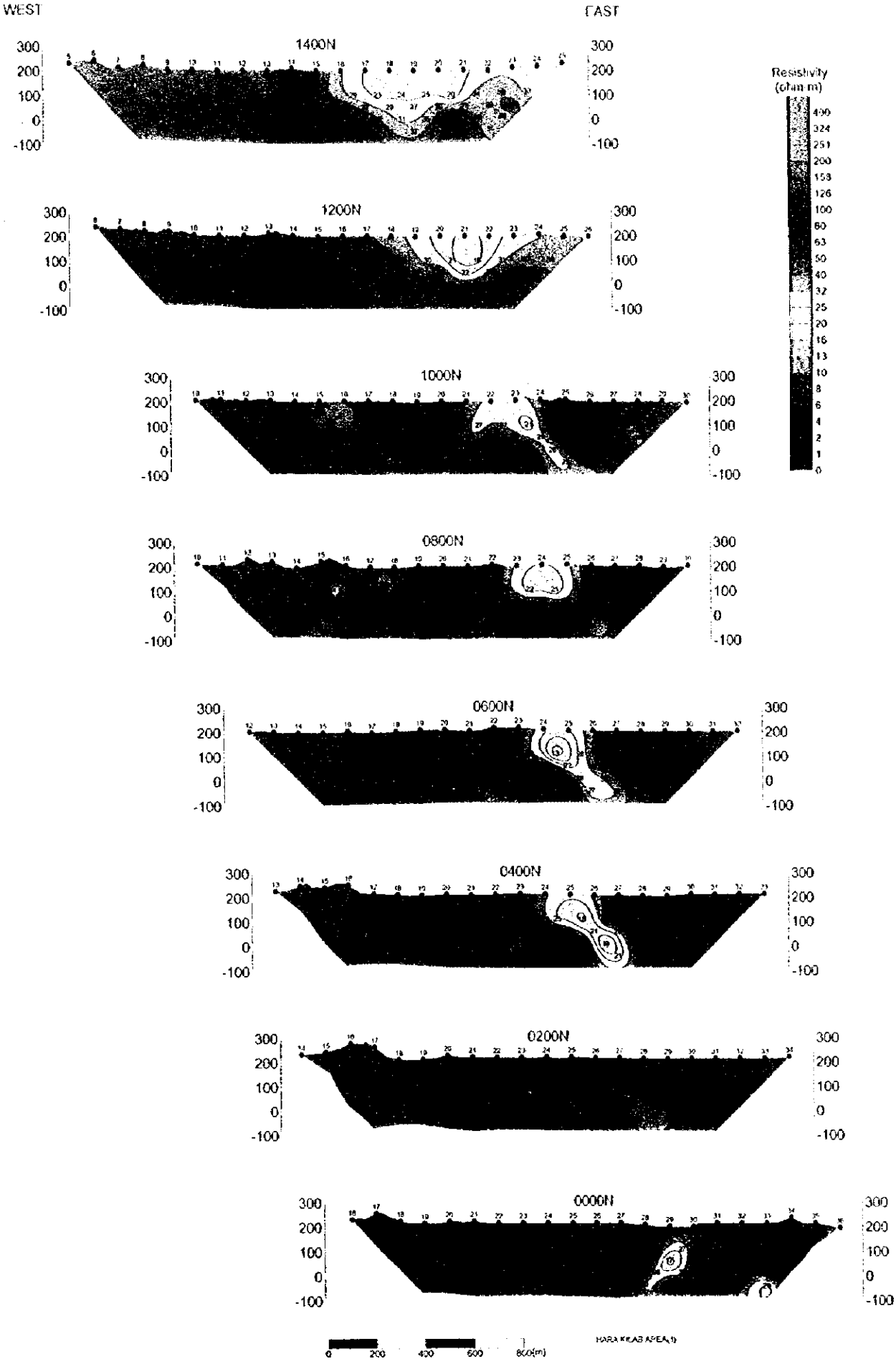

Fig. II-2-32(1) Apparent resistivity pseudo-sections in Hara Kilab area

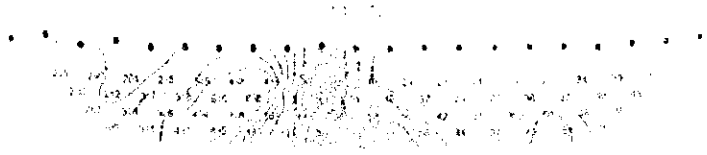

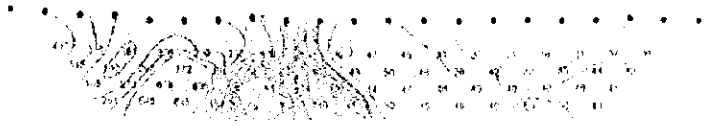

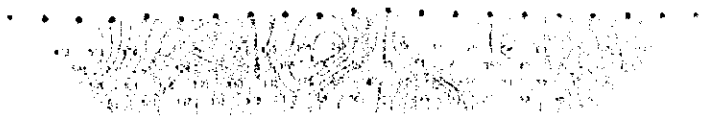

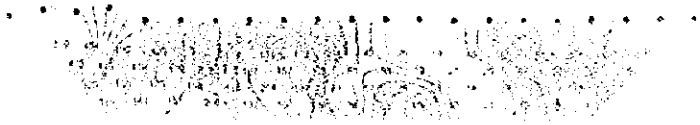

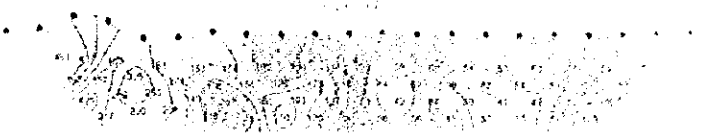

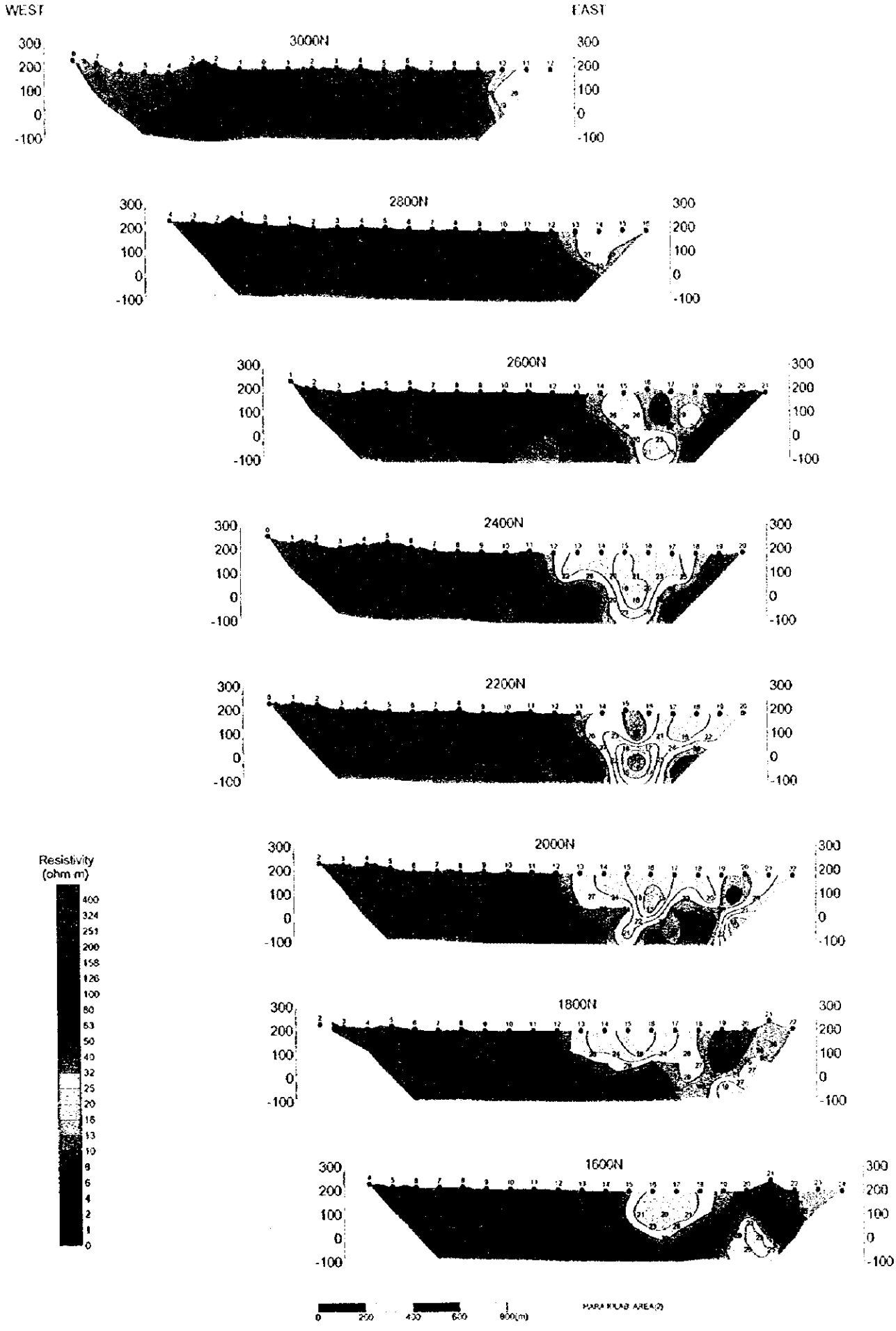

Fig. II -2-32(2) Apparent resistivity pseudo-sections in Hara Kilab area

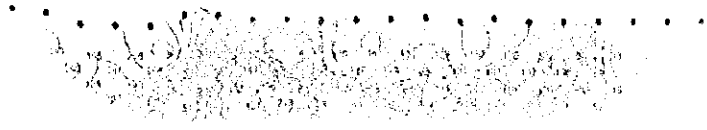

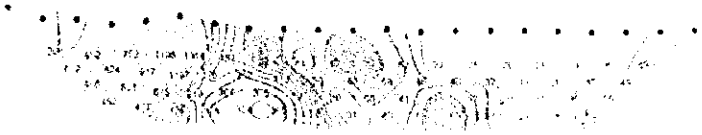

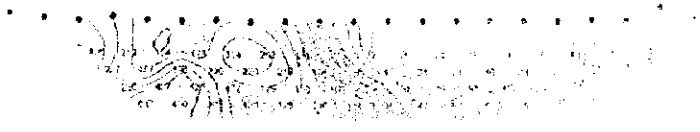

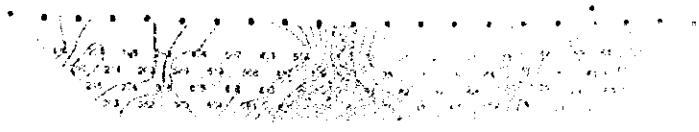

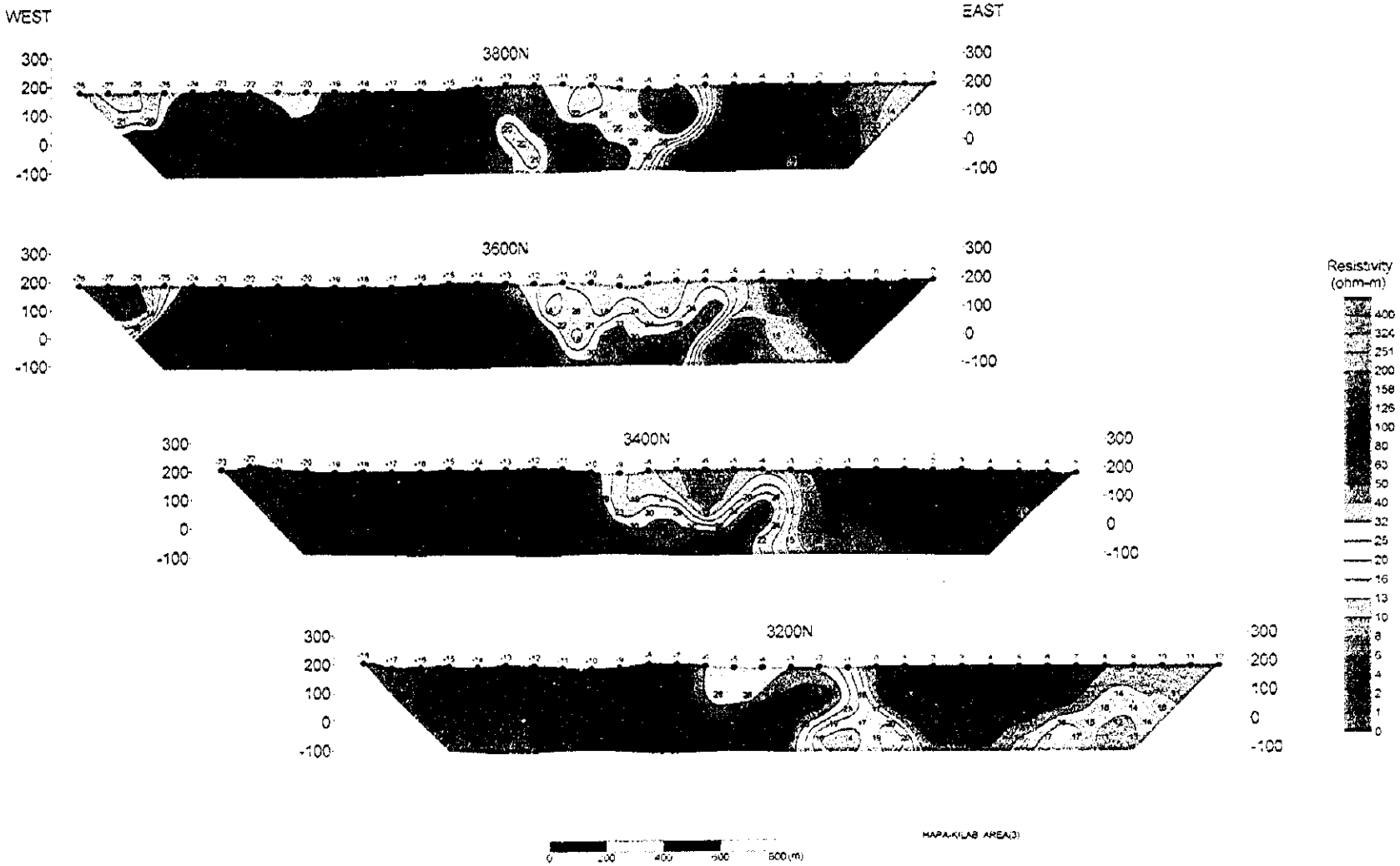

Fig. II-2-32(3) Apparent resistivity pseudo-sections in Hara Kilab area

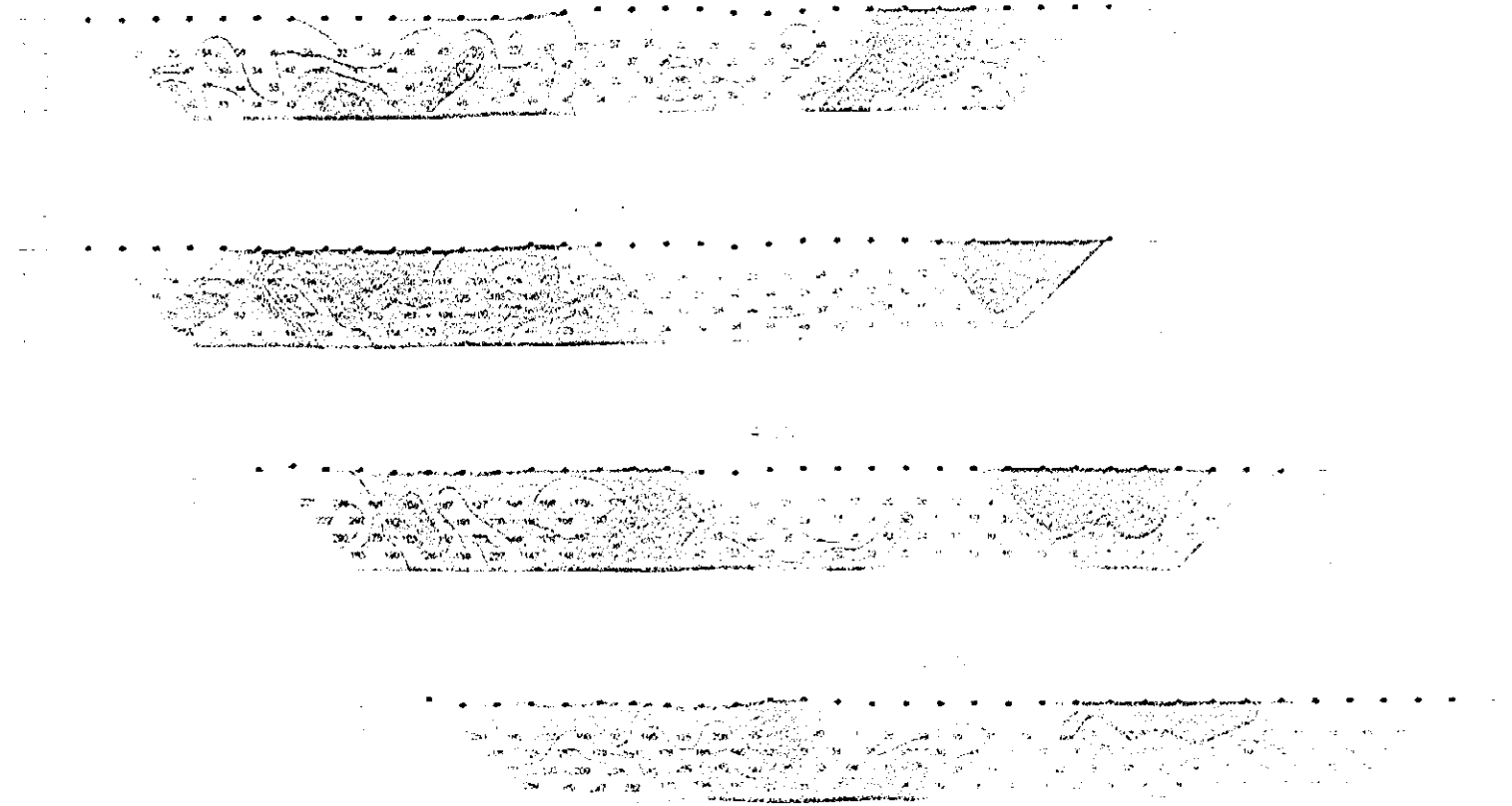

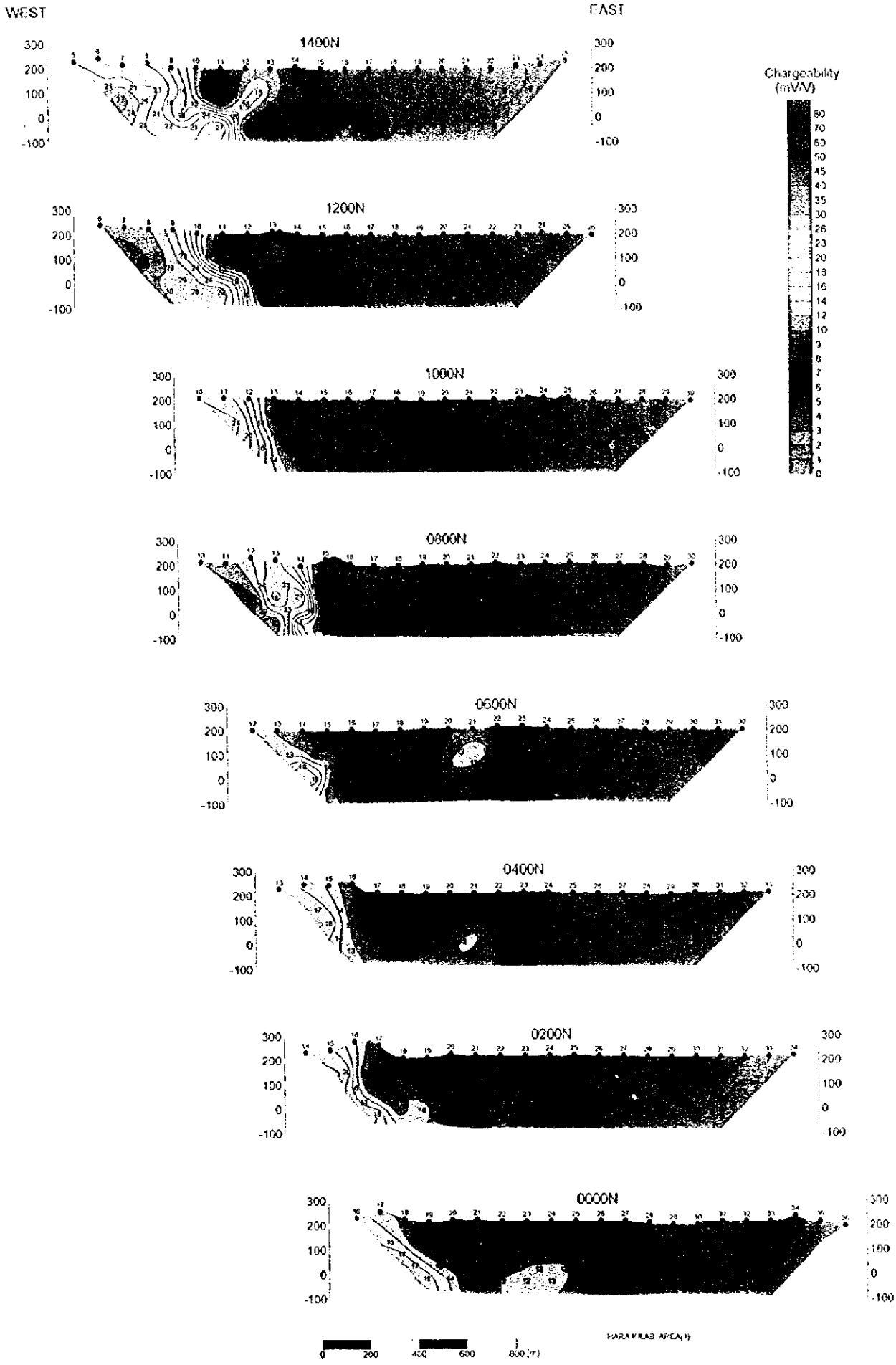

Fig. II -2-33(1) Chargeability pseudo-sections in Hara Kilab area

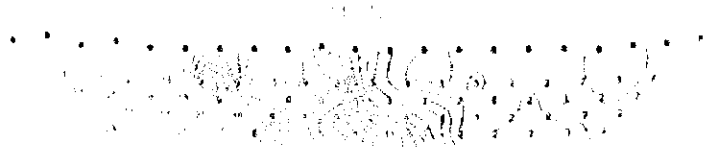

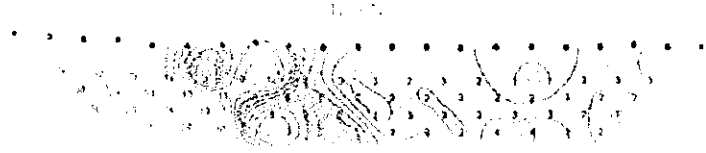

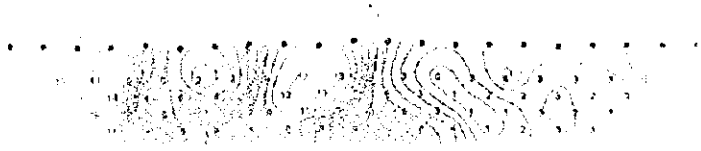

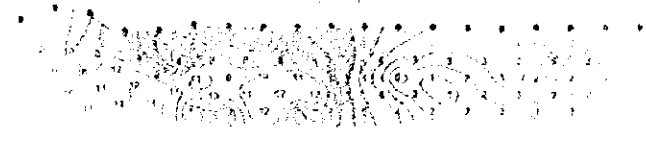

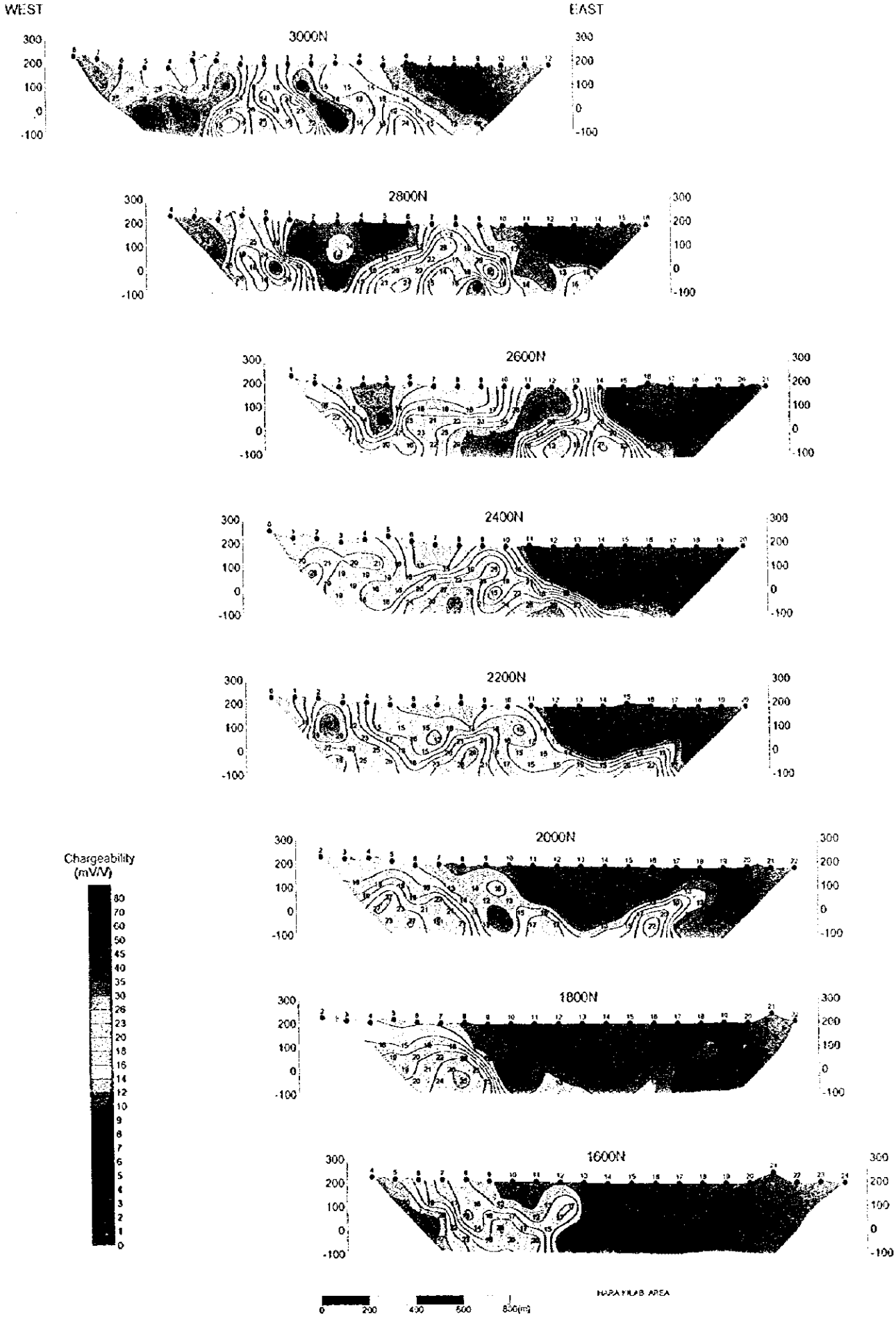

Fig. II-2-33(2) Chargeability pseudo-sections in Hara Kilab area

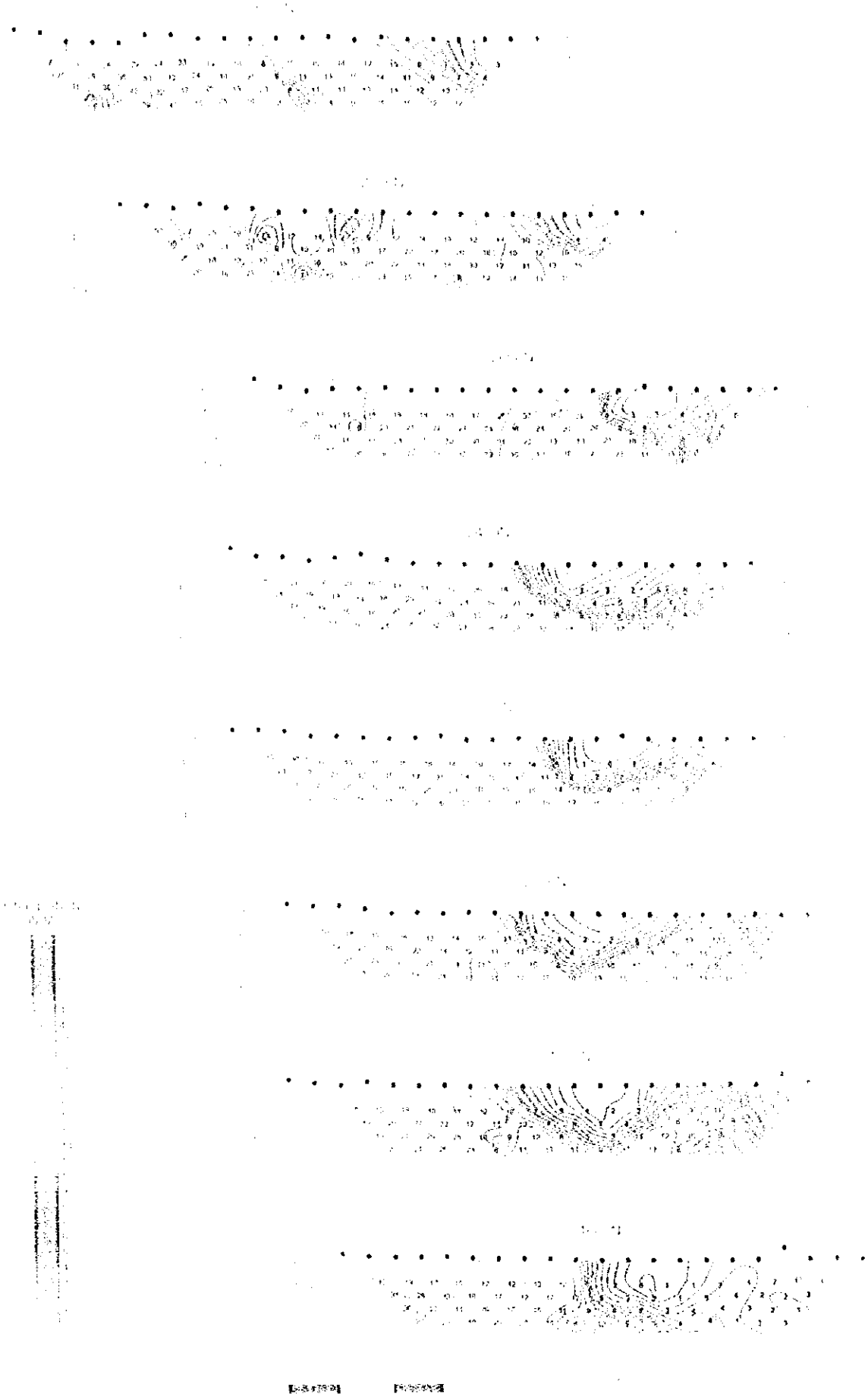

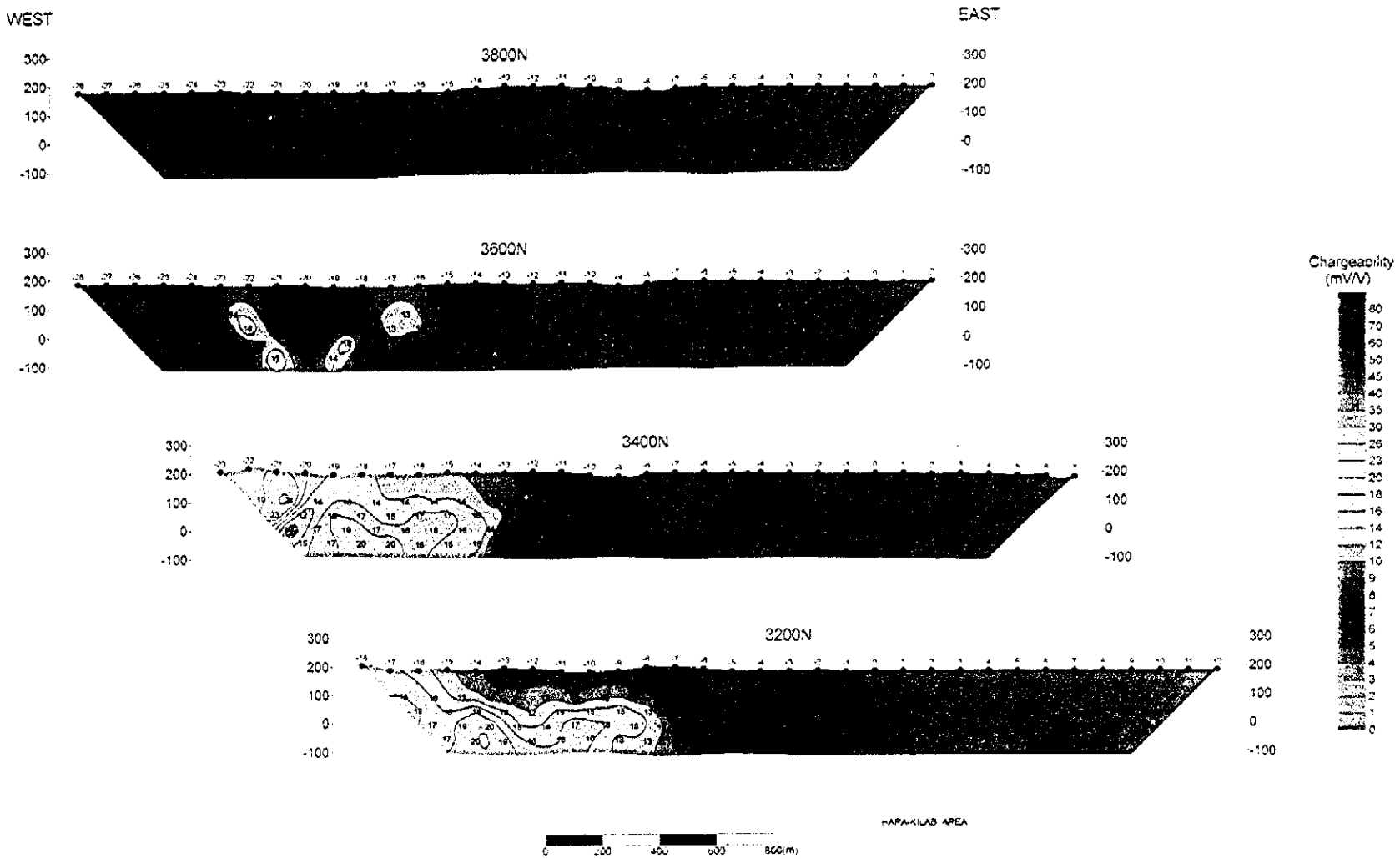

Fig. II-2-33(3) Chargeability pseudo-sections in Hara Kilab area

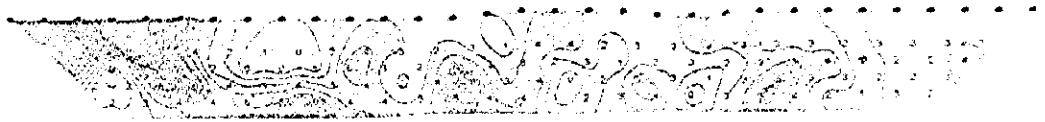

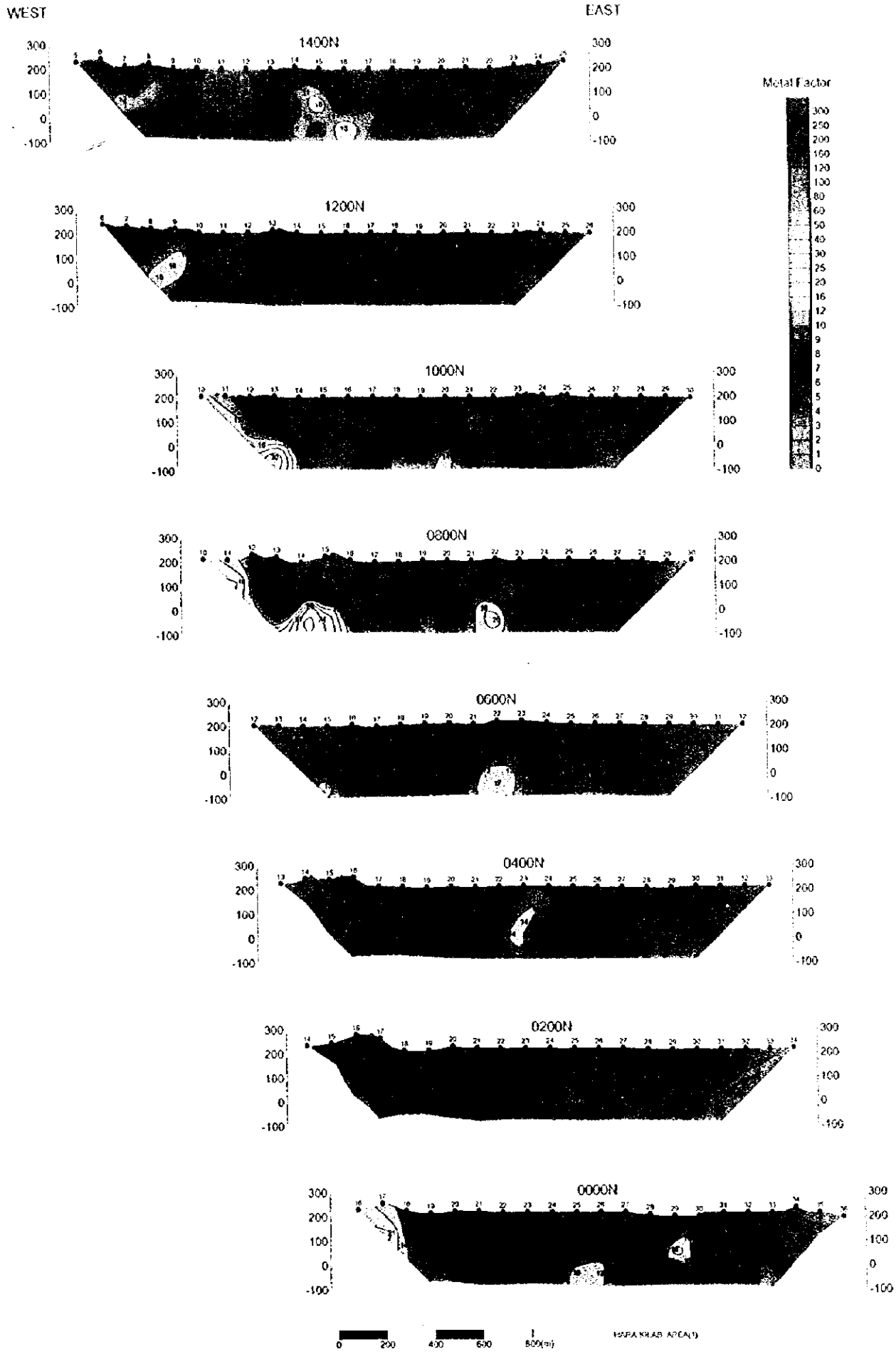

Fig. II-2-34(1) Metal factor pseudo-sections in Hara Kilab area

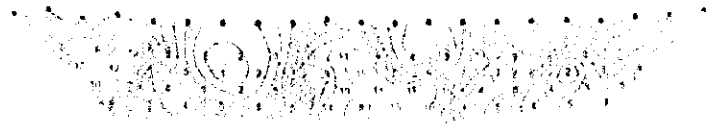

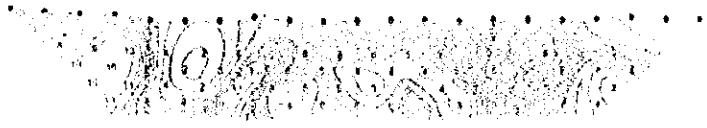

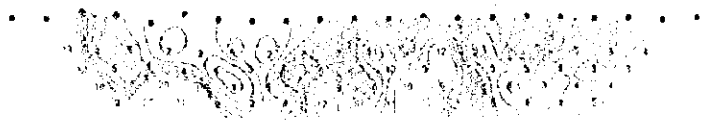

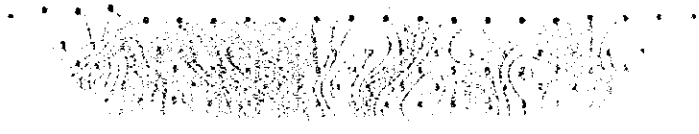

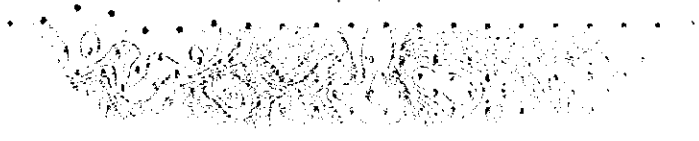

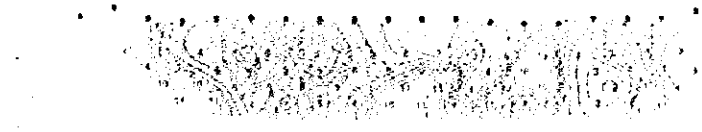

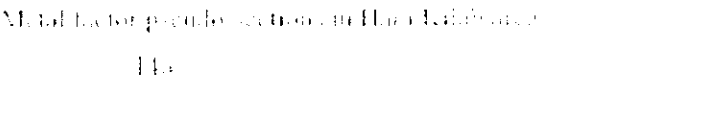

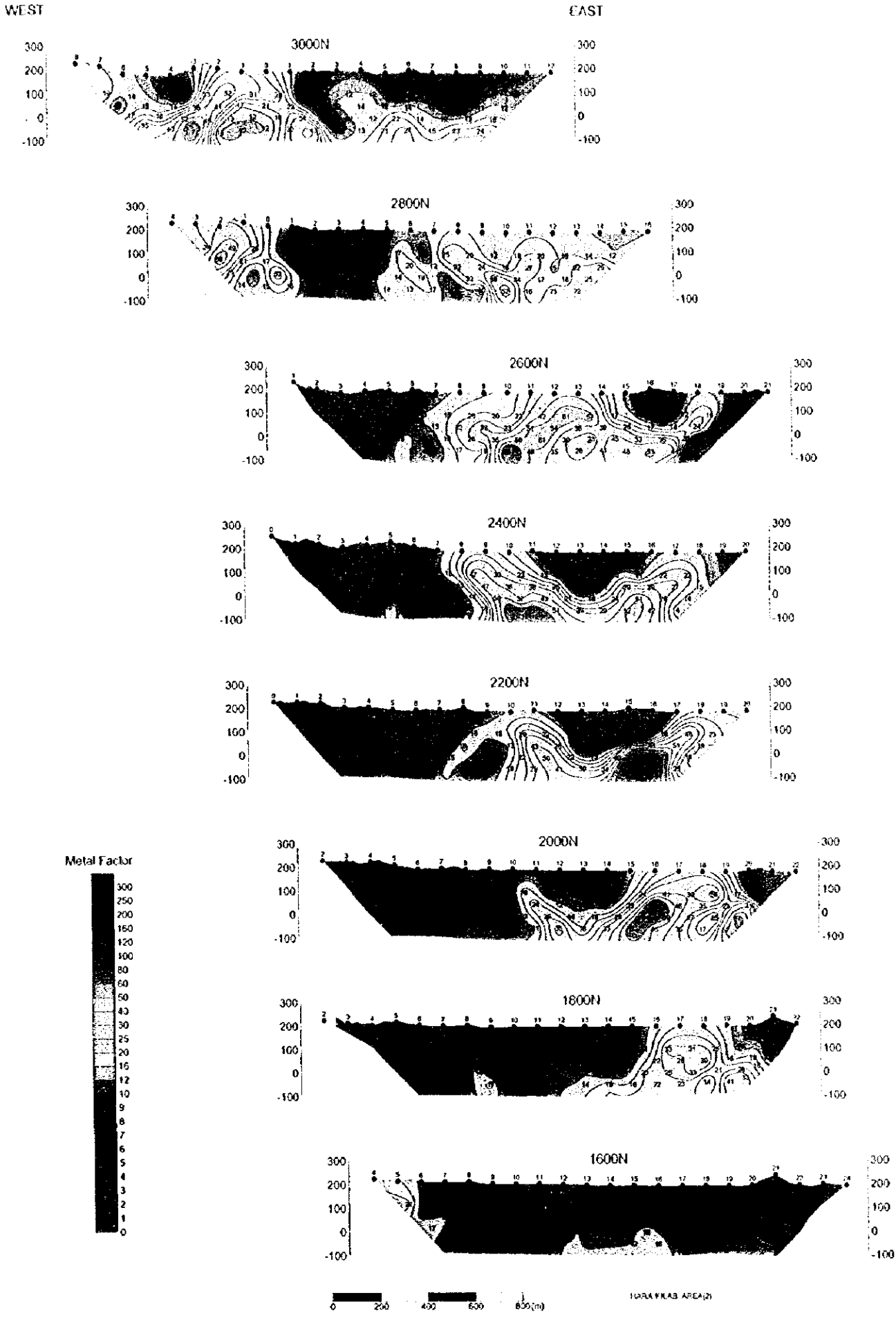

Fig. II -2-34(2) Metal factor pseudo-sections in Hara Kilab area

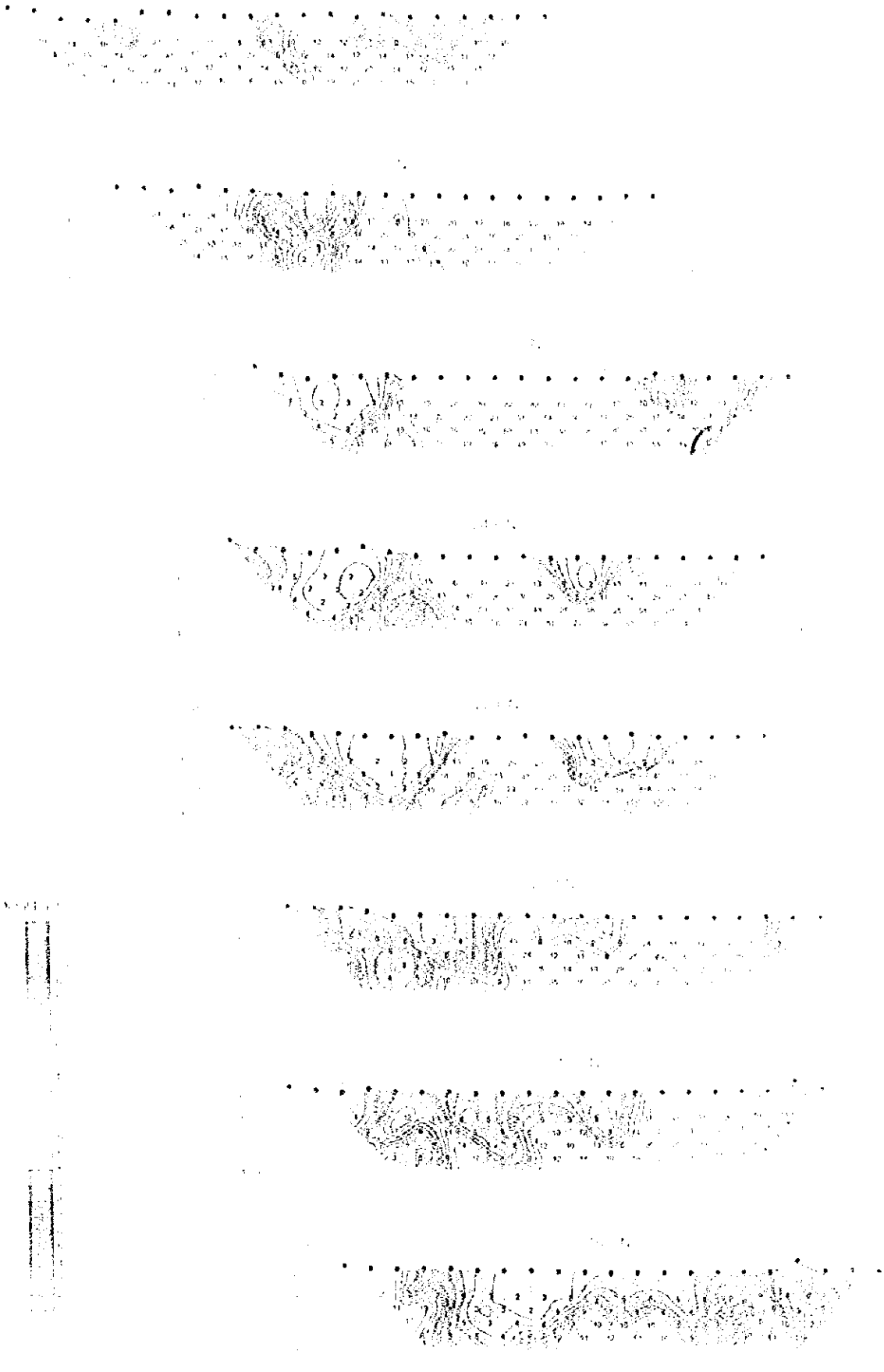

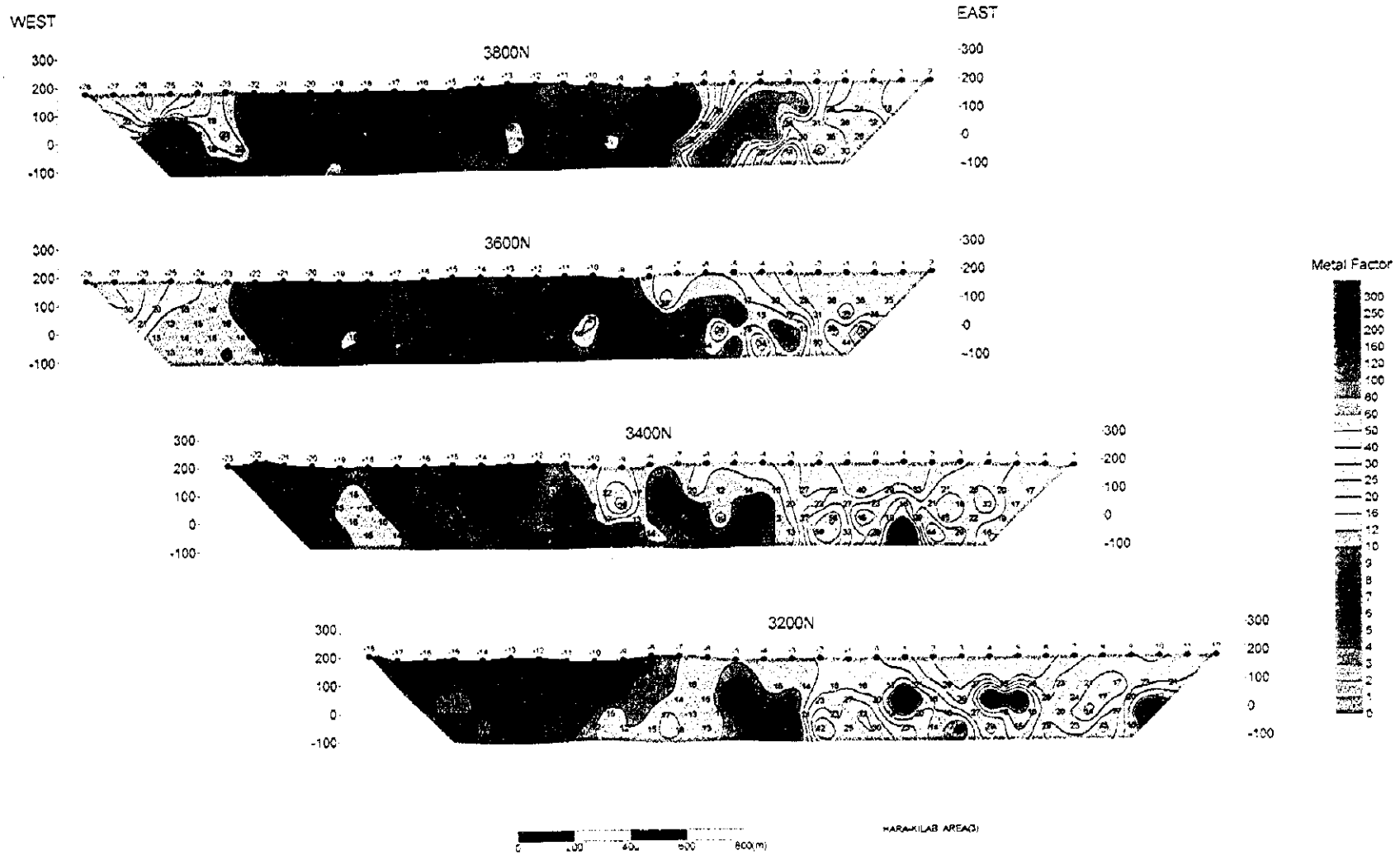

Fig. II-2-34(3) Metal factor pseudo-sections in Hara Kilab area

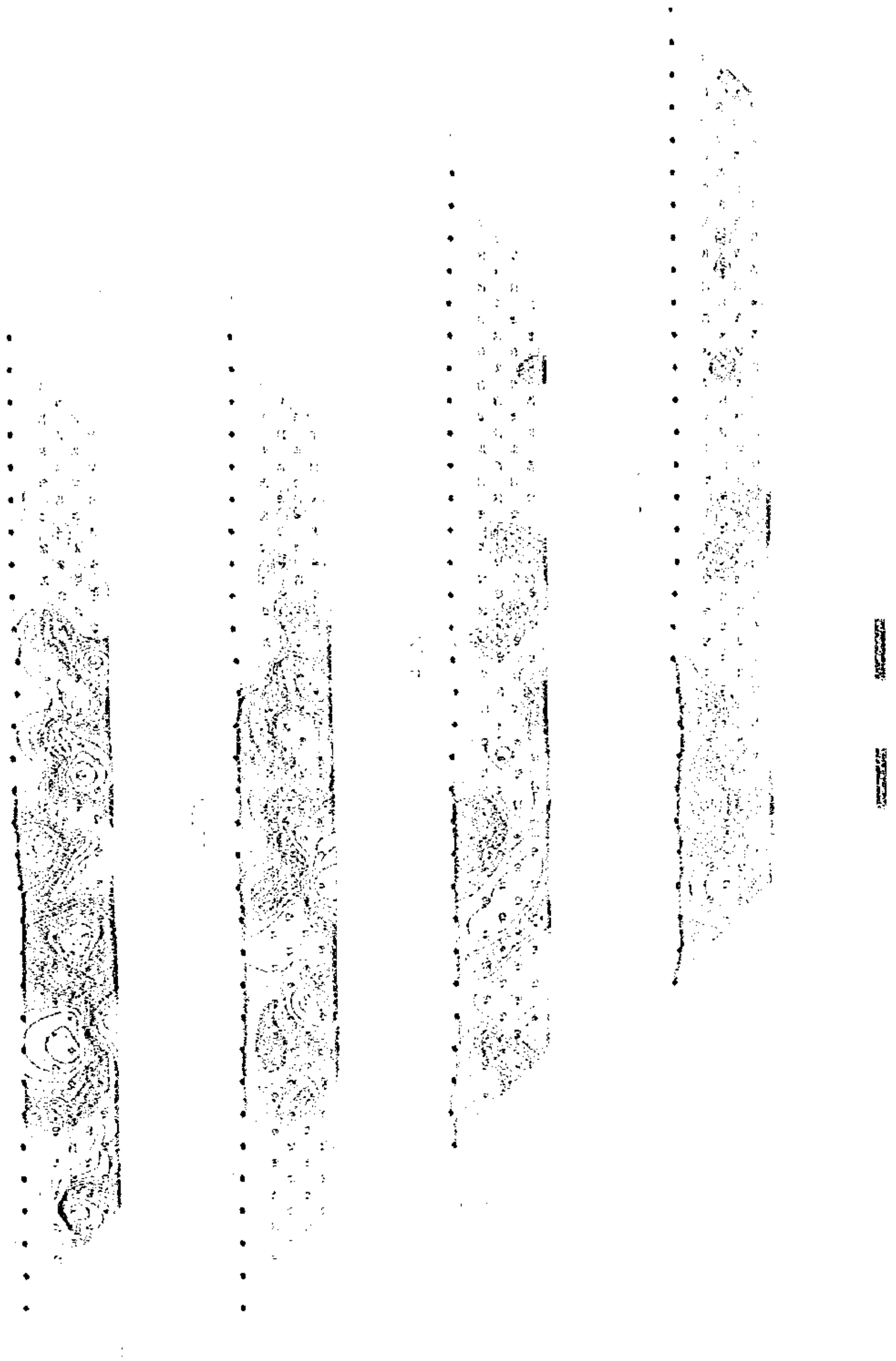

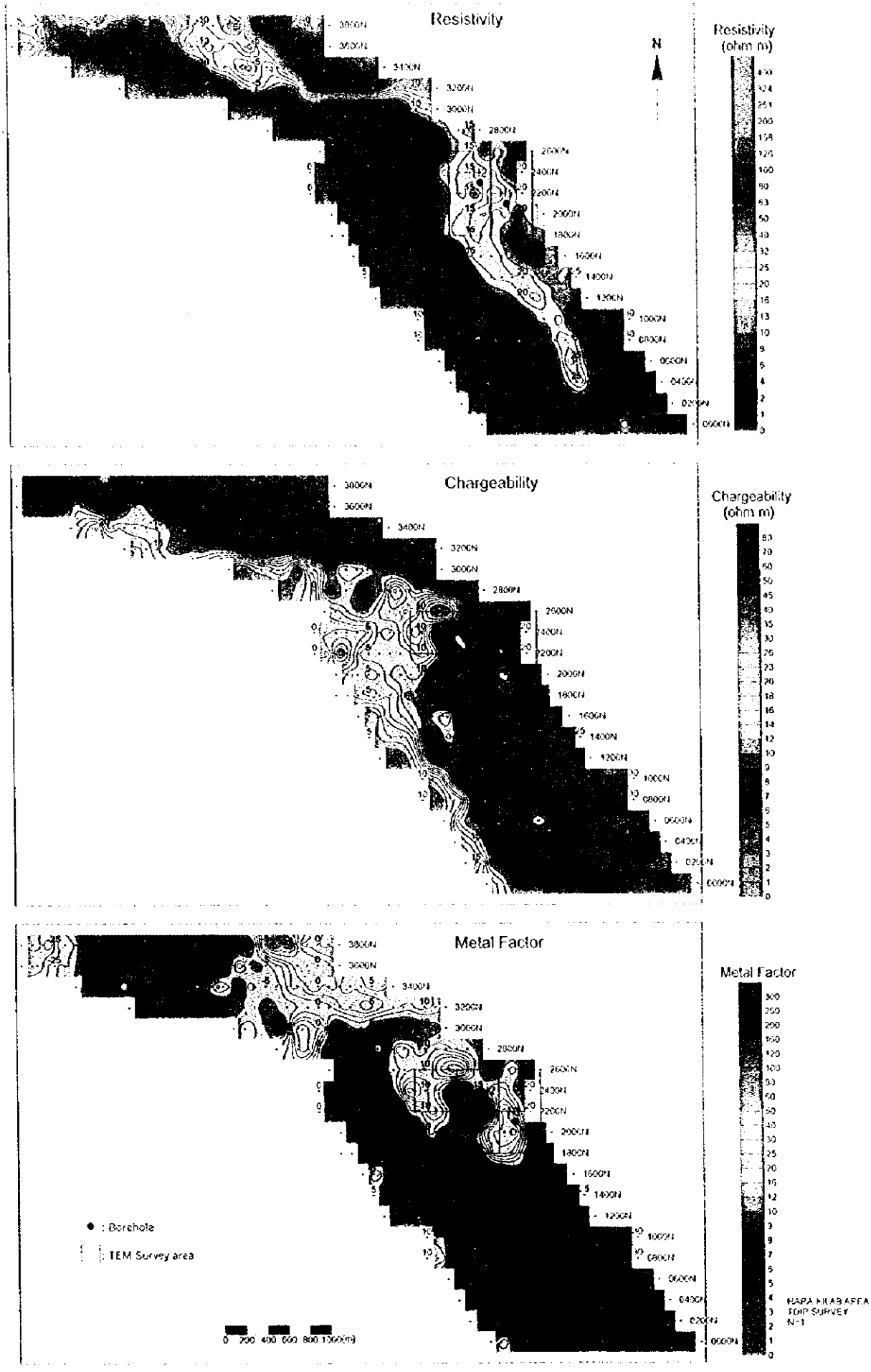

Fig. II-2-35 IP plane map of n=1 in Hara Kilab area

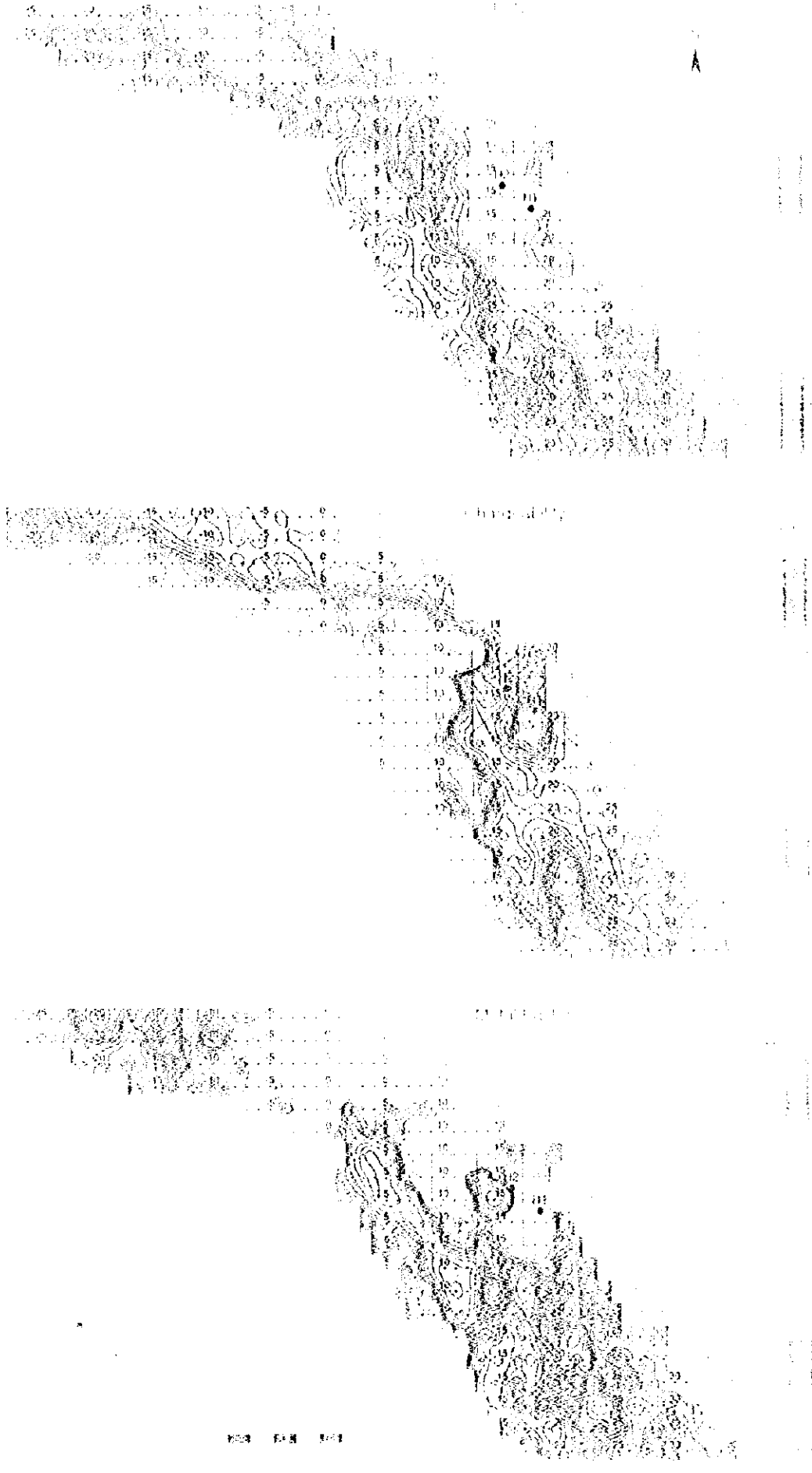

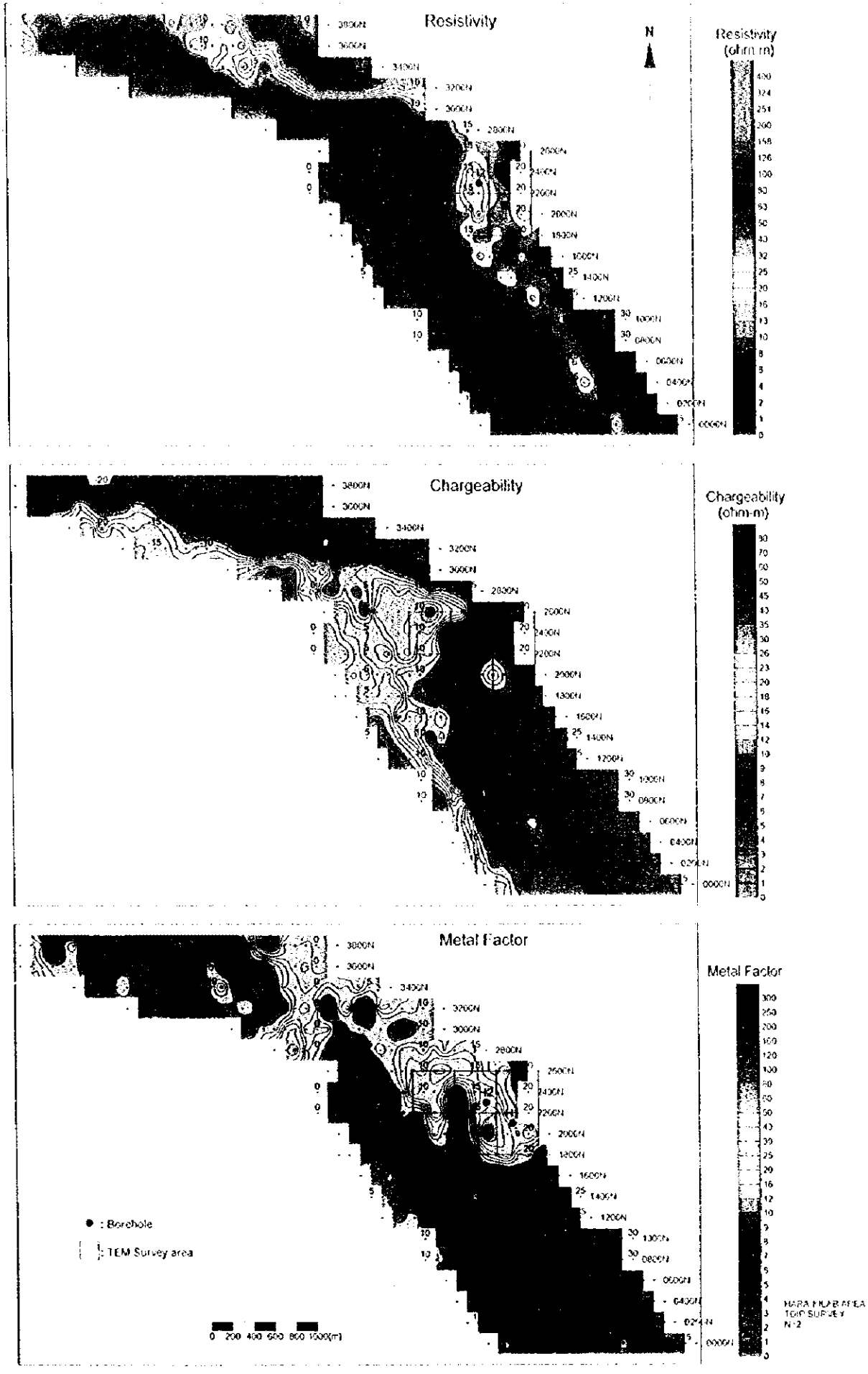

Fig. II-2-36 IP plane map of n=2 in Hara Kilab area

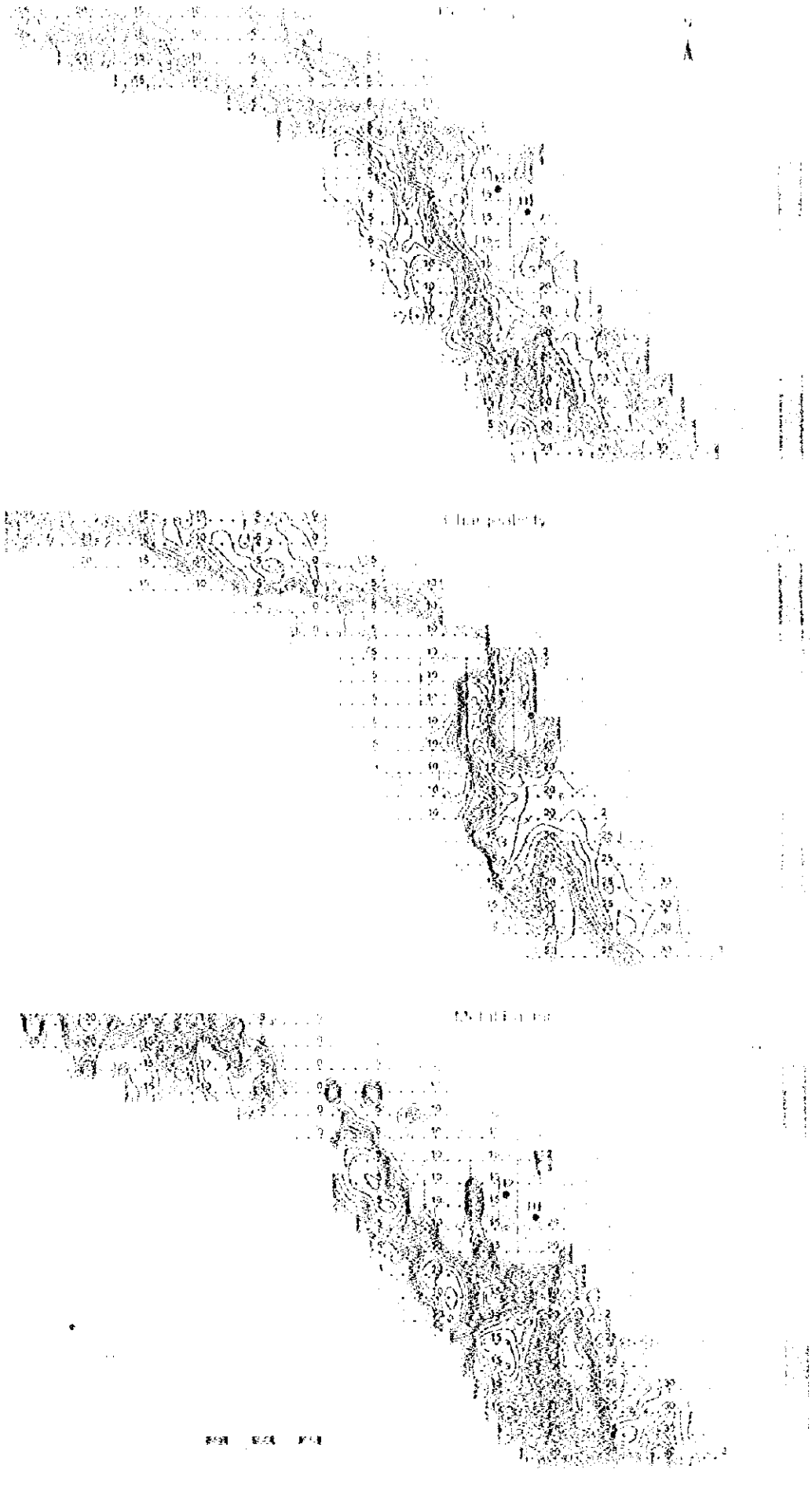

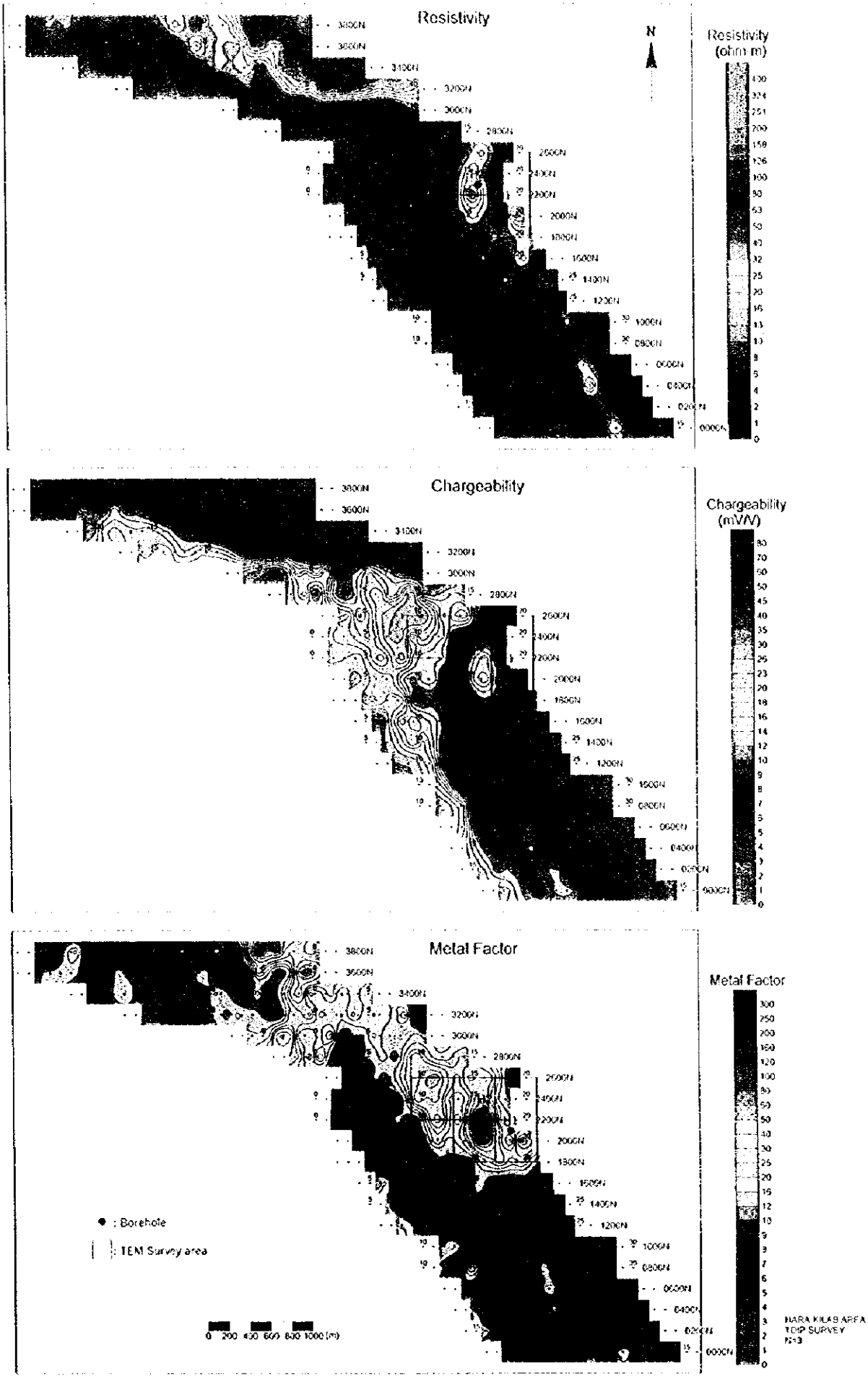

Fig. II-2-37 IP plane map of n=3 in Hara Kilab area

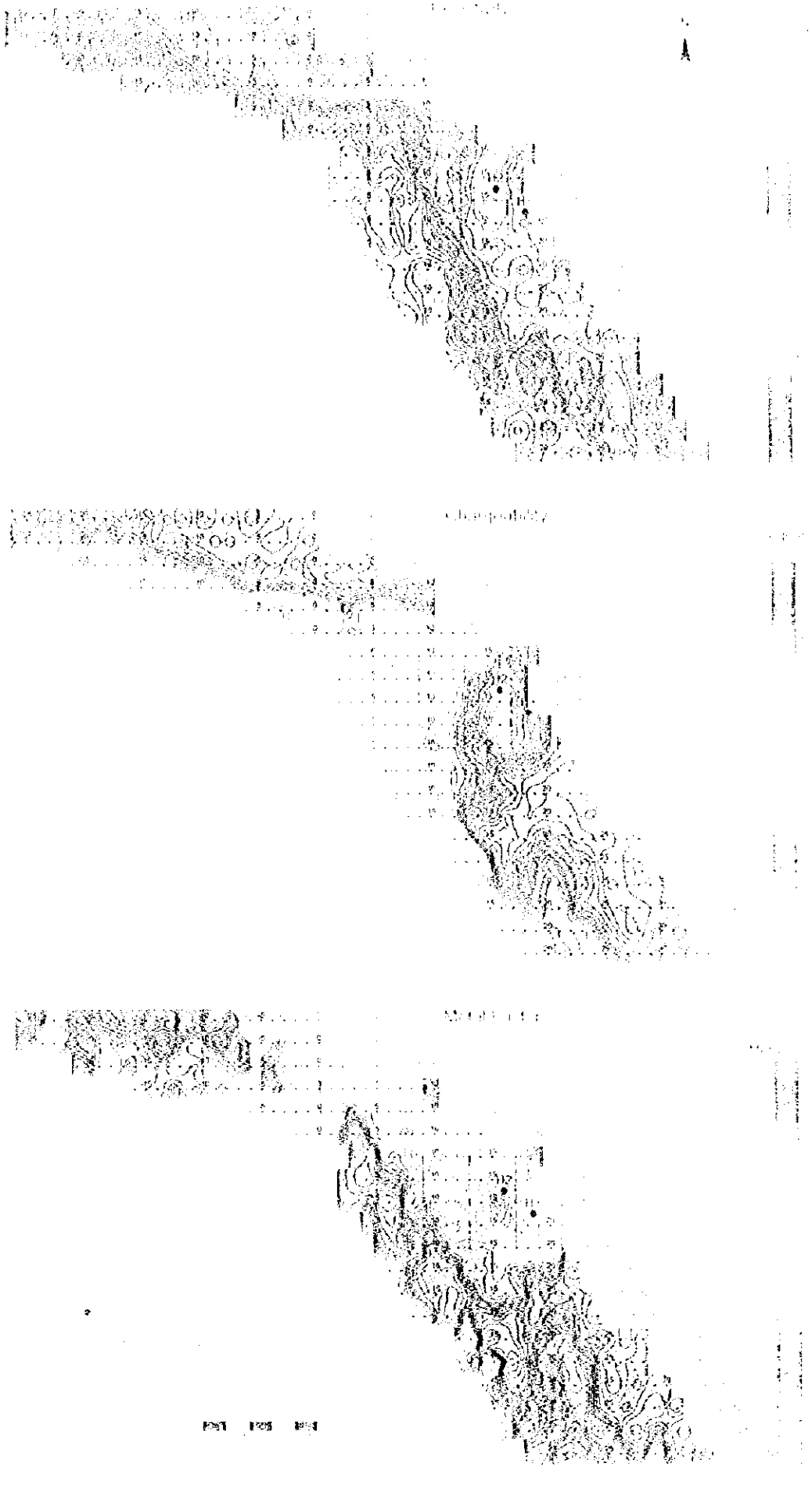

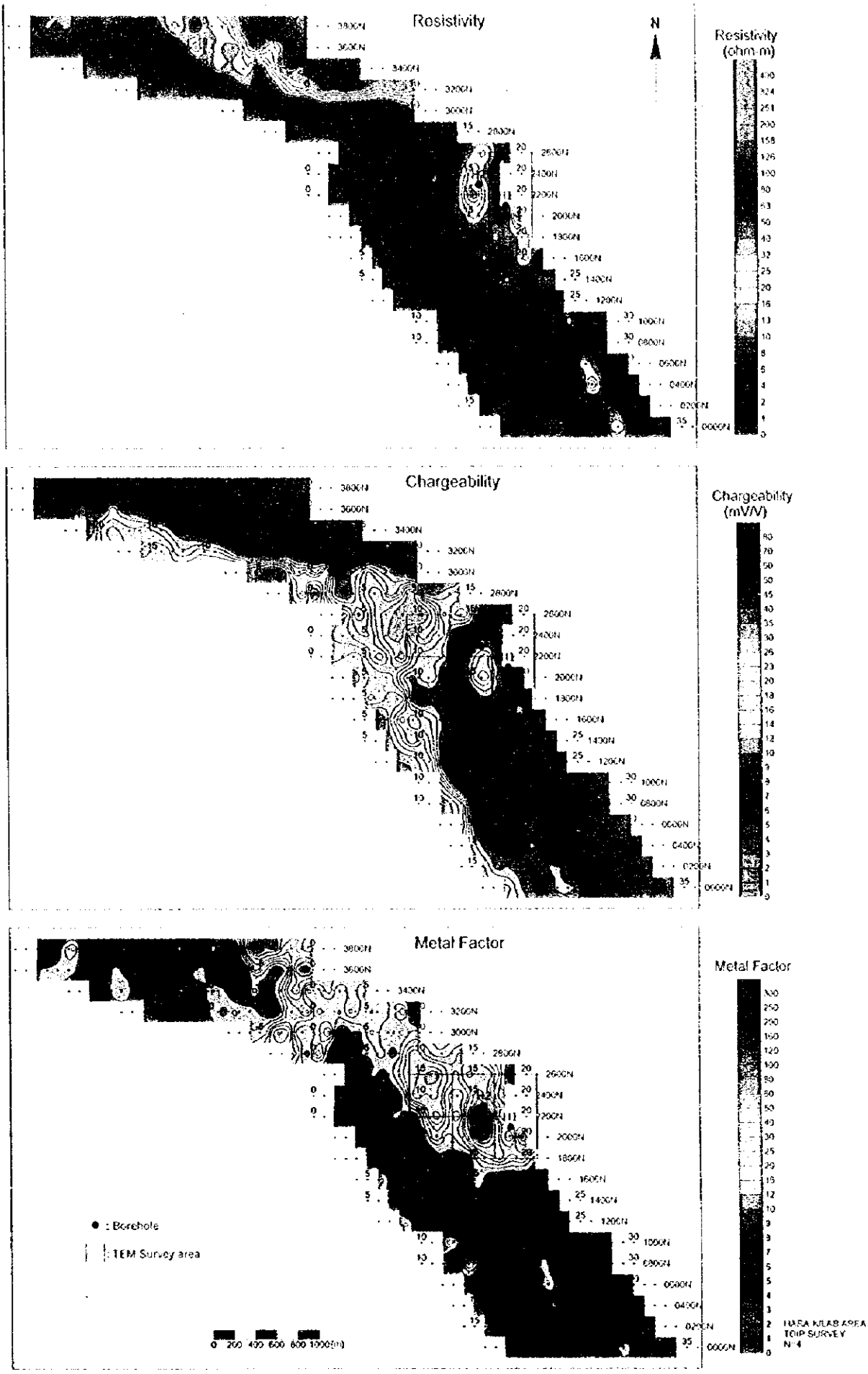

Fig. II -2-38 IP plane map of n=4 in Hara Kilab area

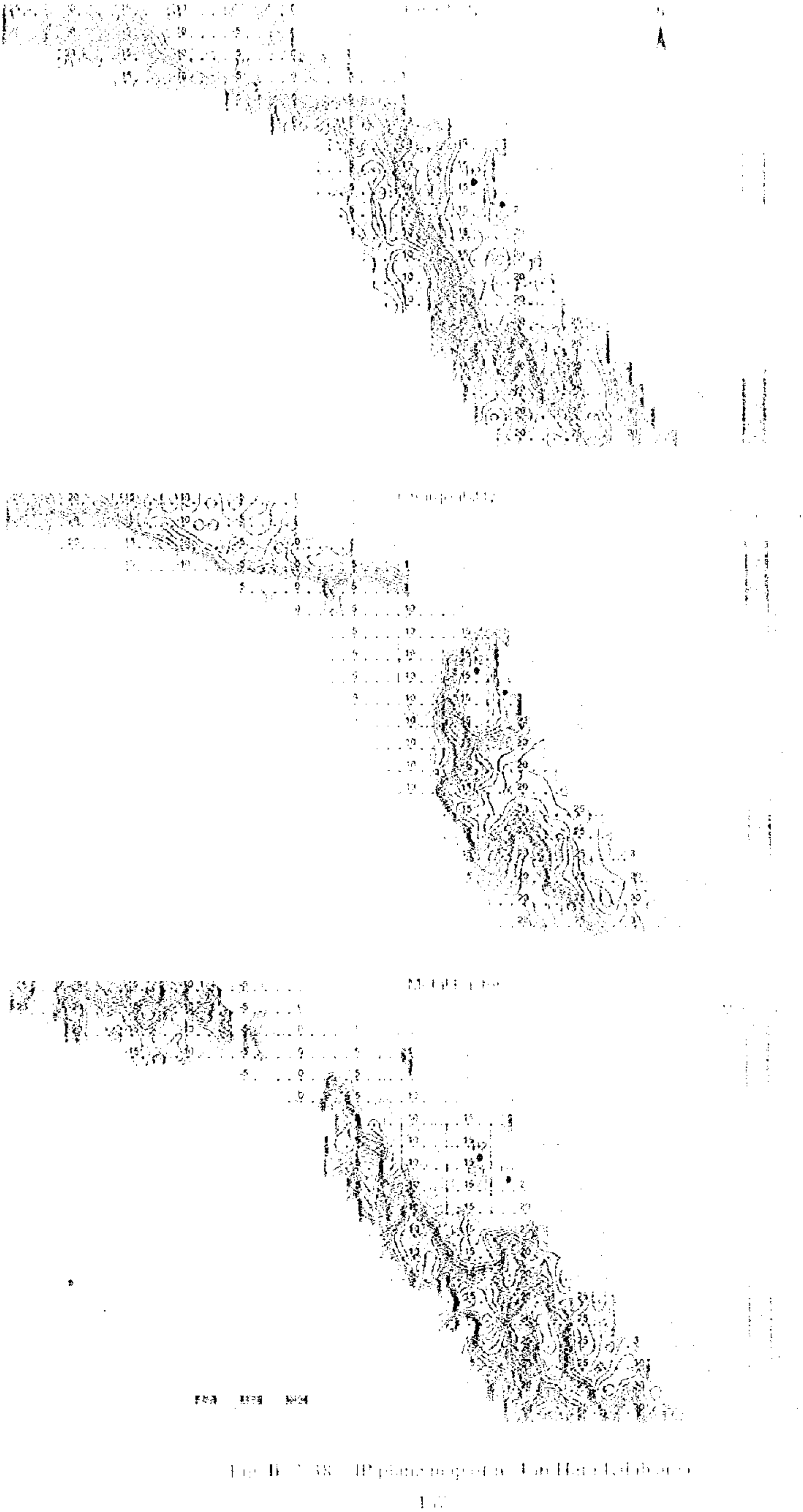

Fig. II-7-38 IP plane map

stations Nos. 15 to 16 of the line 2200N, and also another N-S trending as a center in the vicinity of the station No.11 of the line 2600N shows. The former zone shows high metal values of about 100 (Fig. II-2-37).

In the south part of the area, around the stations 22 to 23 of the lines 400N to 800N, a N-S trending zone of relatively high values is found distributed. Again, around the vicinity of the station No. 15 of the line 800N, it is recognized a small scaled zone of high metal factors at N=3 to 4 (Fig. II-2-34(1)).

(3) 2D analysis

2D analysis was performed for all the lines, however in this report only the sections containing representative anomalies will be described. On these regards, here only the 2D results of the lines 2200N and 2600N will be briefly presented (Fig.II-2-39).

By looking at the 2D modeling results of line 2200N, high resistivity values are seen on all the west part of the area, becoming medium to low resistivity values in the east side. Around the vicinity of the stations Nos. 15 to 16 at depth below 100m, it is seen a low resistivity zone of less than 20 Ω-m. In relation to chargeability, high values are distributed in all the west part, but low values are found distributed at shallow depth in the east part. From the stations Nos. 7 to 17 it is recognized at depth a wide zone with high chargeability values. In relation to metal factor, at depth from stations Nos. 15 to 16, high values above 100 give indications of the possible existence of an orebody around this vicinity.

Regarding line 2600N, as similar as the resistivity calculated in line 2200N, this line presents high values in the west part and low values in the east. Comparatively clear low resistivity values are seen distributed around stations Nos.14 to 15 at shallow depth, and around stations Nos.16 to 17 at deep levels. In relation to chargeability, high chargeability values are seen in the central part of the line and relatively high chargeability values are obtained at the depth of the stations Nos.16 to17. In relation to metal factor, high values are interpreted at the depth of stations Nos. 10 to 17, indicating that there exists the possibility of finding an orebody around this vicinity.

2-5-6 Maqail area

(1) Lines location

During this field season, a total of 9 lines (from 000N to 1600N) were surveyed along E-W direction with a line spacing of 200m. Among these lines, 4 of them (800N to 1400N) had a length of 2.0 km, 4 of them (000N to 600N) a length of 1.5 km and the remaining one (1600N) a length of 1.4km. Total line length consisted of 15.4km.

The Fig.II-2-40 shows the location of all the IP lines surveyed in Maqail.

(2) Results

The results of the TDIP survey in Maqail area are presented here as pseudo-sections of apparent resistivity, chargeability and metal factor in the Fig.II-2-41 to Fig.II-2-43, respectively. Contour maps

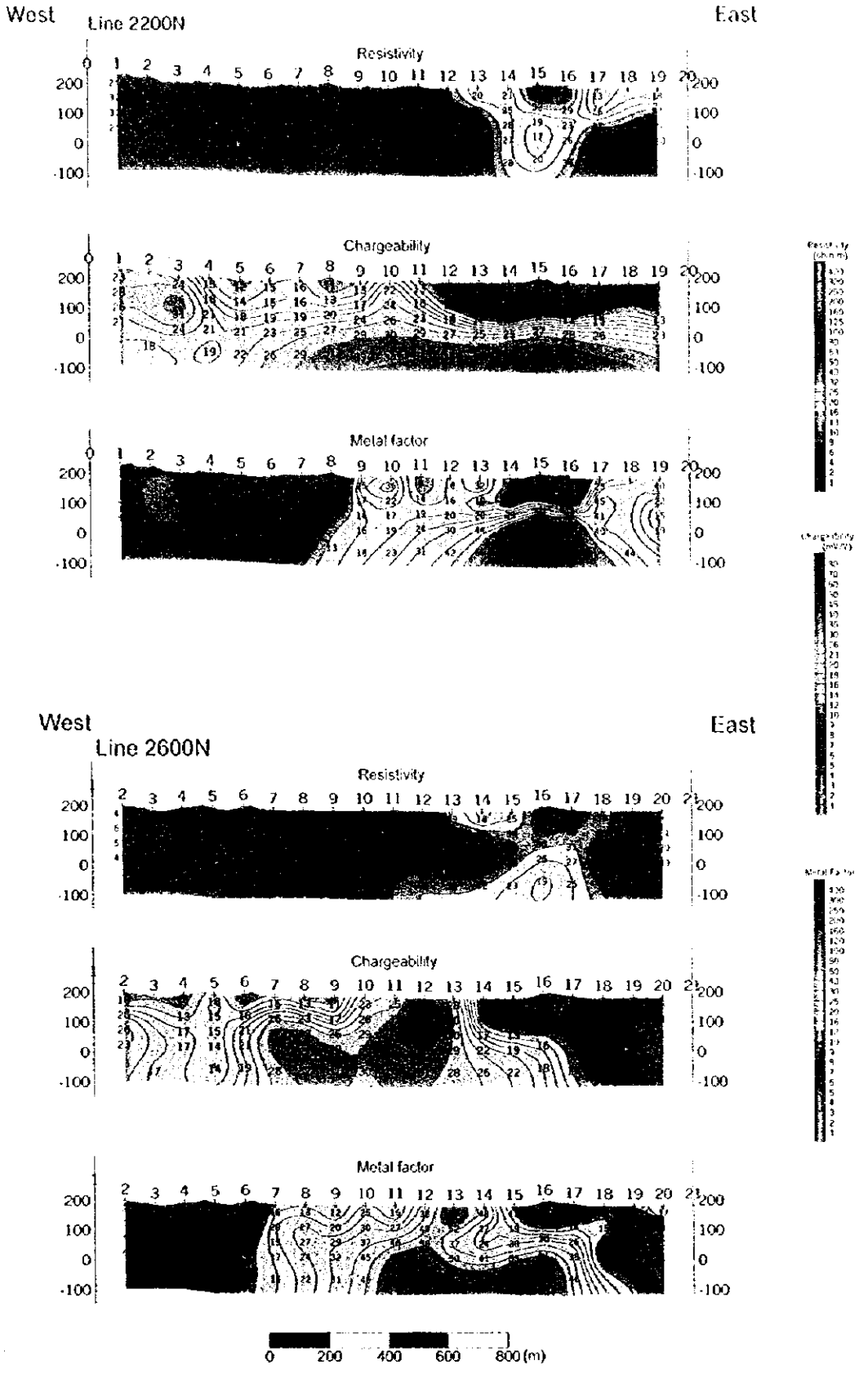

Fig. II -2-39 IP 2D model simulation on lines 2200N and 2600N in Hara Kilab area

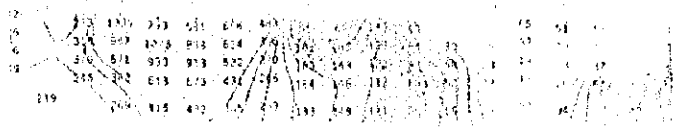

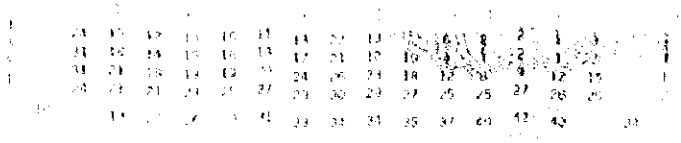

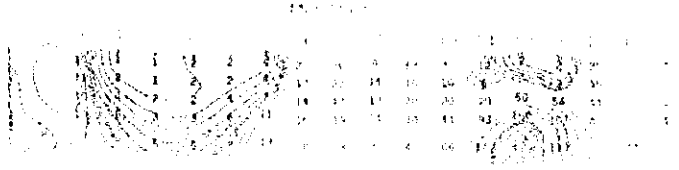

West

Lane 2600H

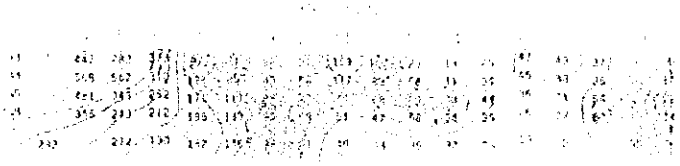

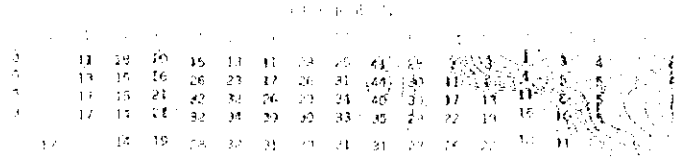

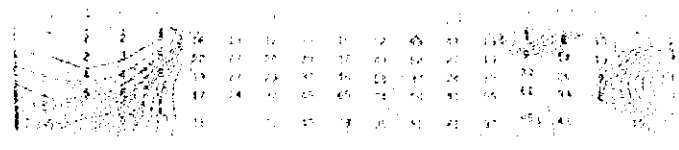

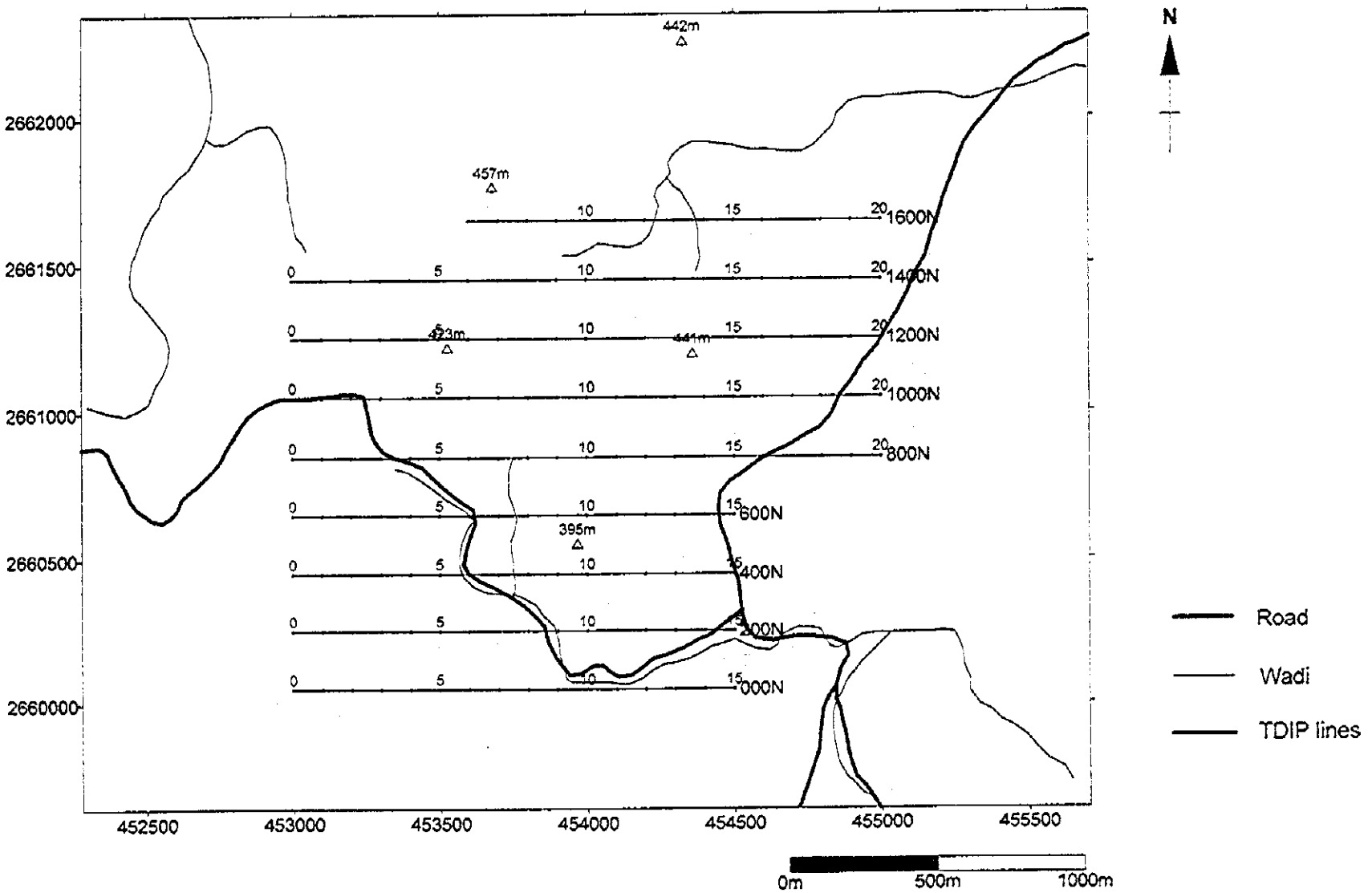

Fig. II -2-40 Geophysical survey location in Maqail area

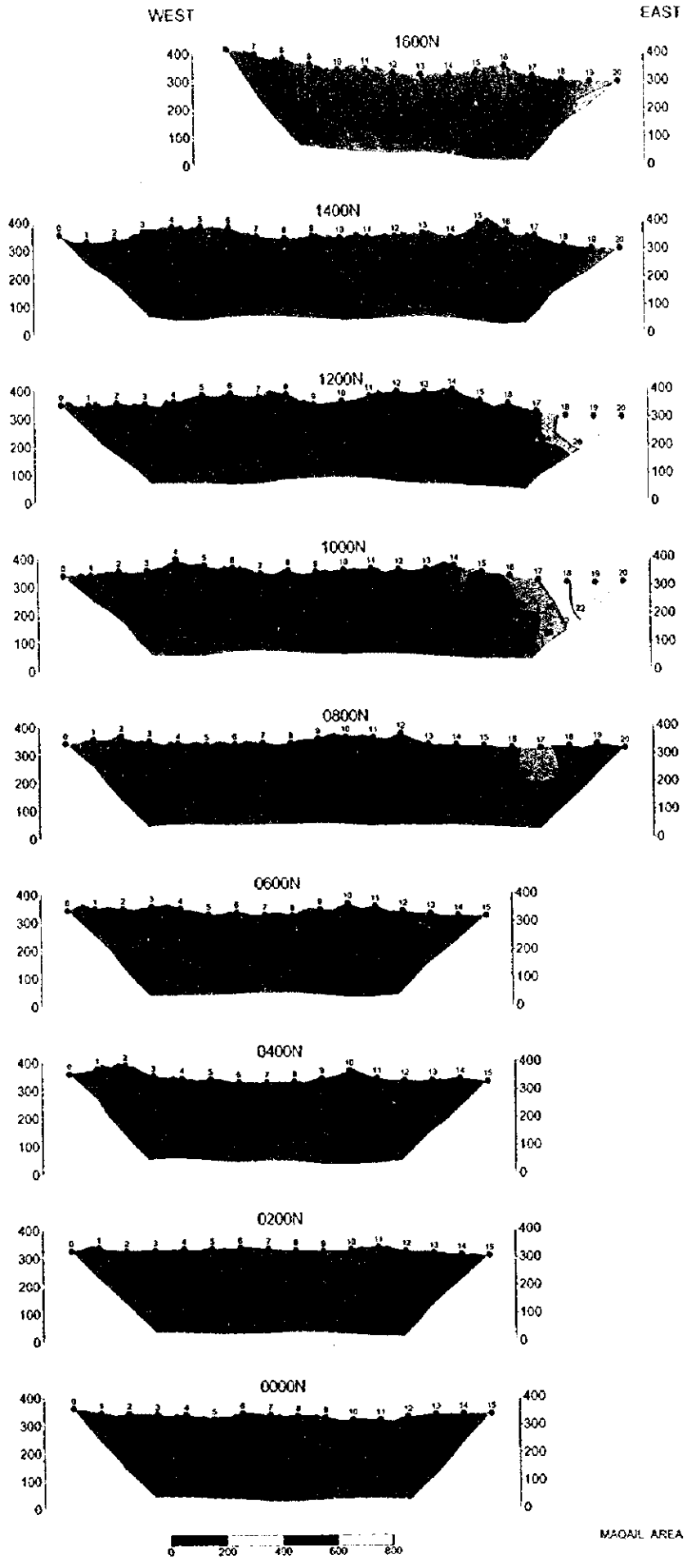

Fig. II-2-41 Apparent resistivity pseudo-sections in Maqail area

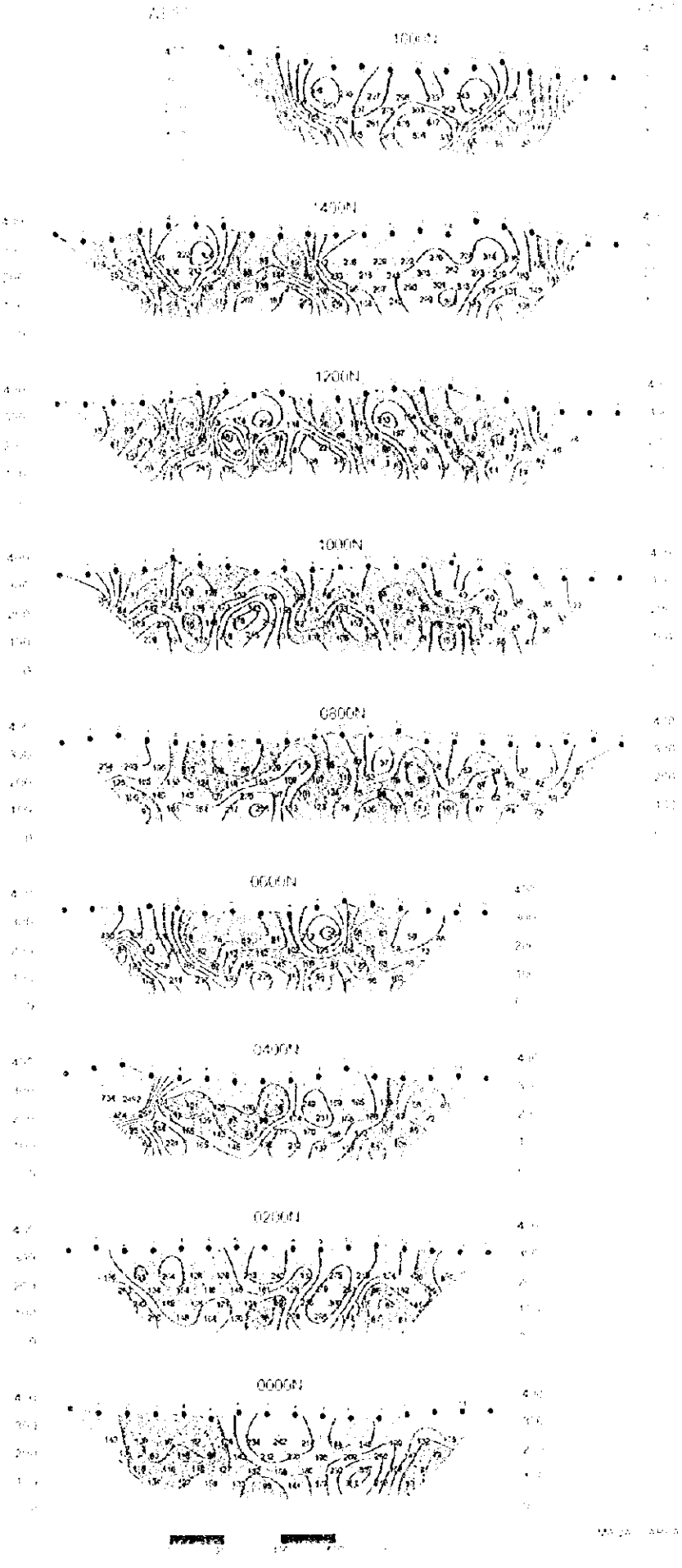

Fig. II-2-41 Apparent resistivity pseudo-sections in Maqail area

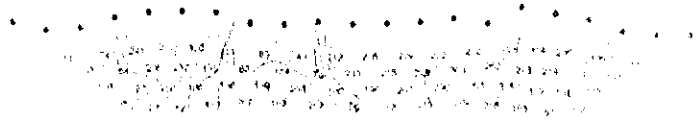

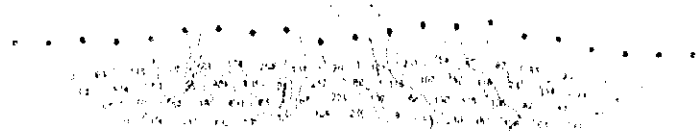

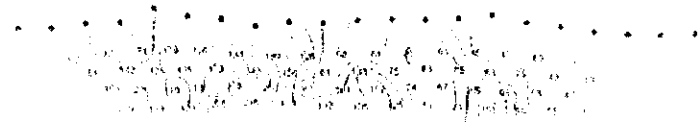

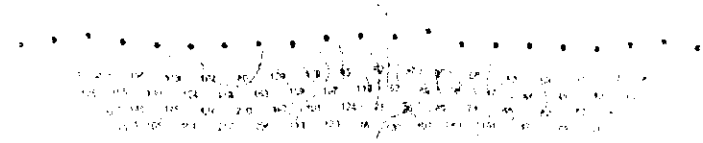

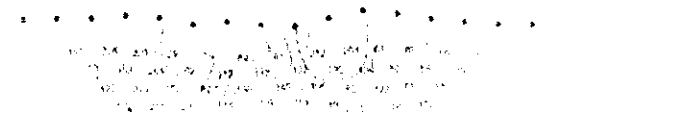

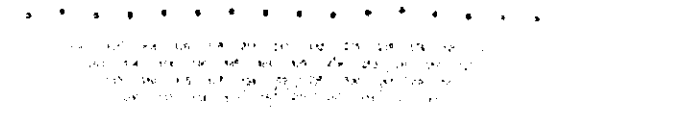

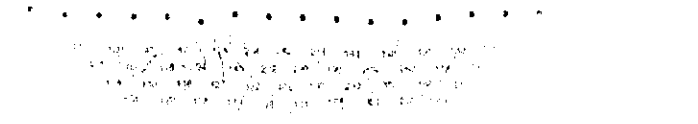

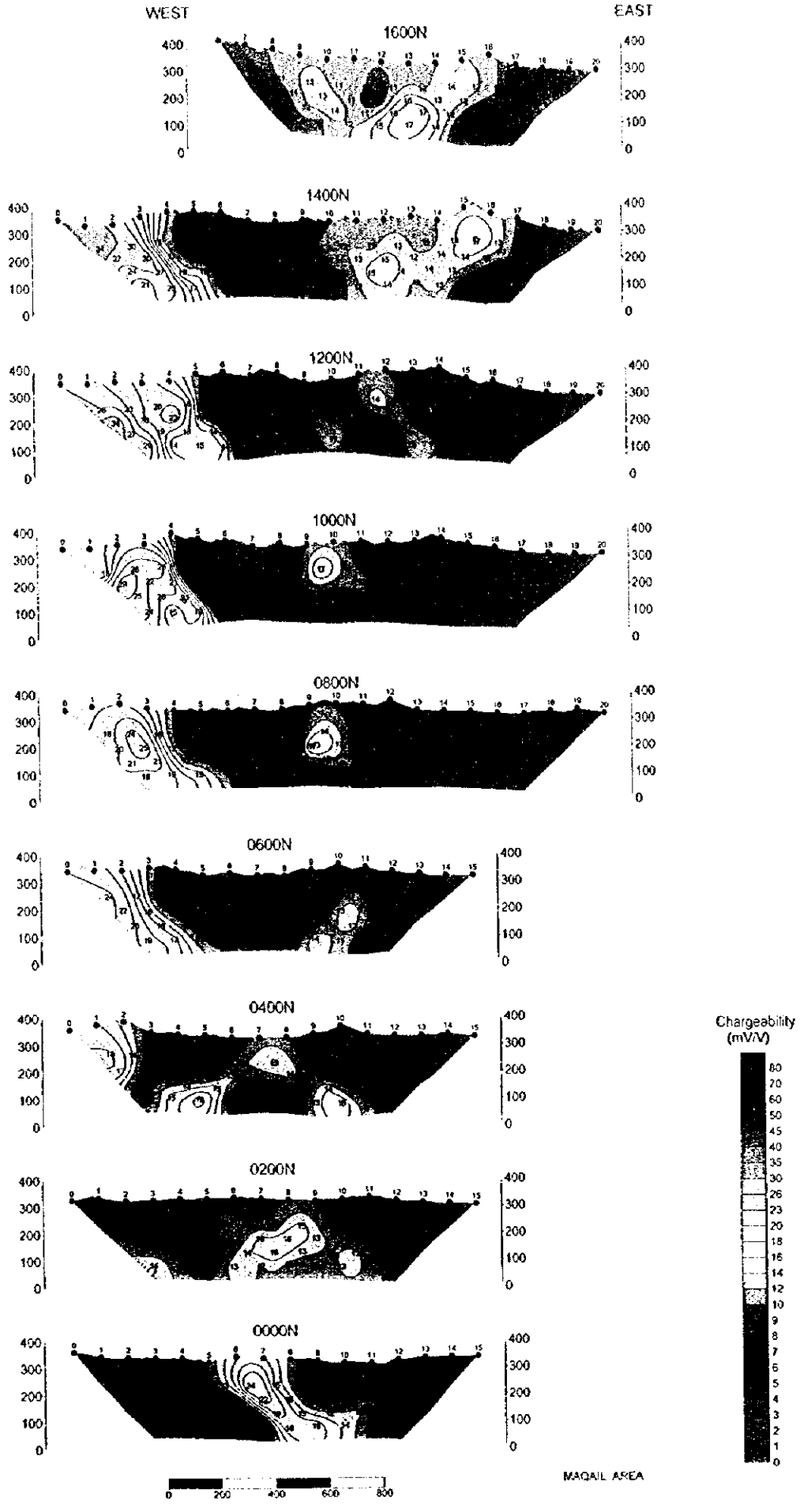

Fig. II-2-42 Chargeability pseudo-sections in Maqail area

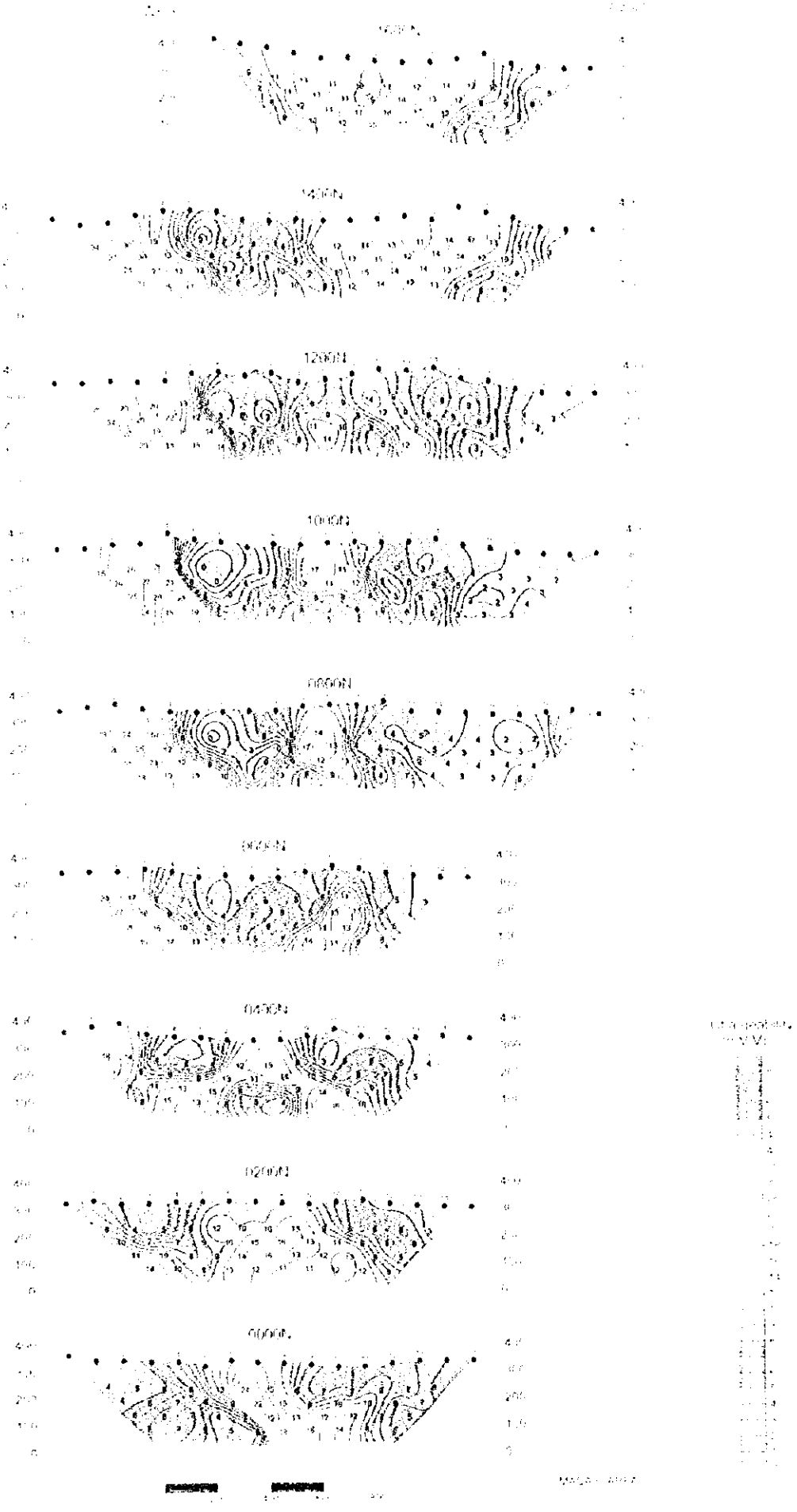

Fig. II-2-12 Chargeability pseudo-sections in Mapai area

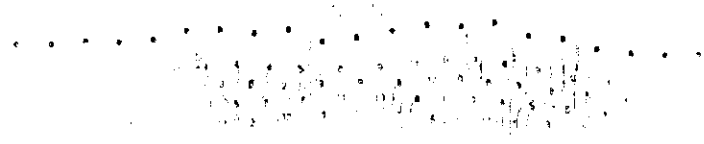

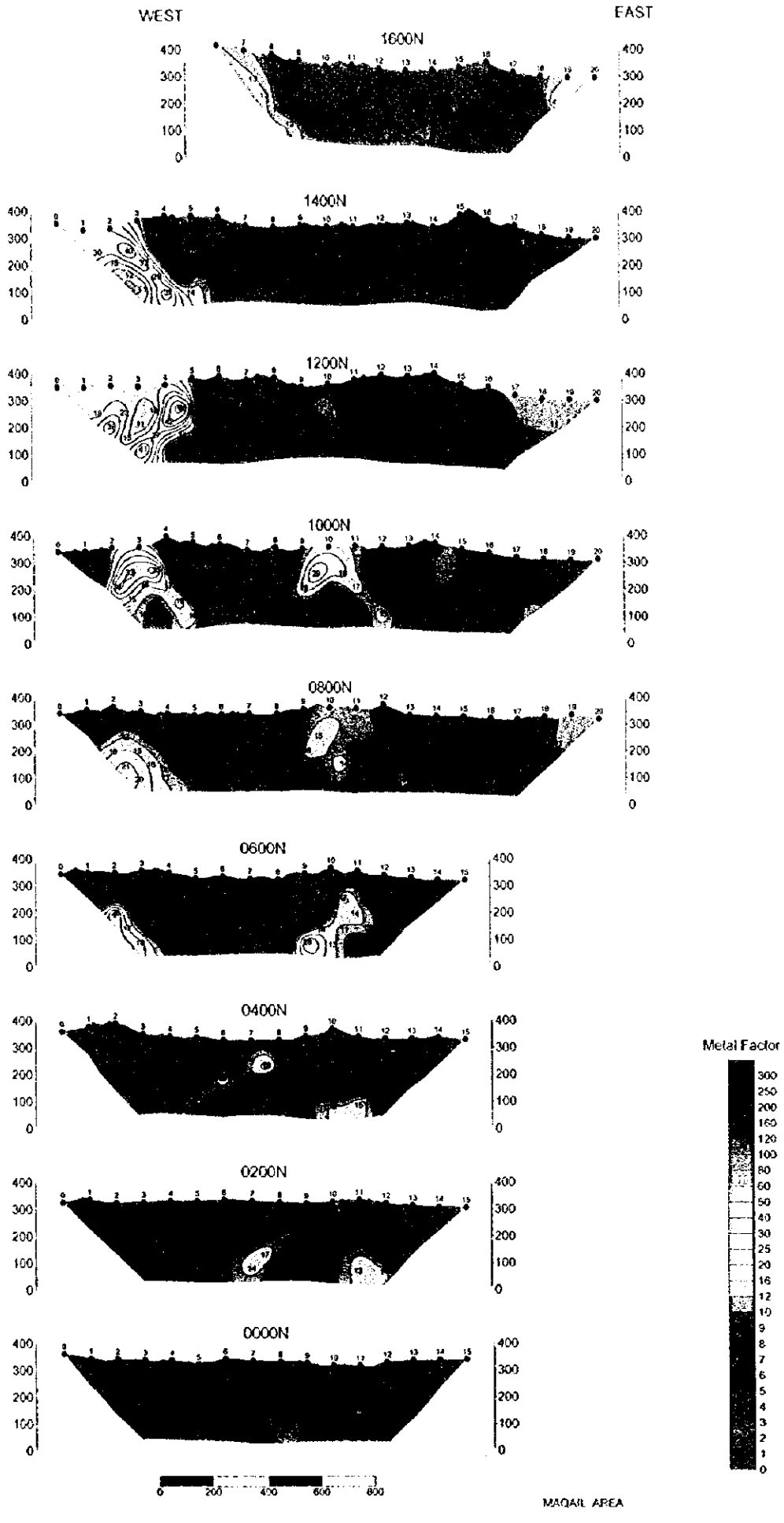

Fig. II -2-43 Metal factor pseudo-sections in Maqail area

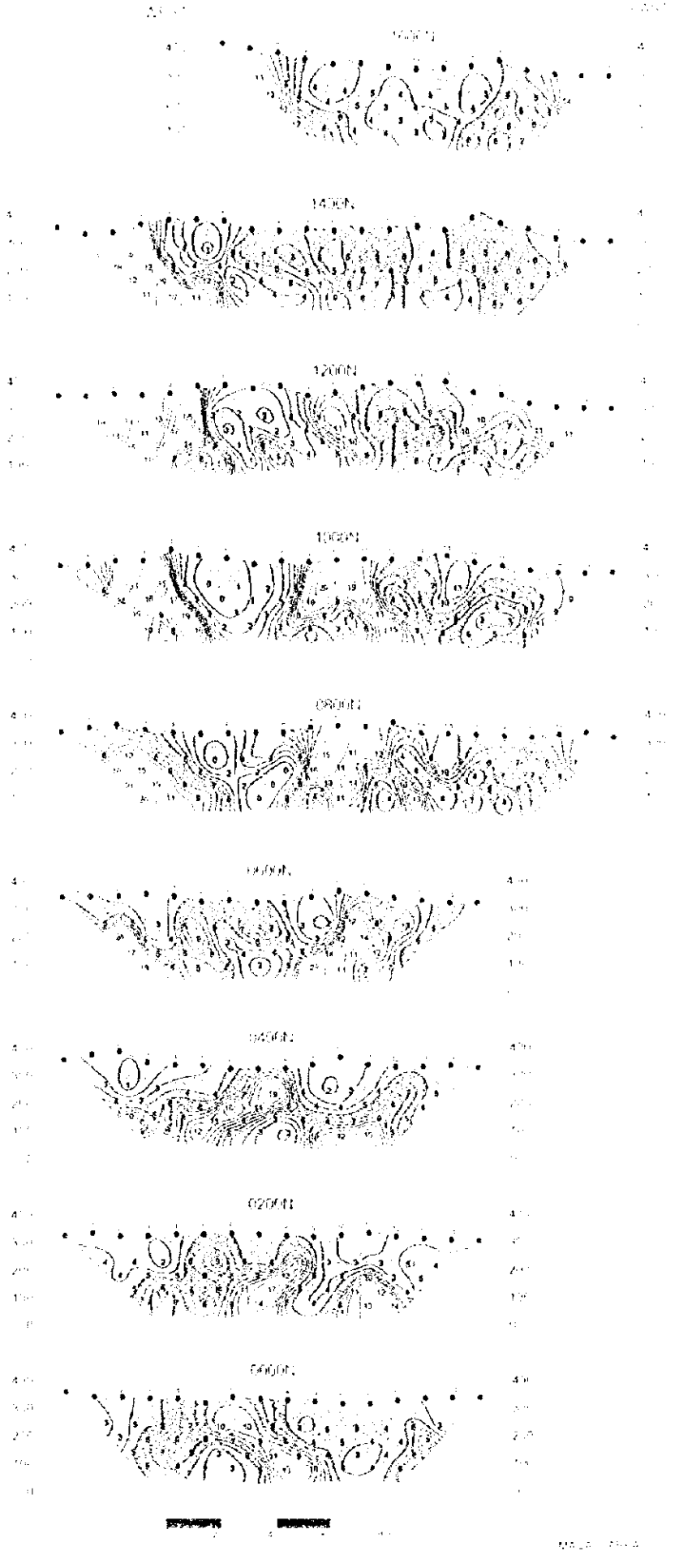

Fig. II-2-13 Metal factor pseudo-sections in Muqail area

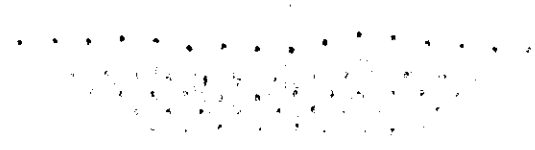

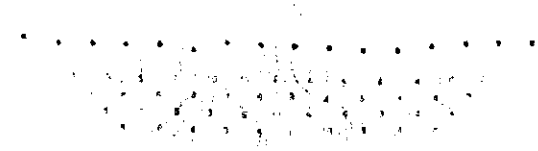

of apparent resistivity, chargeability and metal factor for N=1 to 4 are presented respectively, from the Fig.II-2-44 to Fig.II-2-47.

As compared with other areas, the apparent resistivity distribution in the whole area presents in general higher values (Fig.II-2-46). A relatively low resistivity distribution from N=1 to 4 is recognized in the east part of the area where Quaternary sediments are cropped out. In the central part of the area it is recognized a resistivity structure along a NW-SE trending. Moreover, from station No. 3 of the line 1000N to station No. 5 of the line 1200N a distribution of medium resistivity values is recognized at N=1 (Fig.II-2-44) along a zone where the boundary between V1-1 and V1-2 is assumed.

In relation to the chargeability distribution, high chargeability values are seen widely distributed from shallow to deeper levels (Fig.II-2-46) in the west part of the area where V1-1 is exposed. Another zone consisting of several local high chargeability distributions is seen distributed in the central part almost along an N-S trending structure (Fig.II-2-46). Within this zone, in the vicinity of station No. 10 of line 1000N it can be recognized a relatively clear central anomaly along N-S direction (Fig.II-2-42). In the north side of this central high chargeability zone, it is assumed the boundary between V1-1 and V1-2.

With reference to the metal factor, high metal factor values are seen in the above mentioned west and central parts (Fig.II-2-46). In the west part, a clear contrast is seen in the boundary zone between V1-1 and V1-2. Regarding the central part and around the vicinity of the station No. 10 of the central part of the line 1000N, a high metal factor zone is seen extended along N-S direction. The metal factor pseudo-section shows between the levels N=2 to 4 an anomaly of pants legs shape (Fig.II-2-45 to Fig.II-2-47).

(3) 2D analysis

2D analysis was performed for all the lines; here only the sections containing representative anomalies will be described (Fig.II-2-48).

In the line 1200N, the interpreted resistivity distribution shows in general high values. Around the stations Nos. 4 and 9, a vertical resistivity distribution pattern of medium resistivity are locally found. The boundary between V1-1 and V1-2 is located close to the above mentioned station No. 4. In relation to the chargeability, relatively high values are calculated around the west part of station No. 4 and around the central part, i.e., in the vicinities of the stations Nos.10 to 12. Metal factor anomalies are recognized at depth showing the same pattern as the chargeability distribution mentioned above around the vicinity of the stations No. 4 and west part of No. 10.

Regarding the analysis of the line 800N, medium resistivity zones are to the west part of the vicinity of station No. 3 and around the station No.11. High chargeability is interpreted in the west part of stations Nos. 4 and 10. Metal factor anomalies show the same pattern as the chargeability distribution, i.e., to the west of station No. 4 and around station No.10. Faults are assumed around stations Nos. 4 and 10, because the distribution of the metal factor shows a vertical pattern.

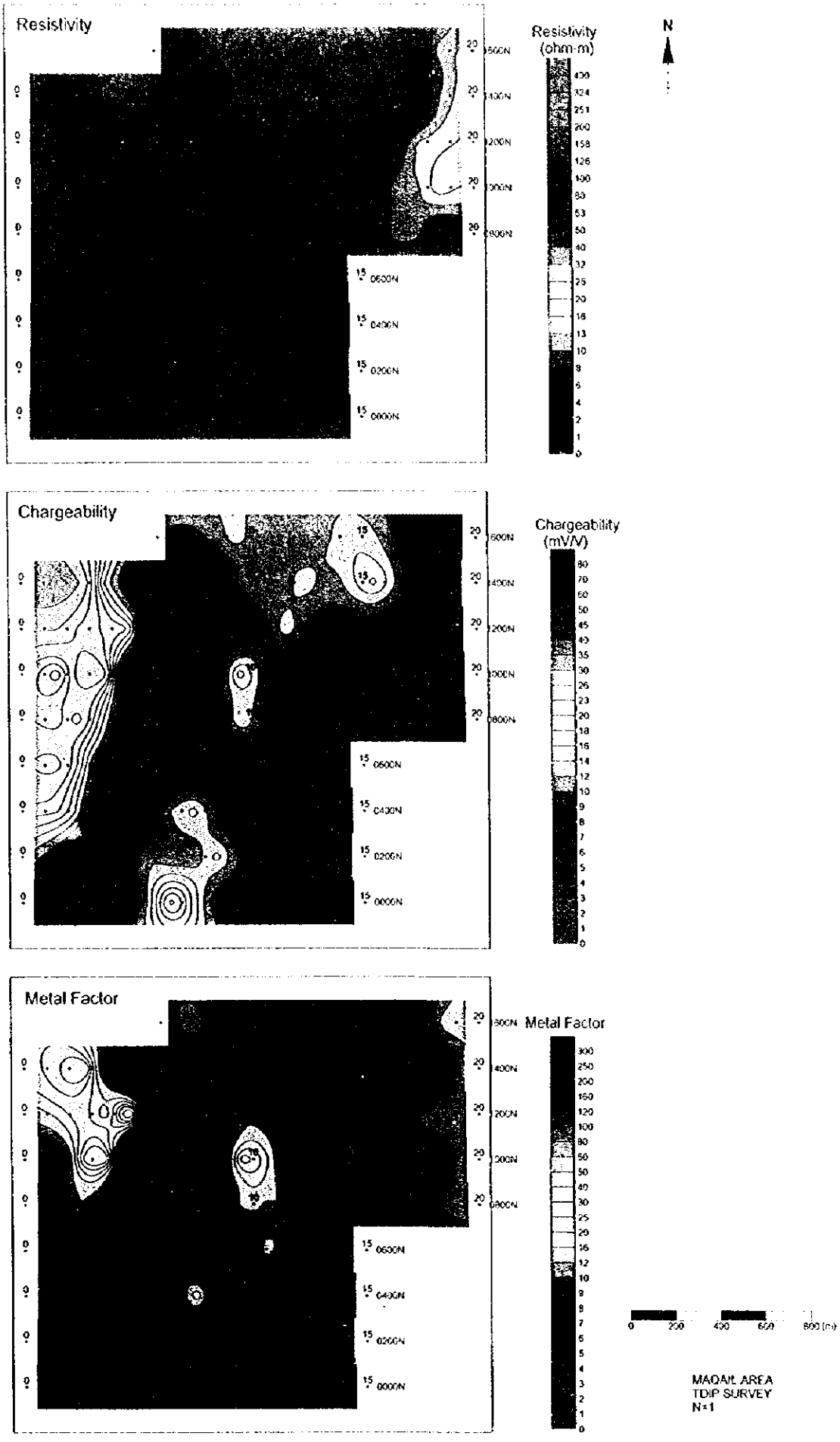

Fig. II -2-44 IP plane map of n=1 in Maqail area

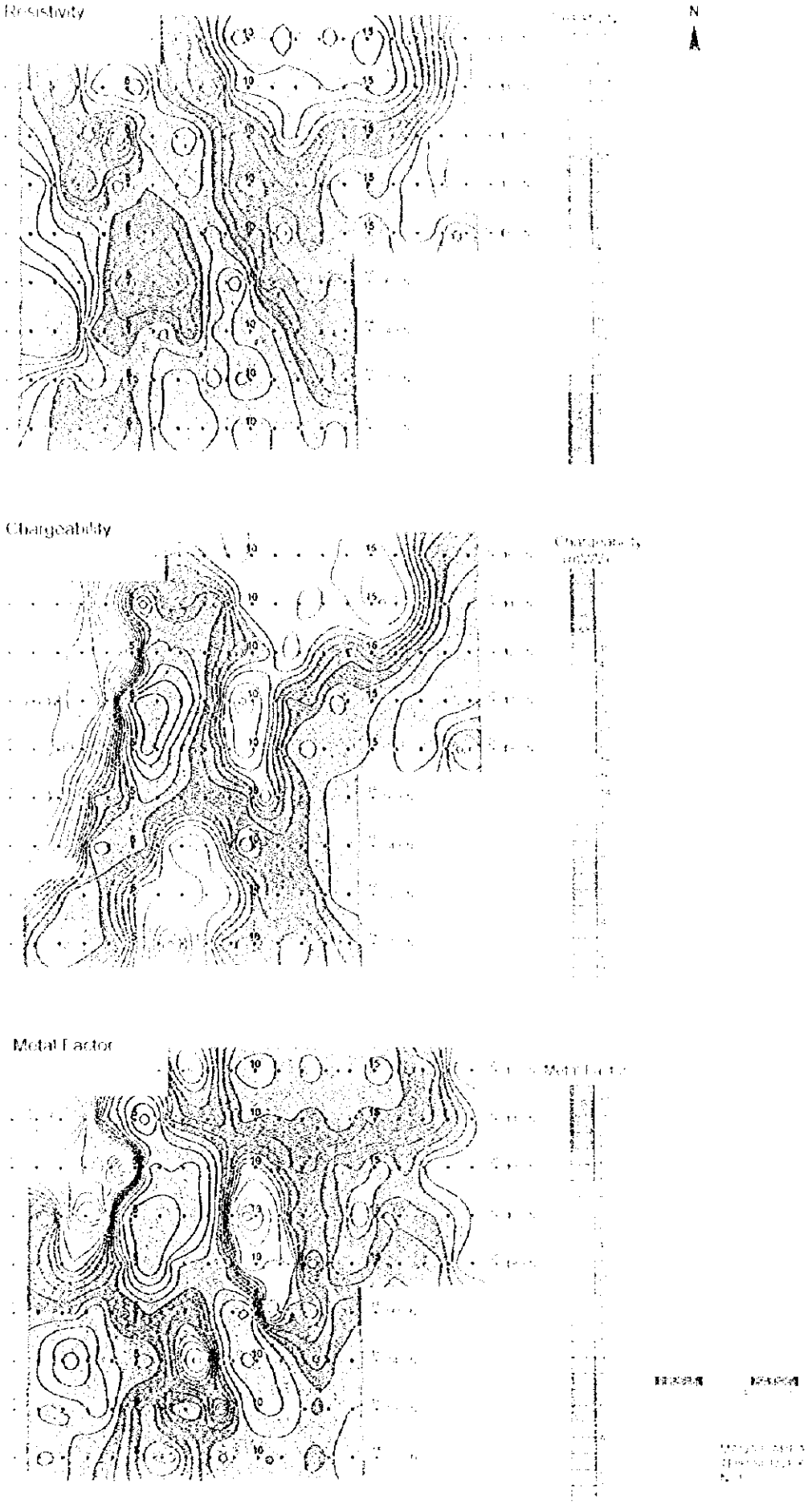

Fig. II-2-11 IP plane map of the Lun Mapai area

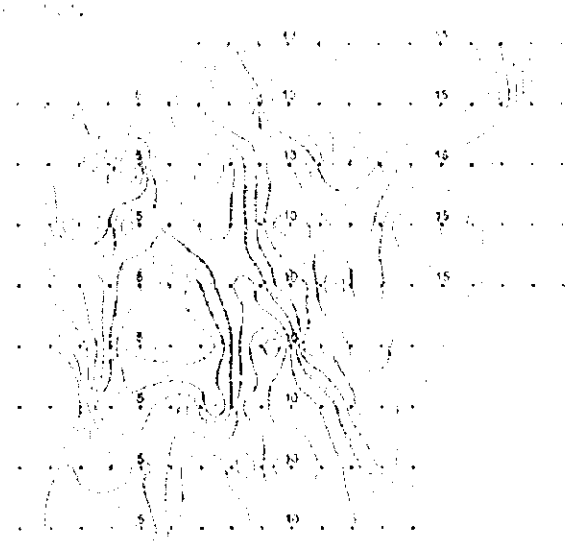

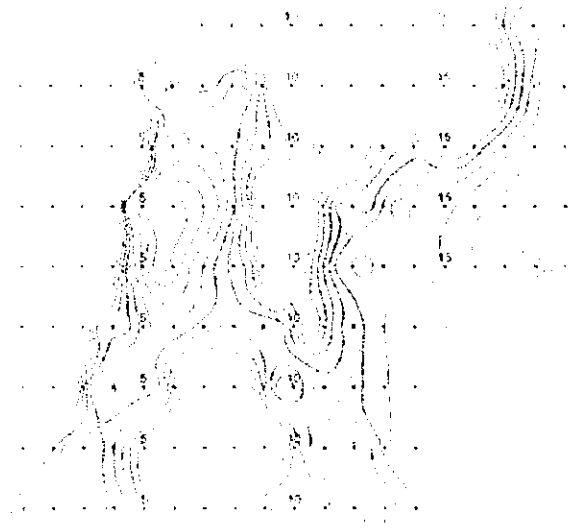

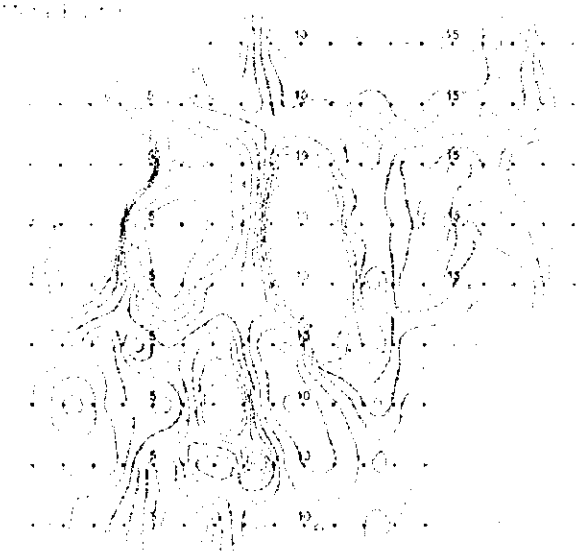

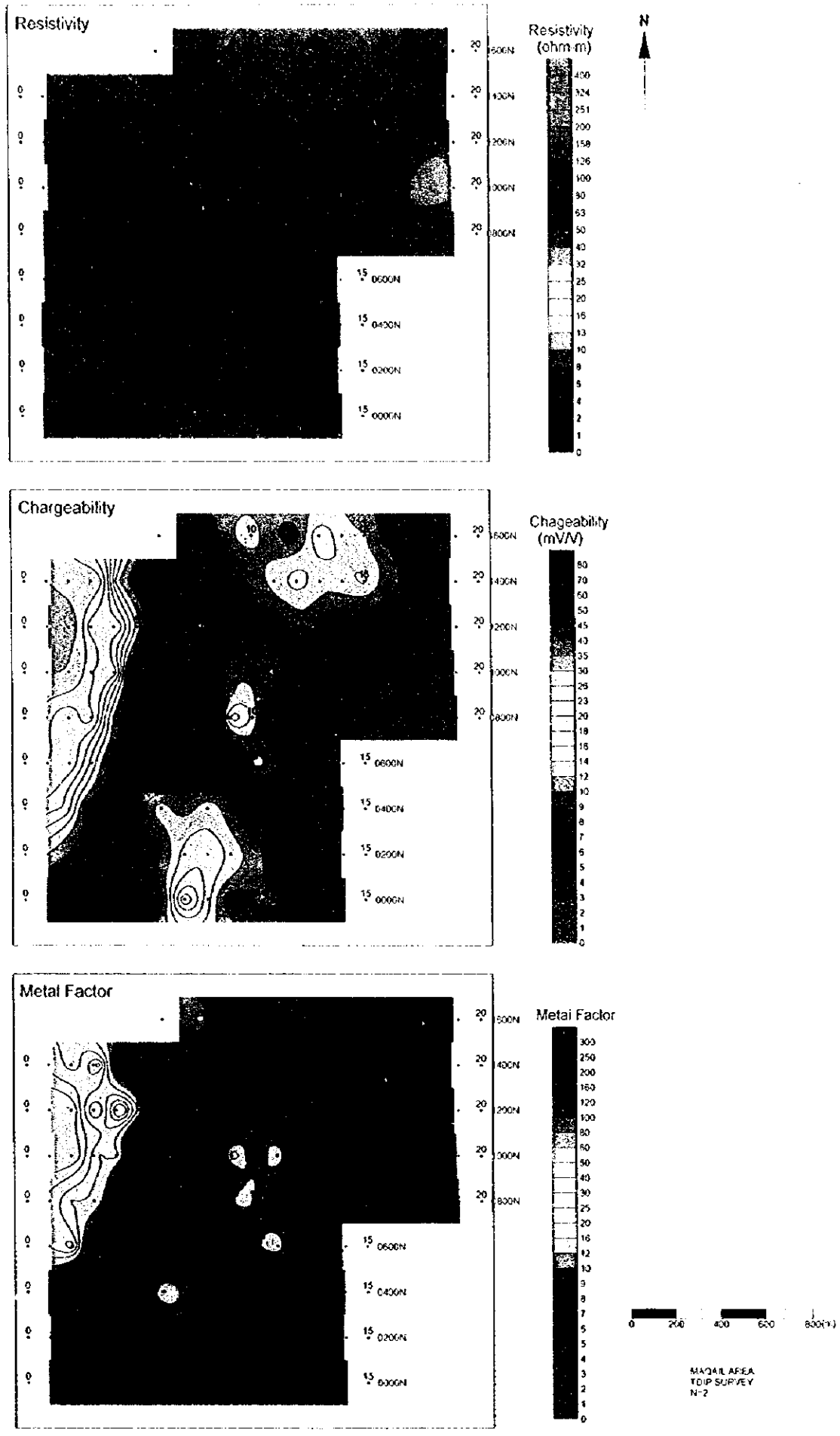

Fig. II -2-45 IP plane map of n=2 in Maqail area

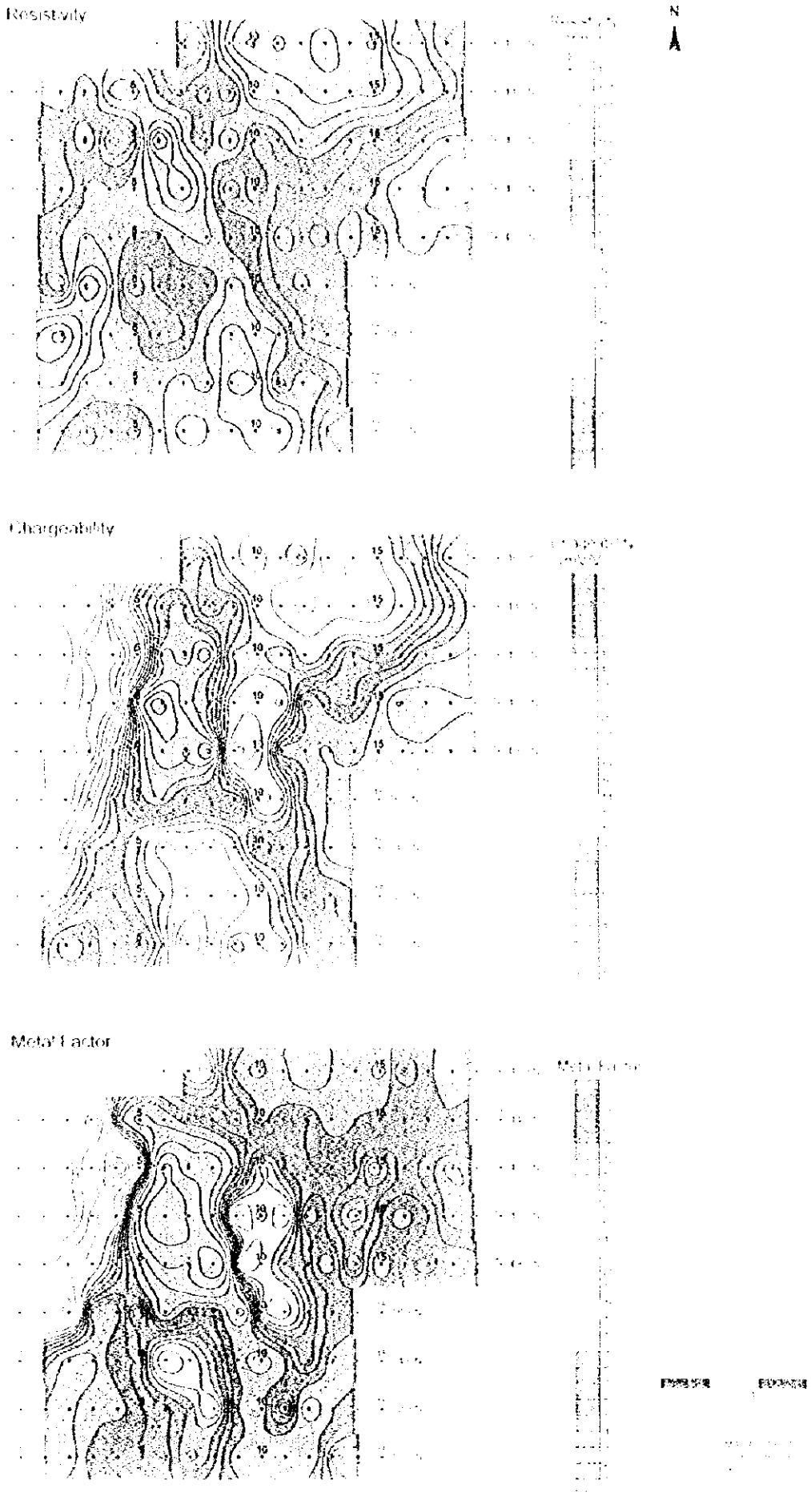

Fig. II-2-45 IP plane map of n=2 in Maquil area

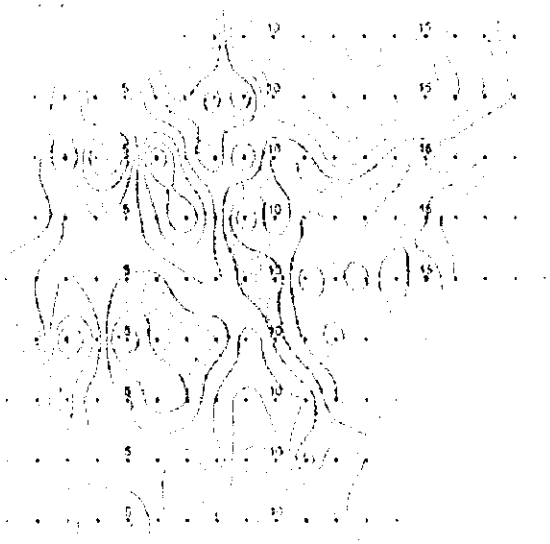

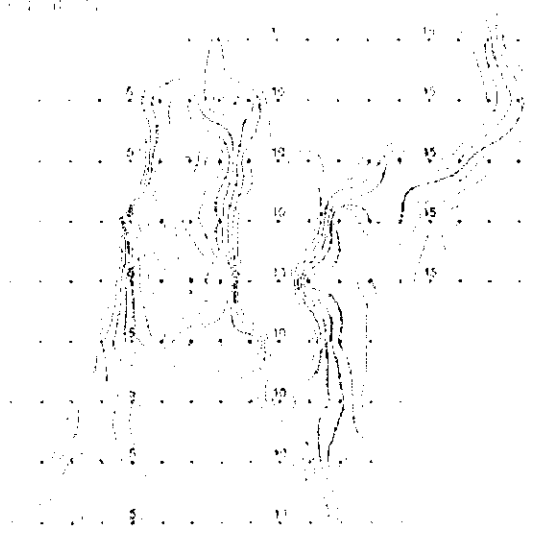

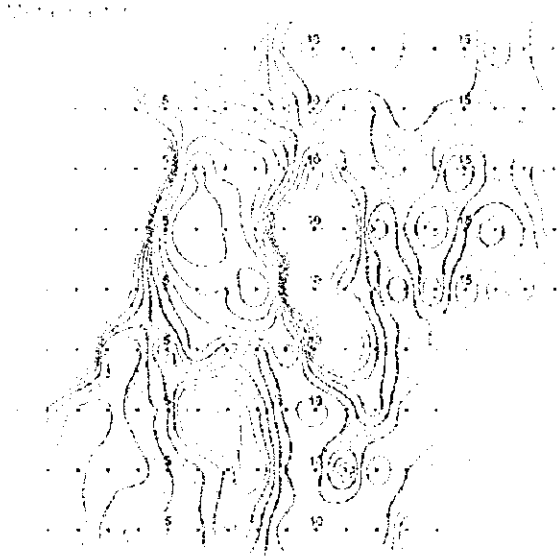

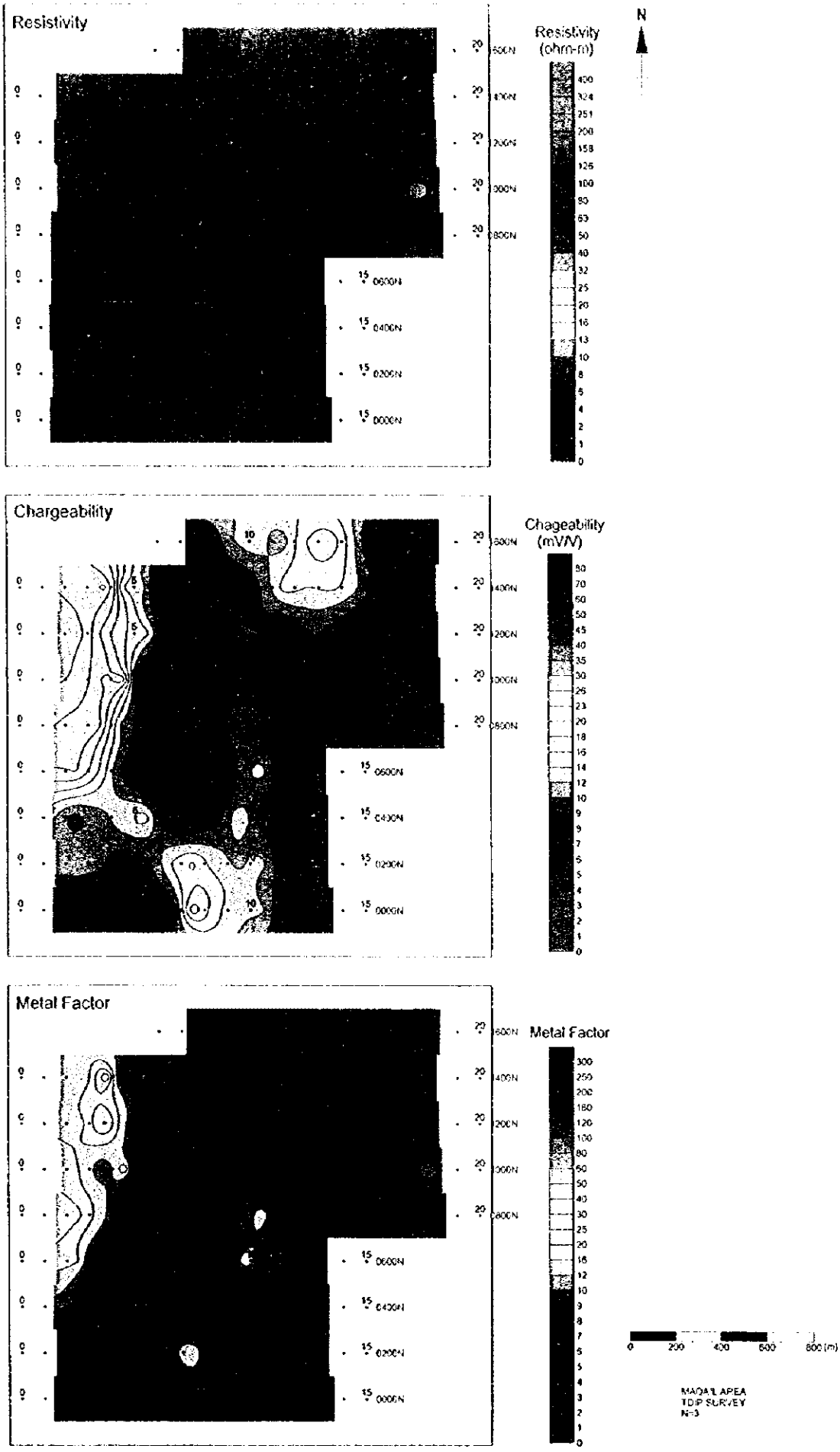

Fig. II-2-46 IP plane map of n=3 in Maqail area

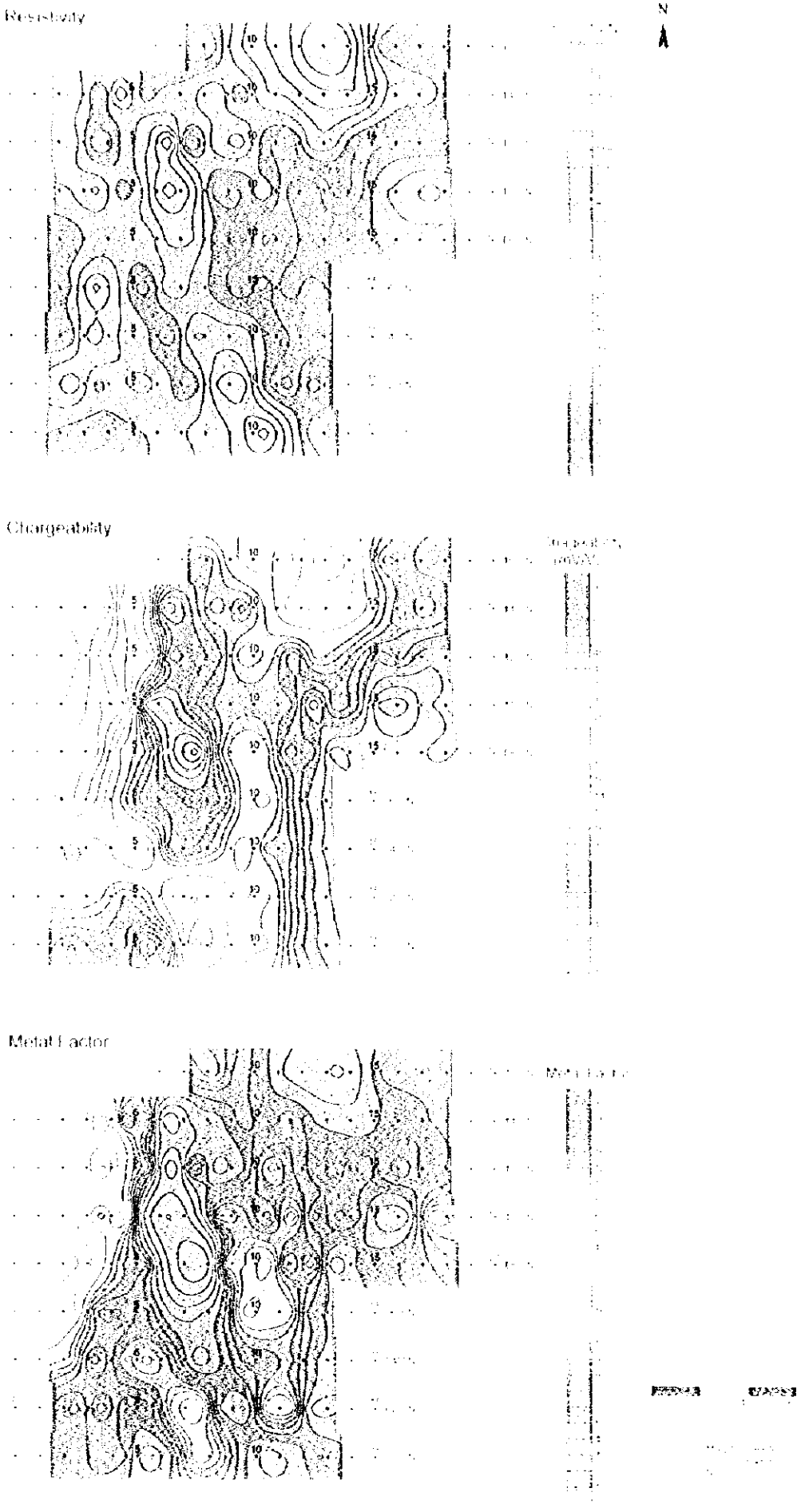

Fig. II-2-46 IP plane map of n=3 in Mapai area

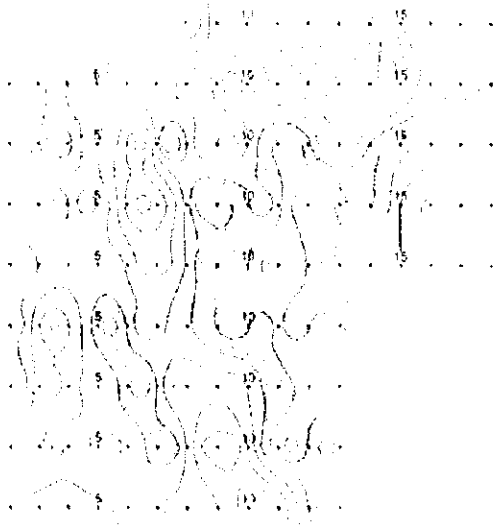

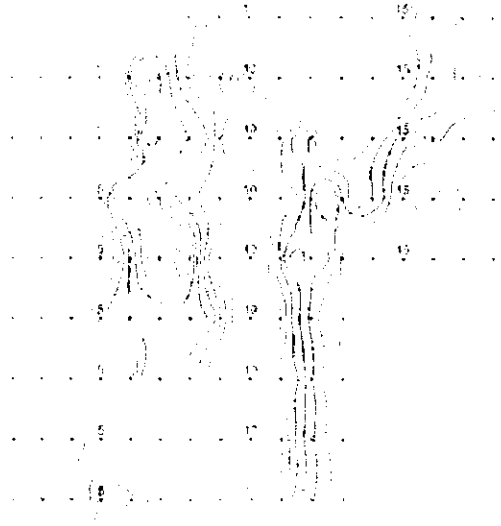

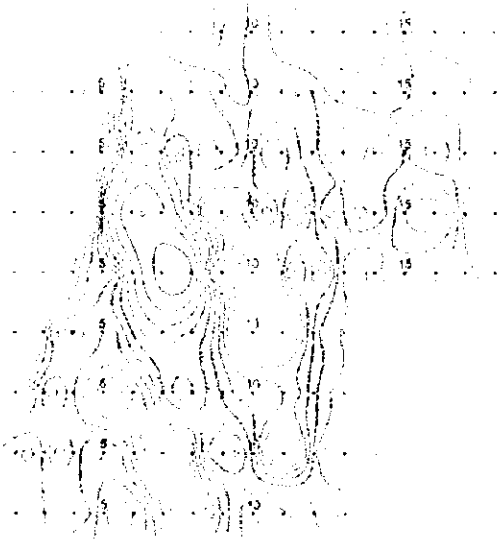

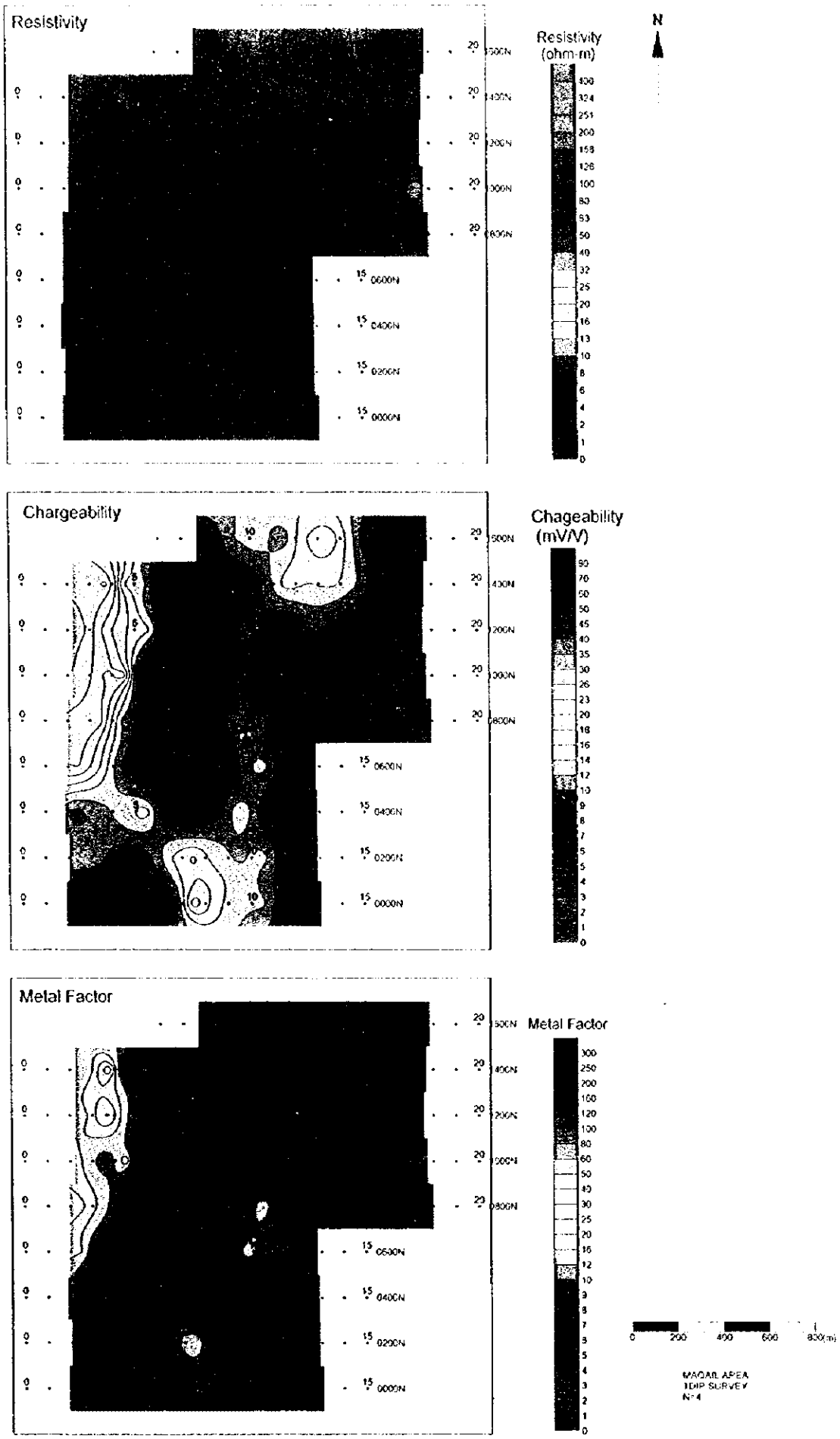

Fig. II -2-47 IP plane map of n=4 in Maqail area

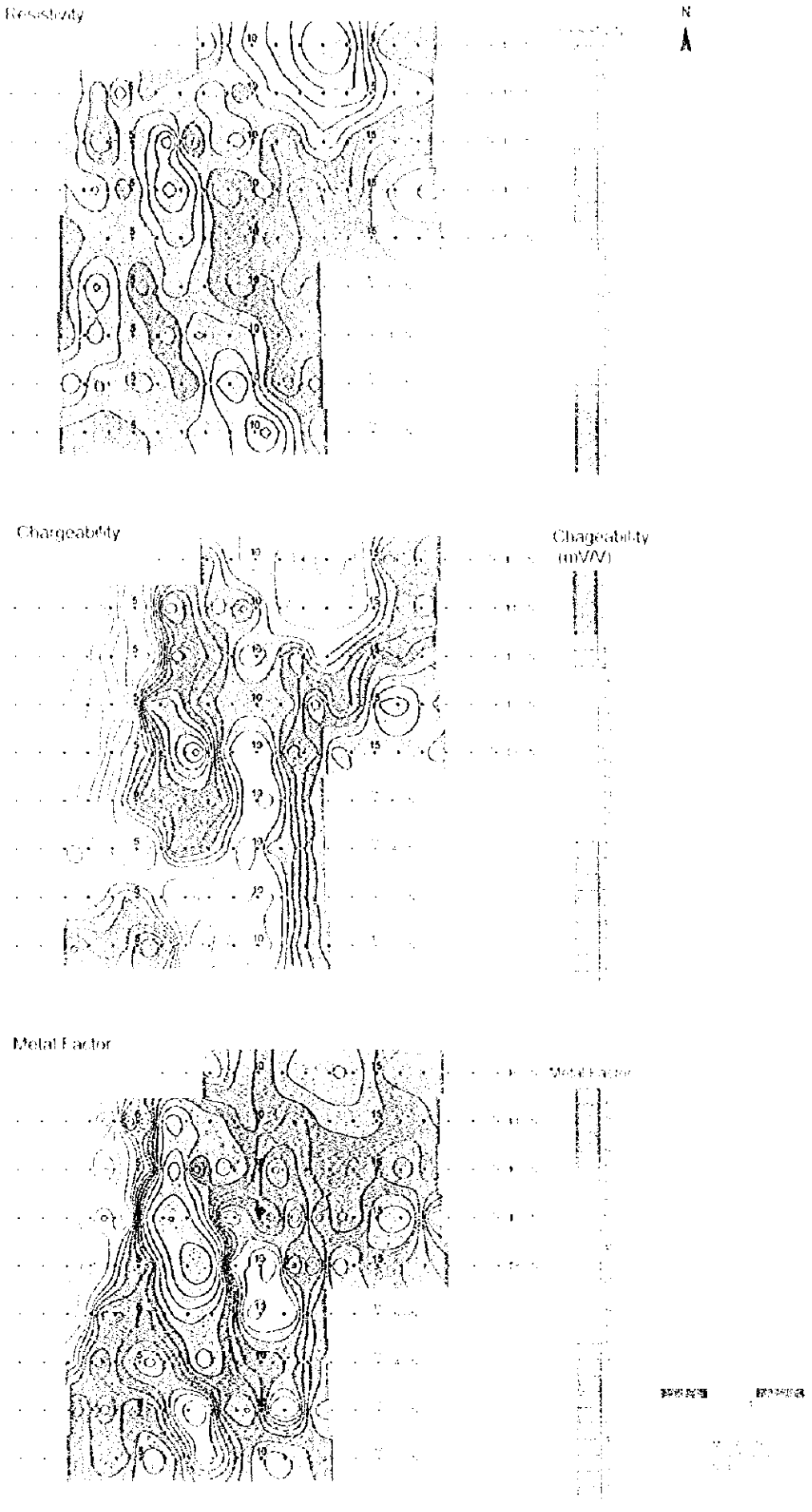

Fig. II-2-47 IP plane map of n-1 m Mapai area

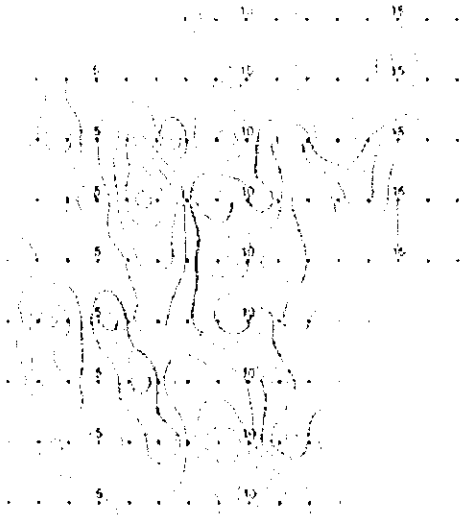

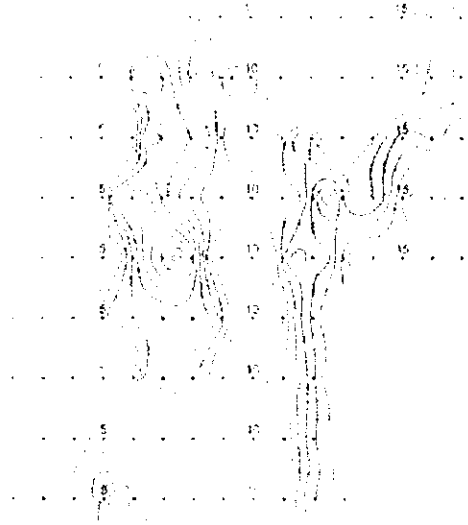

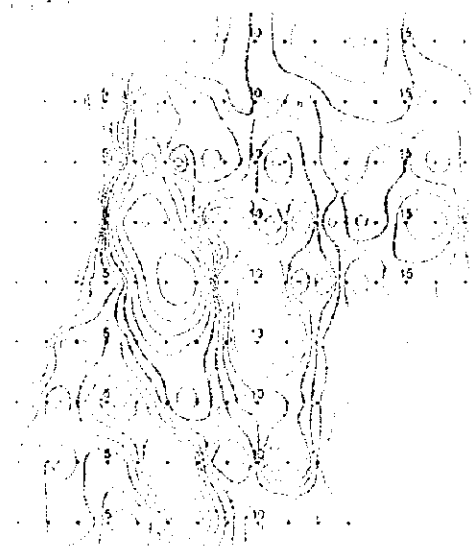

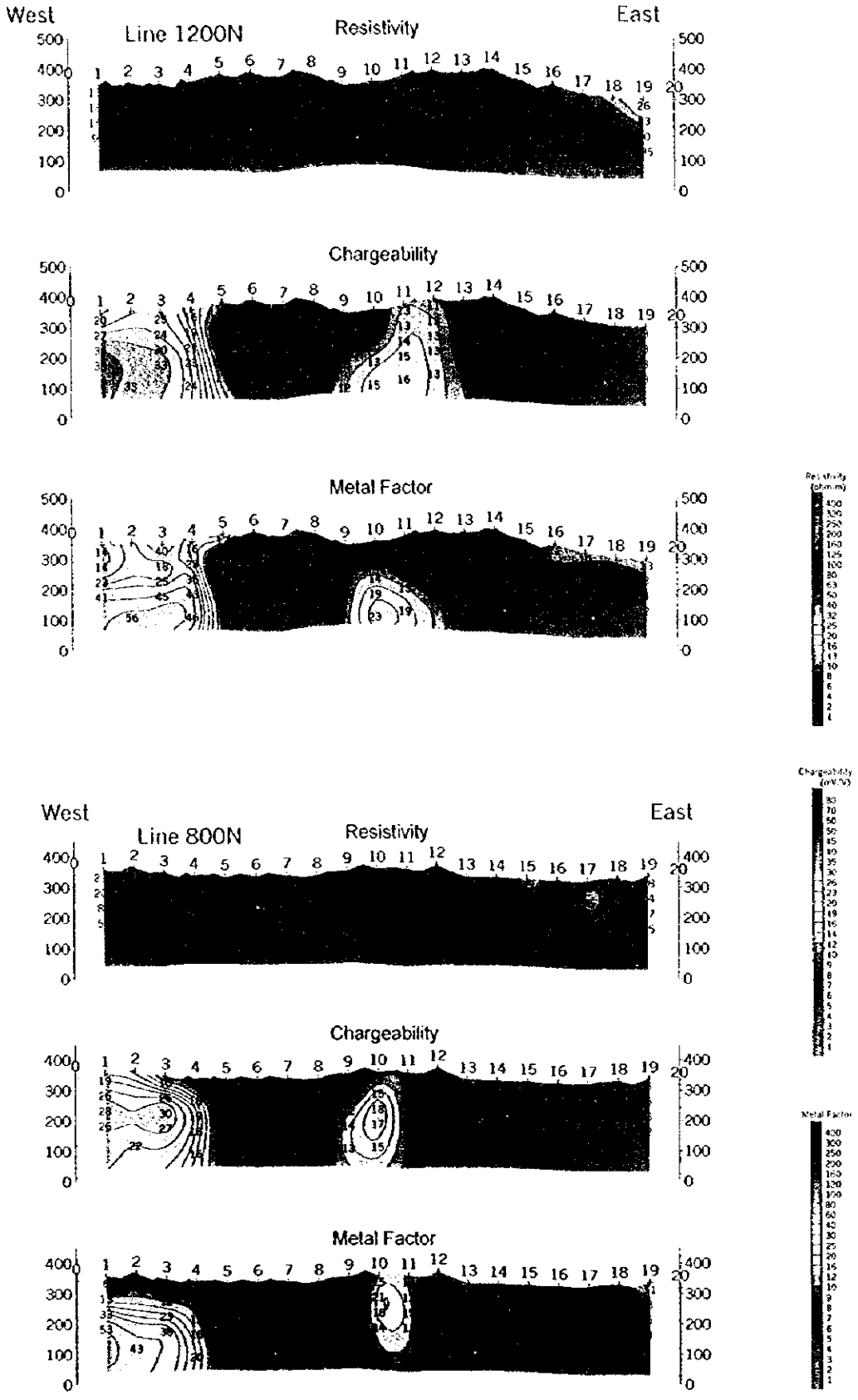

Fig. II -2-48 IP 2D model simulation on lines 800N and 1200N in Maqail area

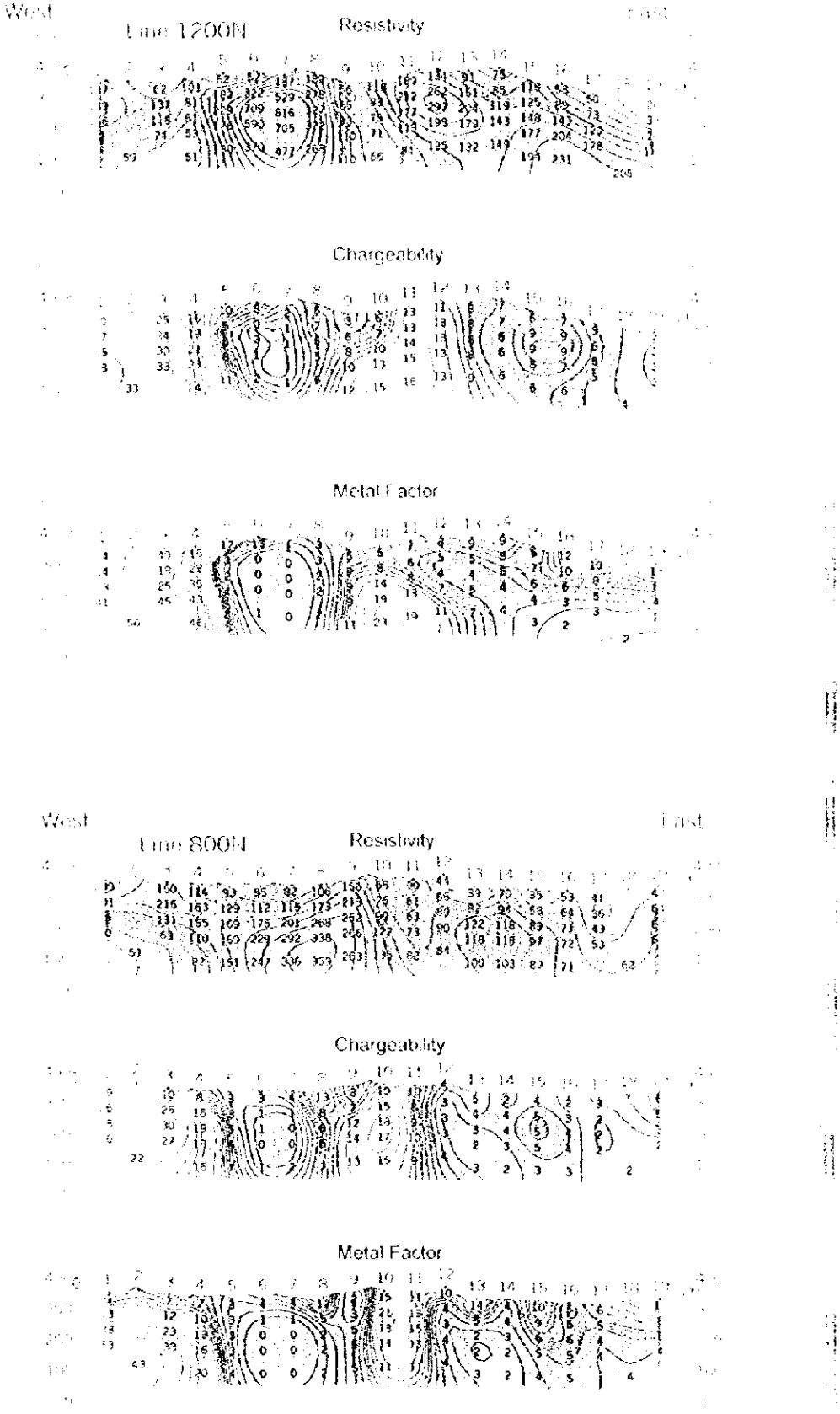

Fig. II-2-18 IP 2D model simulation on lines 800N and 1200N in Magail area